NTNU – Trondheim
Norwegian University of
Science and Technology

Long Step out Umbilicals for Oil and Gas Subsea Pump or Compressor Application

Starting of Permanent Magnet Machine

Andreas Harstad Hallan

Master of Energy and Environmental Engineering
Submission date: June 2012
Supervisor: Lars Einar Norum, ELKRAFT
Co-supervisor: Espen Haugan, Siemens

Norwegian University of Science and Technology
Department of Electric Power Engineering

Problem description

Increased transfer distances for oil and gas gives need for high power pumps installed subsea. One solution possible is to have a variable speed drive on the topside installation with a long power cable feeding the load. For very long distances transformers are necessary. In this work a Permanent Magnet Synchronous Machine is chosen as load for such system which gives the need to reduce the electrical frequency in the starting procedure. Low frequency requires accordingly reduced voltage which alters the motor terminal conditions at starting compared to steady state.

It is assumed that the mechanical load requires a high initial torque to start moving. This assignment seeks to explore if this torque is achievable for a reference system, and which modifications that are most effective to improve starting conditions.

Assignment given: 13. January 2012
Supervisor: Lars Einar Norum, Institutt for Elkraftteknikk, NTNU, Trondheim
Co supervisor: Espen Haugan, Siemens PEC, Trondheim.

Preface

This master thesis is the final part of a Master of Science degree in Electric Power Engineering at the Norwegian University of Technology and Science in Trondheim.

The subject was initially proposed during the fall semester 2011 working with long step out systems power by a topside variable speed drive. This work focused on asynchronous machine loads. Using a Permanent Magnet Machine was proposed by Espen Haugan at Siemens PEC with special focus on starting. Working with this, for me, new type of load gave the possibility to get knowledge about a machine type which has had little focus in the standard courses.

The main supervisor has been Lars Einar Norum from NTNU and Espen Haugen has been co supervisor.

I would like to thank Lars Norum and Espen Haugan for kindly answering questions in the past months. Thanks also goes to all those who I have had valuable discussions with during the semester. Both fellow students and academic staff at NTNU are great contributors to this thesis.

Finally I would like to thank all students in Trondheim for making this a perfect place for personal and professional development.

Trondheim, June 2012

Andreas Harstad Hallan

Summary

Topside Variable Speed Drive (VSD) feeding a subsea load via a long cable is not a new technological challenge [1] and many features in systems feeding asynchronous machines are well known [2] [3] [4] [5] [6]. For a synchronous machine the situation is different as a net positive machine torque is not guaranteed. Therefor an analysis of the start sequence of such machine is of interest.

In this work starting of a Permanent Magnet Synchronous Machine (PMSM) powered by a VSD via a long subsea cable have been studied. Long transfer distance gives need for increased cable voltage, and thus transformers are introduced. The system studied is shown in Figure 1. A dynamic simulation model has been developed in SIMULINK™ SimPowerSystems™ consisting of voltage source, saturable transformers, cable, machine and mechanical load.

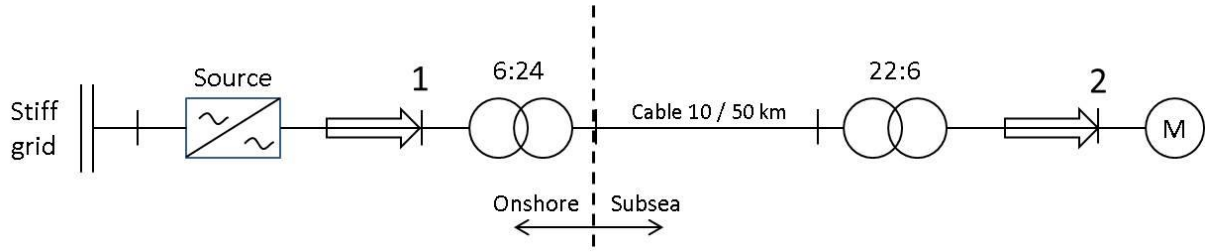

Figure 1 - Single line diagram of the system studied. For 50 km cable the topside ratio is adjusted to compensate steady state voltage drop

To synchronize the machine the electrical frequency is lowered as suggested by e.g. Chapman [7] with the result that the system impedances change compared to steady state and resistance become the dominant parameter. Source voltage amplitude must also be reduced accordingly to avoid iron core saturation. The consequence is that the large cable voltage drop result in insufficient start up torque produced by the machine when a stiction torque around 30 % as described e.g. by Osman [8] is present.

The mentioned dynamic simulation model has been used to compare system modifications proposed in literature to an unmodified base case with a cable length of 50 km. This have been done to investigate how stiction torque affects the start sequence and to draw conclusions about which method gives the most benefits for this type of machine. The main cases tested are increased voltage/frequency ratio, reduced cable resistance and machine damping.

If the electromagnetic torque produced overcomes stiction torque the rotor is set into motion. Because of the rotor and load inertia and the high opposing friction torque rotor oscillations around zero speed is not avoided for any of the cases when stiction torque is applied. Oscillation motion is assumed to heat up the bearing oil such that the static torque is reduced and eventually synchronous operation is achieved after several seconds. It is shown in this work that what separates the cases is the time the machine uses to reach synchronism. A comparison of synchronization times is shown below:

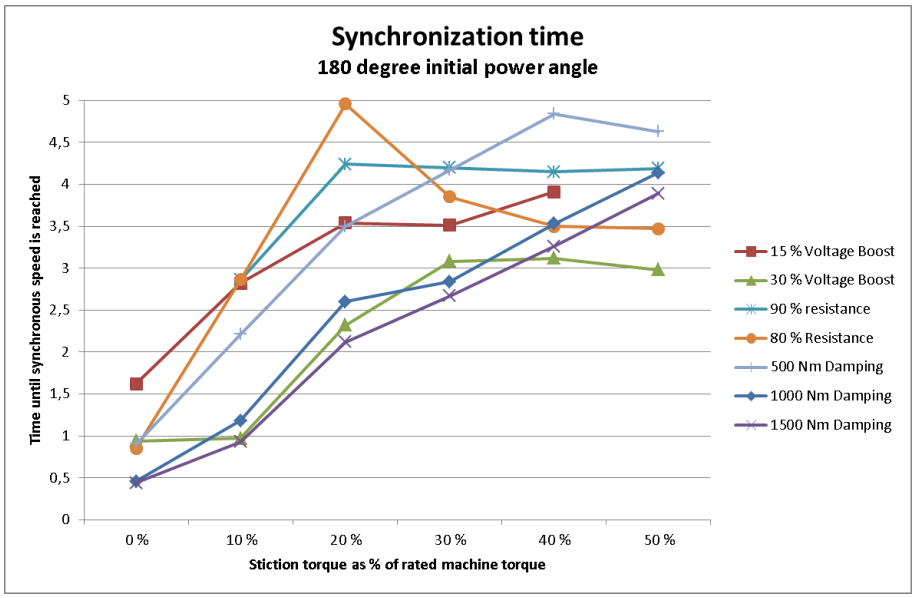

Figure 2 - Comparison of synchronization time as function of stiction torque for all cases

All modifications shows improvement compared to the base case. Damping and voltage boost are the modifications with the most promising results for a broad range of stiction torques. This is expected as damping gives a net positive torque as in an induction machine, and that voltage boost directly increases the machine current. Higher voltage boost is better, but may easily lead to transformer saturation so this method must be used with great care [9]. A rotor design with very high damping may result in a machine with lower air gap magnetic flux and conversely lower electromagnetic torque [10]. The tradeoff between the modifications must be considered for each specific system.

Oscillations are found to be present to the same degree independent of initial power angle. This means that as long as no dynamic control strategy is applied one does not have to take into account the initial angle of the rotor relative to the stator field.

The assumption about reduction in static friction in the mechanical load should be tested in laboratory or existing installations. No cost- or sizing considerations are included in this work. In relation to offshore installations space requirements may often be an issue, but this has to be considered in each specific case. Also resonance conditions must be treated with great care in such system [11] and could be subject for further studies. A great challenge is to achieve general results and models that may be part of a tool box for system development in the future. The model developed here may be a part of such tools.

Sammendrag

Bruk av elektriske frekvensomformere (VSD) til å føde en undersjøisk last via en lang kabel er ingen ny utfordring [1], og mange av utfordringene ved slike systemer tilknyttet induksjonsmaskiner er velkjent [2] [3] [4] [5] [6]. Ved bruk av synkronmaskin som last blir situasjonen annerledes siden man ikke er garantert et netto positivt elektromagnetisk moment. Derfor er det interessant å utføre en analyse av oppstarten av denne type maskin.

I denne rapporten er oppstarten av en permanentmagnet synkronmaskin (PMSM) ved hjelp av en VSD studert. Lang avstand mellom kilde og last gir behov for økt overføringsspenning. Dermed inkluderer systemet transformatorer. Et enlinjeskjema over systemet som er studert kan sees i Figur 1. En dynamisk simuleringsmodell bestående av spenningskilde, transformatorer med mulighet for å inkludere metningsfenomen, kabel, elektrisk maskin og mekanisk last har blitt utviklet i SIMULINK® SimPowerSystems®.

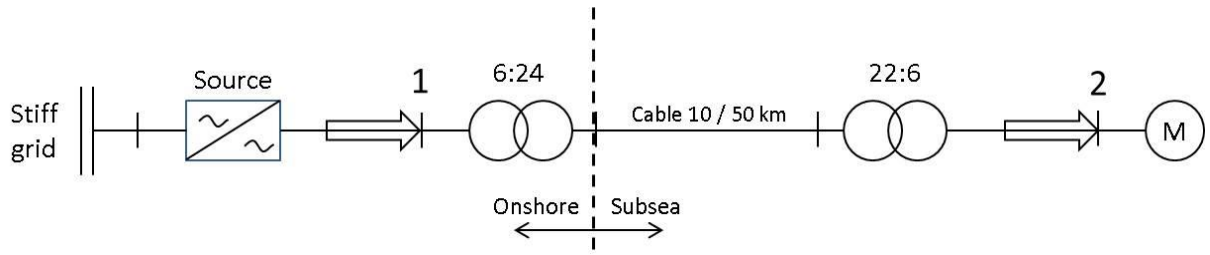

Figur 1 – Systemet vist som enlinjediagram. For 50 km kabel blir vindingstallet på Onshore-transformator justert.

For å oppnå synkron drift av maskinen blir den elektriske frekvensen redusert som foreslått av Chapman [7]. Dette fører til at kabel-, transformator- og maskinimpedansene endres og kabelresistans blir den dominerende parameteren. Kildespenningen må også reduseres i amplitude for å unngå metning av transformatorjern. Konsekvensen av dette er at det store spenningsfallet i kabelen resulterer i utilstrekkelig start moment produsert av den elektriske maskinen når et statisk startmoment rundt 30 %, som beskrevet av f.eks. Osman [8], er til stede.

Den dynamiske simuleringsmodellen har blitt benyttet til å sammenligne systemmodifikasjoner foreslått i relevant litteratur til et umodifisert basissystem med kabellengde 50 km. Dette er gjort for å se hvordan stiksjonsmomentet påvirker startsekvensen, og for å få indikasjoner på hvilke modifikasjon som gir flest fordeler for denne type maskin. De viktigste casene som har blitt utprøvd er økt spenning/frekvens-forhold, redusert kabelresistans og ulike dempemoment i rotoren.

Dersom det elektromagnetiske momentet som produseres av permanentmagnetmaskinen er stort nok til å overvinne stiksjonsmomentet vil rotoren settes i bevegelse. På grunn av høyt treghetsmoment i maskin og last, og det store startmomentet, er det vist at det oppstår oscillasjoner. Disse oscillasjonene rundt 0 fart antas å redusere stiksjonsmomentet gradvis, og simuleringene viser at synkron drift oppnås etter at stiksjonsmomentet er redusert til null. Det er vist i denne rapporten at det som skiller de forskjellige casene fra hverandre er hvor lang tid rotoren trenger for å oppnå synkron fart. En sammenligning synkroniseringstid som funksjon av stiksjonsmoment for alle casene er vist under.

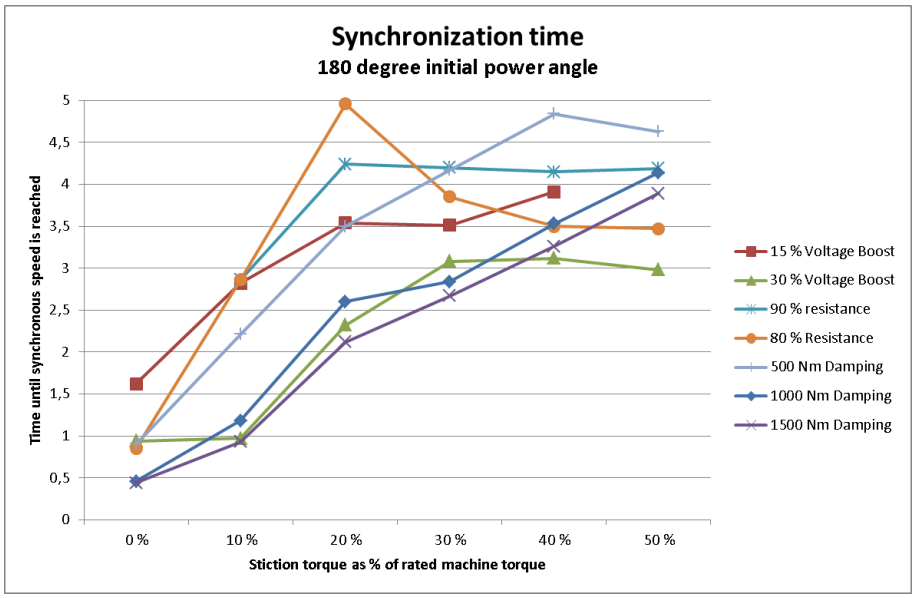

Figur 2 - Sammenligning synkroniseringstid for alle modifikasjoner som funksjon av stiksjonsmoment.

Alle de forskjellige systemmodifikasjonene gir forbedring i forhold til basissystemet. Dempning og økt spenning/frekvens-forhold er de endringene som peker seg ut som mest fordelaktige over et bredt spekter av stiksjonsmoment. Dette er forventede resultater siden dempning gir et netto positivt moment i rotasjonsretningen slik som en induksjonsmaskin. Økt spenning på kilden vil direkte økte spenningen også på maskinterminalene forutsatt at ikke transformatorene er i metning. Økt spenning gir bedre resultat, men må som sagt brukes med forsiktighet siden transformatorjernet lett kan bli mettet [9]. Et rotordesign med økt dempning kan resultere i lavere luftgapsfluks i maskinen med lavere elektromagnetisk moment som resultat [10].

Rotorsvingninger forekommer i alle casene, og i samme grad, uavhengig av hvilke rotorposisjon som var utgangspunktet. Dette betyr at så lenge man ikke skal benytte en dynamisk kontrollstrategi trenger man ikke å ta stilling til rotorposisjonen relativt til statorfeltet ved oppstart.

Antakelsen om reduksjon i statisk friksjon i lasten ved svingninger bør testes i praksis. Enten i et laboratorium, eller i eksisterende anlegg. Det er ikke gjort kostnads- eller størrelsesbetraktninger i denne rapporten. Særlig størrelse kan være svært viktig på oljeinstallasjoner der eksisterende anlegg allerede tar mye plass. Resonans i lange kabler er et tema som alltid må behandles med forsiktighet, og aldri neglisjeres i slike anlegg [11], og bør tillegges ytterligere studier. En stor utfordring er å oppnå generelle resultater og enkle modeller som kan benyttes som verktøy i videre utvikling. Modellen som er utviklet til denne rapporten kan være en del av et slikt verktøy.

Table of Contents

Table of Figures

Table of Tables

1 Long step out umbilicals for subsea pump or compressor application

Subsea processing is getting more and more common due to its large benefits in extracting more oil from fields already in operation, and the possibility to reduce cost in floating production units. Production units on the seabed placed a long distance away from existing installations give a different need for electrical analysis in the power supply system compared to onshore meshed grids with constant frequency [12].

Topside VSD feeding a load via a long cable is not a new technological challenge [1] and many features are well known [2] [3] [4] [5] [6]. The loads in these publications are asynchronous machines. In this work the load is a Permanent Magnet Synchronous Machine, PMSM. Synchronous operation of the machine gives particular problems related to starting. This work seeks to define what is required from a step-out system when starting such machine using a topside variable speed drive system.

Gieras and Wing [13] present the main benefits of magnetic excitation compared to field windings as:

- No electrical energy is absorbed by the field excitation system and thus there are no excitation losses which means substantial increase in the efficiency
- Higher torque or output power per volume
- Better dynamic performance caused by higher magnetic flux in air gap
- Simplified construction and maintenance
- Reduction of prices for some types of machines

Compared to asynchronous machine the main benefit of a PMSM is reduced magnetizing current [14].

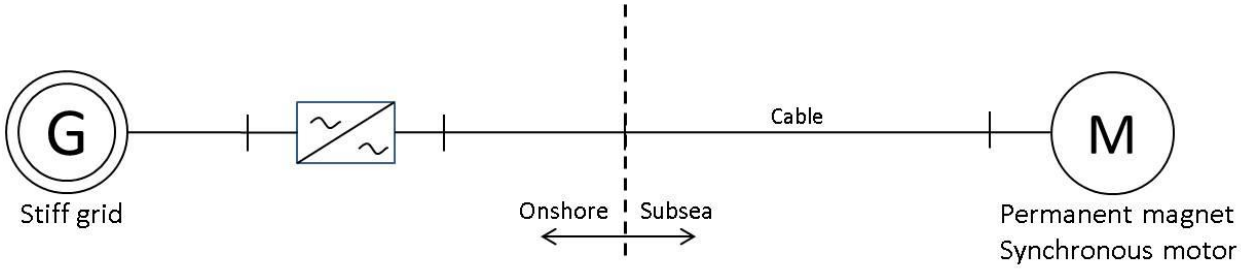

Figure 3 - Short cable VFD system

With new multilevel cascaded inverter technologies medium voltage levels[1] may be achieved directly on inverter output [15]. In shorter step out systems transformers may be avoided as shown in Figure 3.When the distance between power source and load increase the voltage level in cable should be at a higher level then applicable on the motor to reduce power losses and voltage drop. Figure 4 shows a single line diagram where step up and step down transformers are included.

[1] 7.2 kV output is possible from Perfect Harmony [1]

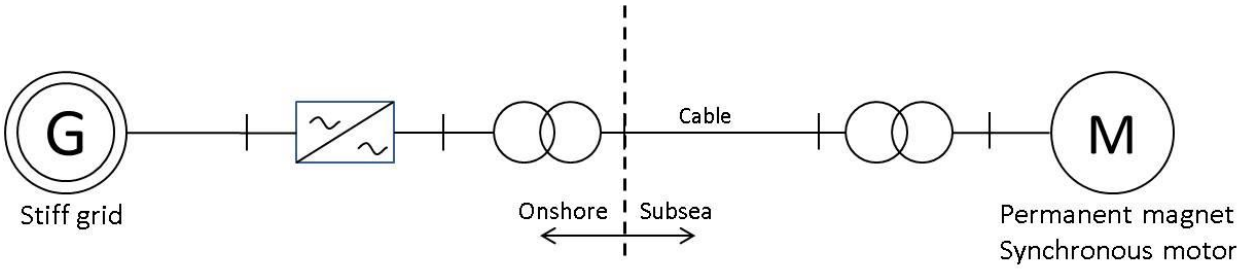

Figure 4 - Long step out variable frequency drive system with step up and step down transformers.

The above system is to be studied in this work. Different cable lengths will be chosen to illuminate challenges imposed by increased transfer distance with main focus on long cables. Both hand calculations and dynamic simulations of motor starting are used to test different improvement proposals from asynchronous machine systems and other solutions relevant for synchronous machines only.

2 Starting of synchronous machine

2.1 Introduction to synchronous machine starting

Chapman [7] gives three alternative approaches for starting of a synchronous machine.

1. Reduce the speed of the stator magnetic field to a low enough value that the rotor can accelerate and lock in with it during one half-cycle of the magnetic fields rotation.
2. Use an external prime mover to accelerate the synchronous motor up to synchronous speed before connecting the terminals to the power source.
3. Use damper windings to provide asynchronous starting.

By using a variable speed drive the first alternative is possible. For subsea application alternative (2) is not an option. According to Pyrhönen et.al. [10] alternative (3) is a possibility for motors with well designed damper windings. Alternative (1) is the option seaming most likely to be the main starting method. Below two main issues with starting of a permanent magnet machine in a long step out system is presented. Machine features are also studied in more detail later. See chapter 3.5.

2.2 Voltage drop problem

The need for voltage reduction at starting frequency again leads to a reduction in voltage at the cable end. This voltage is crucial to overcome stiction torque which usually is present for some time during start up [16]. Ensuring sufficient start up torque is the main objective of this work. Figure 5 shows a very simplified system model to illustrate the voltage distribution problem.

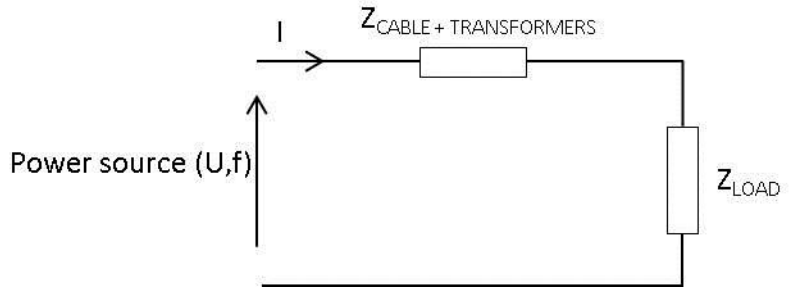

Figure 5 - Simplified system view. Voltage division between load and system.

Series reactance of cable and transformer is frequency dependent and conversely very small at low frequencies. Resistance is in lesser degree dependent on frequency. Table 1 gives an example of which parameter is the dominating part of the series impedance at different frequencies.

Table 1 - Linear frequency variation in cable impedance imaginary

f [Hz]	R* [ohm/km]	ωL* [ohm/km]	$\frac{R}{\lvert Z \rvert} * 100$ [%]
3	0.287	0.038	99.2
60	0.287	0.754	35.5

***Arbitrary cable data**

It can be seen that resistive voltage drop is very dominant at low frequency. The total resistance of a cable is usually higher then that of the motor such that $Z_{CABLE + TRANSFORMERS} >> Z_{LOAD}$ in Figure 5. Thus the initial voltage drop in the cable is very high relative to that in the motor.

Extended cable lengths studied in this work makes transformers necessary, and the iron core of a transformer, like all iron cores, may easily saturate at low frequencies if the applied voltage is not reduced in accordance to the frequency [7]. This combined with a very unfavorable voltage distribution might make it challenging to achieve successful motor start.

Proposed solutions to this problem is to oversize the step up transformer iron or use a lower resistance cable [1] [11]. These among other solutions are tested in this work.

2.3 Reaching synchronism problem

A simplified expression for electrical torque presented by e.g. Machowski et. al. [17] for round rotor machines is (2.1):

$$T_{EM} = \frac{\pi}{2} F_r . \emptyset_f sin\delta_{fr} \tag{2.1}$$

Assuming constant rotor magnetomotive force and air gap field flux the torque is a sinusoidal function of the angle between these two fields. This is illustrated in Figure 6.

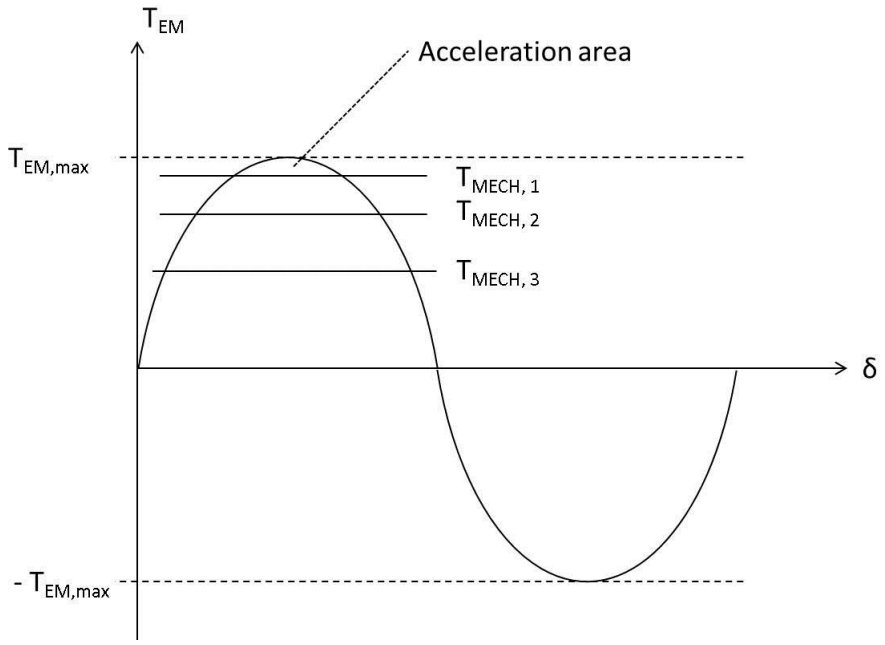

Figure 6 - Electromagnetic- and mechanical torque initially for the synchronous motor

The rotor is reluctant to start because the mechanical system needs some time to heat up. Figure 6 shows the acceleration area as the difference between the mechanical friction initially and the electromagnetic torque produced in the motor. The surplus of electromagnetic torque is used for rotor acceleration. Acceleration is restricted by the high friction, and may limit the synchronization ability of the rotor. A running rotor reduce this static friction fast, but it is assumed that also oscillating motion of a non-synchronized rotor reduce the static friction illustrated by the horizontal torque lines moving downwards to increase acceleration area.

Synchronous operation is achieved when the mechanical- and electromagnetic torques are equal, and the rotor is settling at the equilibrium point to the left of $T_{EM,MAX}$ in Figure 6 [17]. If synchronous operation is reached at low frequency further acceleration of the machine up to rated may be achieved as long as the mechanical torque does not exceed a stable operation point. If steady state

operation is to close to T_{MAX} the motor may easily loose synchronism if mechanical torque suddenly increases [17].

3 Model description

3.1 SIMULINK™ SimPowerSystems™ model

The simulation model used as basis for this work consists of a scalar controlled voltage source and a permanent magnet machine as shown in Figure 8. Between these two there are multiple points for measurements to investigate the impact of cable and transformers. The visual layout is inspired by Siemens projects [18], but all elements are either standard SimPowerSystems™ blocks or custom made for this application.

Figure 7 is a simplification of the system shown in Figure 8.

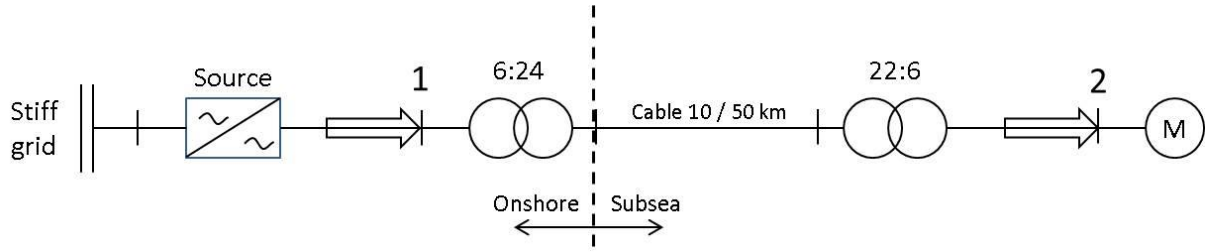

Figure 7 - Single line diagram of the long step out umbilical system

Each main component in Figure 7 is described in the following chapters and put together to the SimPowerSystem™ shown below. This is the basis for simulations of motor start.

The main objective is to investigate if high enough torque may be achieved at low frequency such that synchronous starting is successful with different configurations. In this system topside transformer voltage ratio is adjusted to compensate steady state voltage drop. See Power system description in Appendix A1. Simulations are run and output data is treated via Matlab™ scripts. These scripts are found in Appendix E where also system parameters may be changed according to the scenario one wish to illuminate.

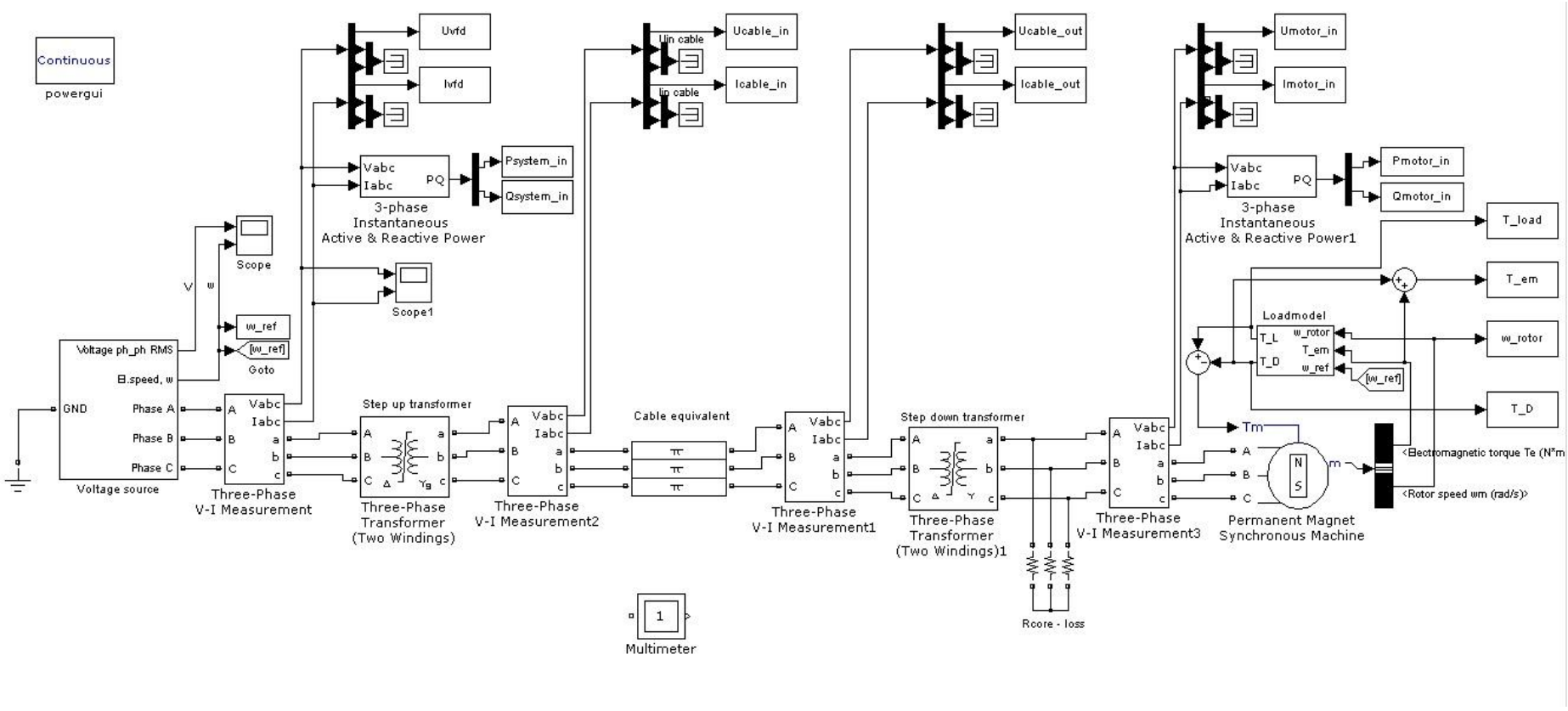

Figure 8 - SIMULINK SimPowerSystems start up system

3.2 Voltage source

Starting of a synchronous machine require low frequency. A three phase voltage source with adjustable voltage and frequency has been developed for this task. Feedback is referred to as impractical by e.g. Råd [19], and in this work constant voltage/frequency ratio is chosen as control strategy.

The source is developed in SimPowerSystems™ and the block as it appears in start system is shown in Figure 9.

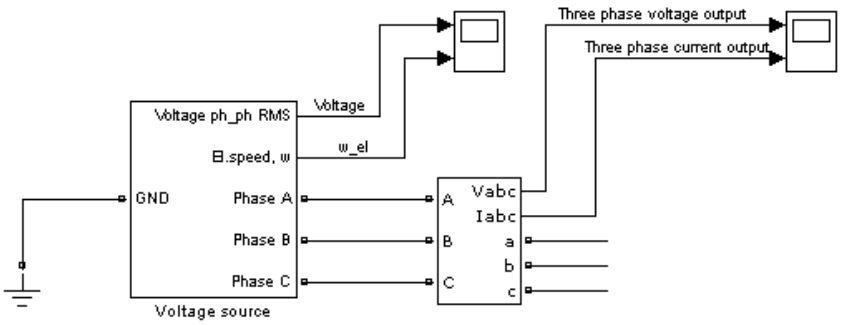

Figure 9 - Three phase source

The block shown in Figure 9 contains several subsystems. All phases are equal except for a 120° phase shift, and that the reference signals for voltage amplitude and frequency are obtained from phase A only. The subsystems and mathematical derivations may be found in Appendix C.

The reference signals for voltage and frequency are obtained at the input to the sine function on the form (3.1):

$$K(t) = \mathrm{U(t)} * \sin(2 * \pi * \mathrm{X(t)}) \qquad (3.1)$$

Where K is the single phase to neutral voltage, U(t) is voltage amplitude reference and X(t) is t*f(t). See details in Appendix C.

As an example the voltage output for one phase when the frequency is ramped from five to 20 Hz in 3 seconds is shown in Figure 10. Also included in the figure are voltage and frequency references. In this case the voltage/frequency-ratio is kept constant. The block has the ability to adjust this if necessary. This feature will be used in simulations to create voltage boost.

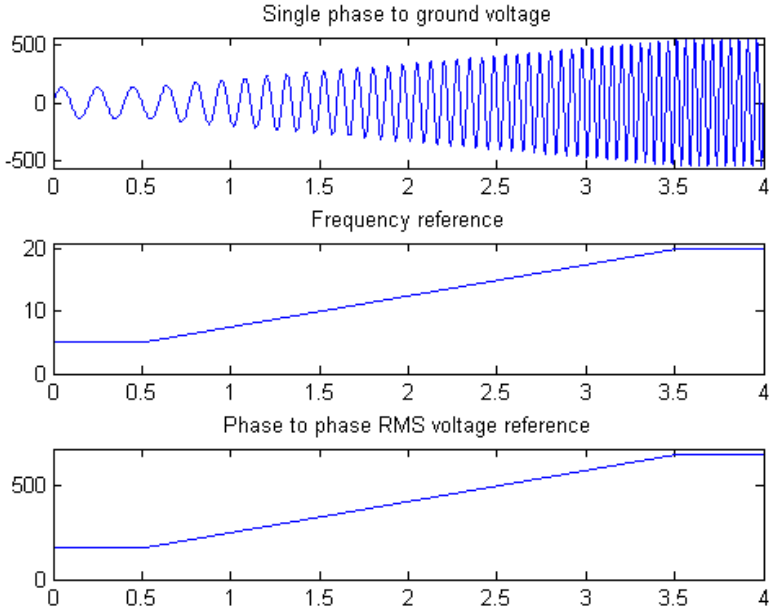

Figure 10- Single phase output with references

3.3 Transformer

3.3.1 General

As cable length increase power loss increase correspondingly. Transformers increase the voltage level to reduce current and thus ohmic losses in the system [19]. Voltage level, power rating and connection method is chosen dependent on the system. In this work the equivalent model in Figure 11 is used to implement the transformer.

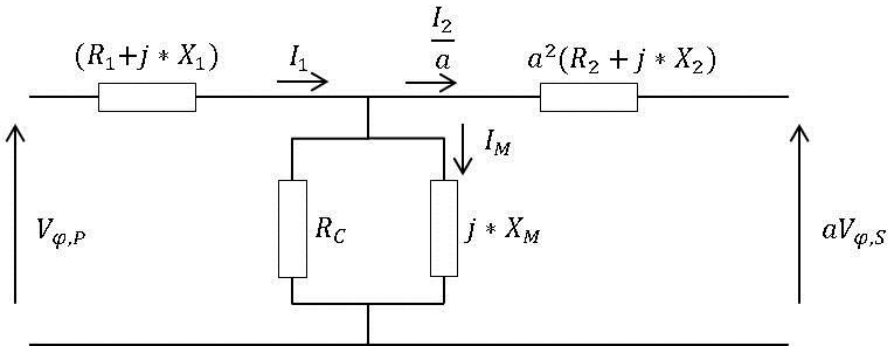

Figure 11 Transformer equivalent circuit referred to primary side. SI units.

In Figure 11 "a" denotes transformer turns ratio. See (3.2).

$$a = \frac{V_{\varphi,P}}{V_{\varphi,S}} = \frac{N_P}{N_S} \tag{3.2}$$

R_1 and R_2 represent winding resistive losses, and X_1 and X_2 is a representation of winding leakage inductance. The parallel branch containing R_C and X_M copes with core loss and magnetization respectively. Both the currents in this branch are nonlinear so the resistance and reactance are approximations of the real excitation effect [7]. In steady state calculations the magnetization and core loss currents are often neglected because these currents usually are in the order of 0.5 % compared to the winding currents and power transfer [20]. In the dynamic simulations iron core saturation is included. This effectively means that the magnetizing inductance varies with the applied primary side voltage, and the transformer draws very high magnetizing current for high voltage/frequency ratios. Thus the secondary side voltage is not proportional to the winding ratio as in (3.2).

3.3.1.1 Voltage level / winding ratio

The voltage level must be chosen according to system design. Power flow analysis gives steady state voltage drop in the cable. The power loss is reduced at higher voltage, and the cost of insulation increases.

3.3.1.2 Power rating

The transformer must be capable of transferring the current required at all times for the system.

3.3.1.3 Connection method

In a three phase transformer the primary and secondary may be connected in one of three different ways, or derivations of these [7]:

- Wye – wye (Y – Y)

- Delta – delta (Δ - Δ)
- Delta – wye (Δ - Y) (or opposite)

All the above configurations have distinct advantages and disadvantages. Relevant resources as Chapman [7], Harlow [20] or Grainger [21] should be consulted for details. Here, it is only briefly argued why the latter alternative is preferred. See Figure 12.

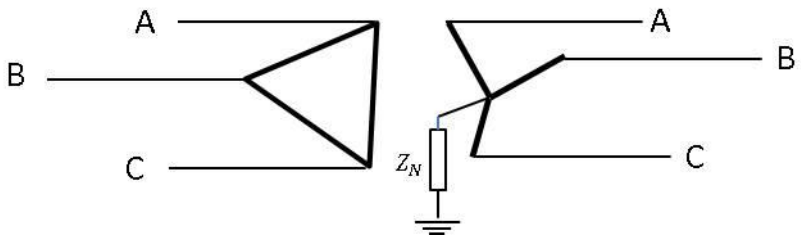

Figure 12 - Delta-wye connected transformer

Delta – wye connection result in a 30 degree lag for the secondary voltage referred to primary [7] [20]. In a step out system where no paralleling of transformer occurs this is no concern. If the wye side is grounded unbalances voltages on this side cause high circulating currents in the delta connection [20]. These currents are not seen in the secondary windings. The transformer must be properly designed to prevent overheating caused by these circulating currents.

One of the major advantages of the Δ-Y connection is that is provides harmonic suppression [9]. The third harmonic currents are able to circulate around the path formed by the Δ-connected winding. If the fundamental frequencies are 120^o apart, the third harmonics are in phase and do not appear as physical currents on the terminals of the windings. This also apply for all zero sequence currents, and is important because zero sequence currents give great mechanical stresses on machinery [9].

The second of the most important advantages is that this connection provides ground current insulation between the primary and secondary side of the transformer. A single phase to ground fault will not affect the Δ-side of the transformer because no return path exist for the current. If the neutral point of the Y is grounded a fault may be detected easily such that damage on equipment or personnel does not occur [22].

3.3.1.4 Saturation

The lowest frequency possible is a DC-voltage. If DC is applied on the primary of a transformer the coil will act as to a short circuit since the opposing voltage is proportional to the rate of change in flux as shown in Figure 13. A transformer might be constructed in various ways to modify the saturation characteristic. It is common to either use a higher cross section iron core, or to insert an air gap in path of the magnetic flux. Inserting an air gap gives a flatter curve then the one presented in Figure 16 such that higher voltages may be applied, but also gives a higher steady state magnetizing current caused by the higher reluctance in the transformer core [9].

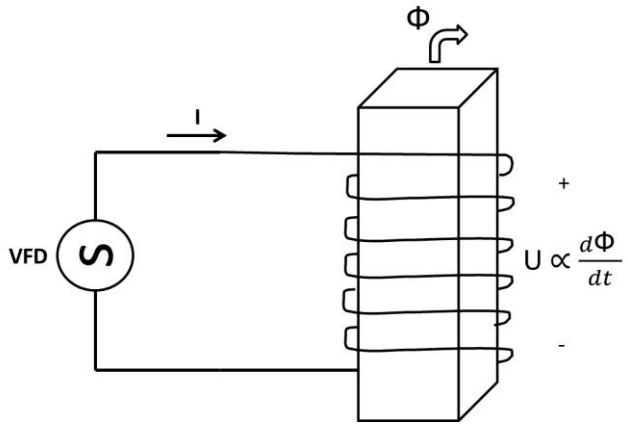

Figure 13 Iron leg of transformer

A high voltage input at low frequency may in this way cause high current and saturation of step up transformer. Therefore the variable frequency drives is set to maintain a constant volt/hertz ratio at starting [4].

3.3.2 Simulink model

The Three-Phase Transformer (Two Windings) block implements a three-phase transformer using three single-phase transformers as in Figure 11 [23]. The block as it appears in SIMULINK is shown in Figure 14.

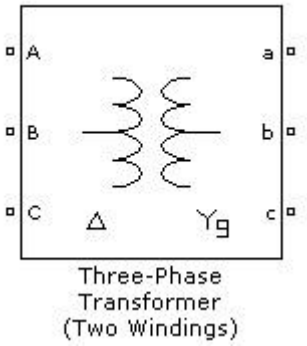

Figure 14 - SIMULINK SimPowerSystems transformer model

Parameters and connection method are chosen in the block parameter selection box shown in Figure 15. For saturable transformers the magnetizing inductance, Lm, is replaced by a saturation curve.

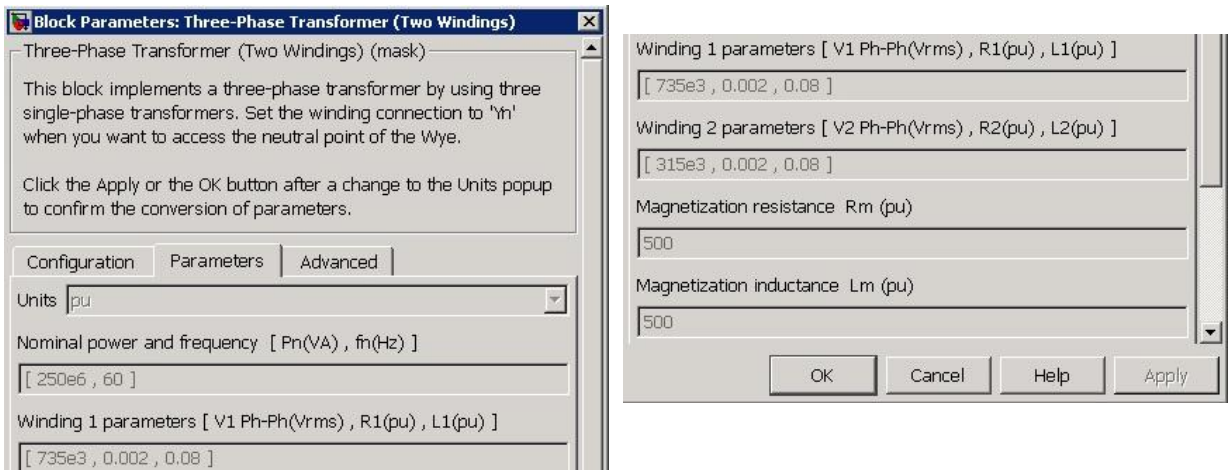

Figure 15 - Parameter selection box in SimPowerSystems

The saturation curve may be set as a piecewise linear relationship between magnetizing current and flux [24]. This is the method chosen in this work to simulate transformer saturation at start-up. See Figure 16.

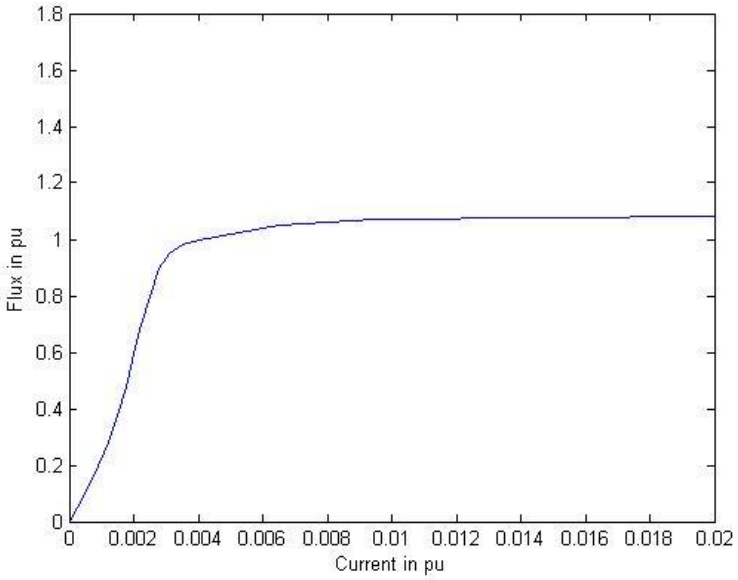

Figure 16 - Saturation curve for a typical transformer in Matlab

In Figure 16 the base values for pu calculations are (3.3)(3.4):

$$I_{base} = \frac{P_N}{V_1} * \sqrt{2} \tag{3.3}$$

$$\lambda_{base} = \frac{V_1}{2 * \pi * f_n} * \sqrt{2} \tag{3.4}$$

The base flux is defined as the peak value of the sinusoidal flux when the primary winding is connected to a 1 pu voltage source. λ_{base} defined above represents the base flux linkage. It is related to the base flux by the number of turns in the primary winding as shown in (3.5) [24]:

$$\lambda_{base} = \text{Base flux} * \text{number of turns in primary winding} \tag{3.5}$$

When values are expressed in pu the turns ratio is 1.

3.3.3 The chosen transformers

Data are taken from a different project [25] and modified slightly to correspond to other chosen components. See Table 2.The values are assumed to be in the range of what is representative for in a real system of this approximate rating.

Table 2 - Transformer data used in simulations [18]. 10 km.

Transformer data		Topside step up	Subsea step down
Rated power	[MVA]	5.00	5.00
Rated frequency	[Hz]	66.67	66.67
Primary side voltage	[kV]	6	22
Secondary side voltage	[kV]	24*	6
Reactance, ux	pu	0.06	0.086
Resistance, ur	pu	0.005	0.006
Magnetizing reactance	pu	"Saturation curve"	"Saturation curve"
Magnetizing resistance	pu	426	870

***For 50 km cable the topside transformer ratio is chosen as 6:25.6 (see Appendix A1)**

Steady state system simulations and calculations with 10 km cable presented in Appendix A1 argues that the step up transformer topside should have a higher turns ratio then the subsea transformer. This is to compensate the steady state voltage drop. Thus it is assumed that cable insulation is designed for this higher voltage. For longer cables this voltage drop is higher, and the turns ratio is adjusted in the simulations. Table 2 represents the base case.

Figure 17 shows the chosen saturation curves for this work. Both are from a previous Siemens project [25] and are thought to be representative as the power ratings of the loads are approximately equal, and both projects are step out systems with the same cable.

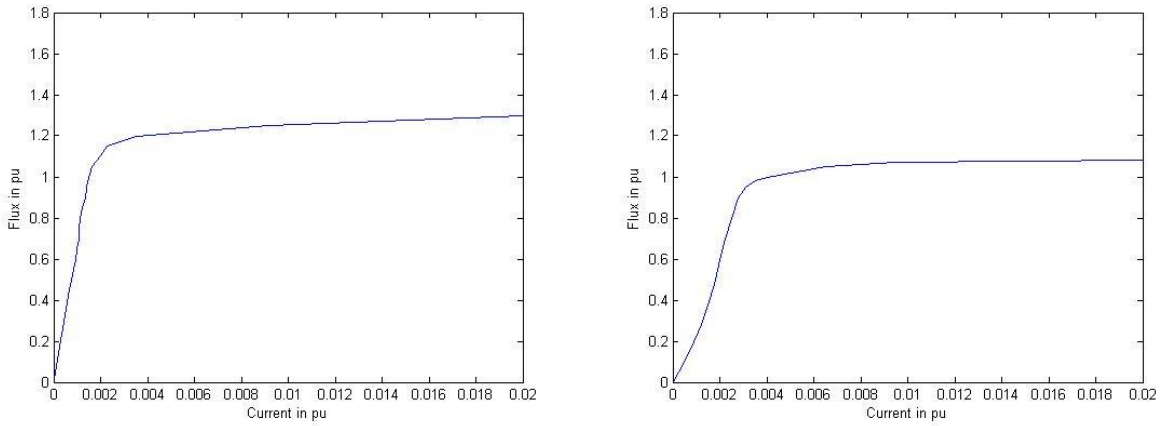

Figure 17 – Left: Topside transformer saturation curve [25]. Right: Subsea transformer saturation curve [25].

Comparing the two it can be seen that the topside transformer have a higher flux capacity then the subsea transformer. Larger iron core gives higher current carrying capacity and the possibility to use higher voltage/frequency ratio then subsea.

3.4 Cable model

3.4.1 General

In this work the subsea cable is chosen to be modeled as a PI-equivalent. Resonance phenomena are not a subject here. Therefor PI-sections, with a finite number of states, are sufficient [26]. The single phase pi-section line block as it appears in SIMULINK is shown in Figure 18 together with the three phase equivalent used here.

Figure 18 - Pi section blocks in SimPowerSystems. Single phase (left) and three phase (right)

This block models the series resistance and inductance, and the shunt capacitance of each phase. The equivalent capacitance is a function of both capacitances to ground, and between the phases. See Figure 19.

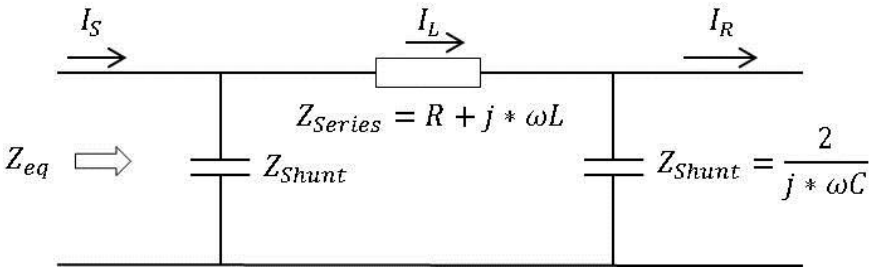

Figure 19 - Content of PI-equivalent block

Parameters for the cable equivalent are chosen per km line as shown in Figure 20.

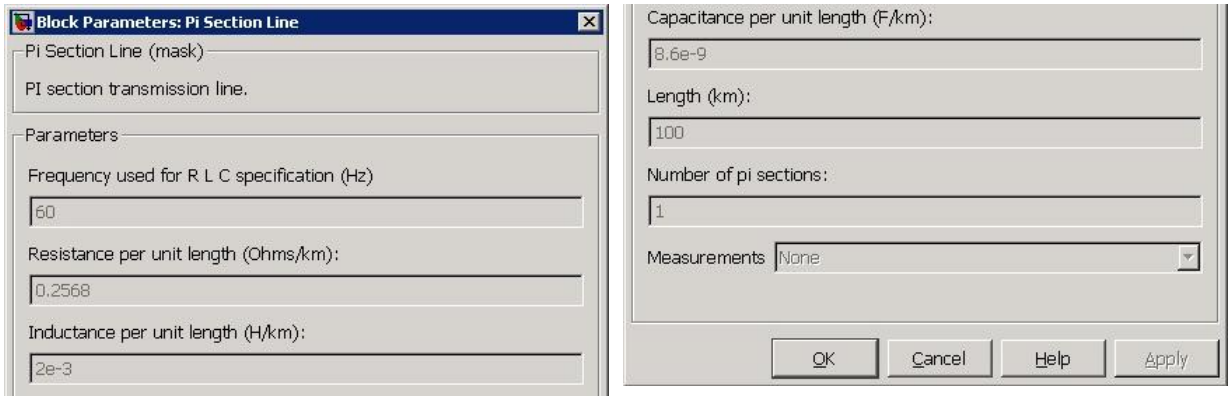

Figure 20 - Parameter selection for the PI-section block in SimPowerSystems

In SimPowerSystems™ hyperbolic correction of parameters is used for all lengths. This is to account for the fact that propagation speed of the magnetic field around the cable is finite [26]. Generally this result in decrease of series R and L, and increase in shunt capacitance [26]. The corrections become more important as line length increase.

When starting the synchronous machine in this work the frequency varies from almost zero up to rated. Reactances are frequency dependent and will vary within a high range. In the series

impedance the resistance has a much higher part of total impedance at starting then at rated conditions. Using the standard Matlab-parameters shown in Figure 20 as illustration gives:

Table 3 - Linear frequency variation in impedance imaginary

f [Hz]	R [ohm/km]	ωL [ohm/km]	$\frac{\boldsymbol{R}}{\lvert\boldsymbol{Z}\rvert} * \mathbf{100}\ \%$
3	0.287	0.038	99.2
25	0.287	0.314	67.4
60	0.287	0.754	35.5

As can be seen in Table 3 the expected result is obtained. Resistance is reduced relative to the inductance in the series impedance as frequency increase. Resistance also increases with frequency because of uneven current distribution in the AC cable, but not at the same extent as the reactance [27]. Therefor this is not included in this work.

The number of pi sections used depends on the frequency range to be represented. Mathworks [26] gives the frequency range of a PI line model as (3.6):

$$f_{max} = \frac{N * v}{8 * l_{tot}} \tag{3.6}$$

Where:

N Number of PI sections

v Propagation speed. $v[km/s] = \frac{1}{\sqrt{L' * C'}}$. Inductance and capacitance per km

l_{tot} Line length

In this work no harmonics are included in the source model. Harmonics in the multiples of three imposed by magnetizing currents in transformer is cancelled in phase to phase voltages, see chapter about transformer. However resonance must be treated with great care when construction a system using variable speed drives and long cables [2]. If the model is to take resonance into account knowledge of the converters dominant harmonic frequencies should be compared to the systems frequency range.

The most critical part of the simulations is the initial synchronization at low frequency. Therefor it is important to investigate cable parameters at these low frequencies. The equation above becomes important if a real converter is to be used in the system as resonance phenomena are important in long cable sections.

3.4.2 The chosen cable

One pi section per 5 km cable is chosen in this work, and is thought to be sufficient. It is shown in Appendix A1 that series impedance is sufficient for low frequencies because the charging current is neglectable. However the model may also be used for acceleration of the machine. Thus pi-equivalents are chosen to have an equal basis for the simulation results in further work.

In this work a cable produced by Nexans is chosen. The parameters per kilometer are shown in Table 4.

Table 4 Cable parameters. Nexans 22 kV umbilical

Resistance	R_C [ohm/km]	0.214	
Inductance	L_C [H/km]	$0.746 * 10^{-3}$	
Reactance @ 3 Hz	X_C [ohm/km]	0.014	Typical starting frequency
Reactance @ 66.67 Hz	*X_C [ohm/km]*	*0.313*	
Capacitance	C_C [F/km]	$0.136 * 10^{-6}$	

Values are included in the model via the Matlab script used to initialize the simulations. See Appendix E.

3.5 Permanent magnet machine

3.5.1 Torque equations and design

PM synchronous motors are usually built with one of following rotor configurations [13]:

(a) Salient poles with laminated pole shoes and a cage winding
(b) Interior-magnet rotor
(c) Surface-magnet rotor
(d) Inset-magnet rotor
(e) Rotor with buried magnets symmetrically or asymmetrically distributed

The rotor configuration effect the inductance seen from the motor terminals as the reluctance of the stator and rotor iron, and air gap become a function of rotor position if the rotor is magnetically salient. Briz and Degner [28] shows that this might be exploited by some controllers but in this work no feedback is assumed so these types of control is not an option. Gieras and Wing [13] gives the general three phase electromagnetic power equation when neglecting stator winding resistance as (3.7):

$$P_{em} = 3 * \left[\frac{V_1 E_f}{X_{sd}} * \sin(\delta) + \frac{V_1^2}{2} * \left(\frac{1}{X_{sq}} - \frac{1}{X_{sd}} \right) * \sin(2 * \delta) \right] \quad (3.7)$$

V_1 Input terminal voltage
E_f EMF induced by the rotor excitation flux
δ Power angle
X_{sx} Synchronous reactances in q- and d-axis

For a salient pole synchronous motor the synchronous reactances are (3.8):

$$X_{sd} = X_1 + X_{ad} \qquad X_{sq} = X_1 + X_{aq} \quad (3.8)$$

X_1 Stator leakage reactance
X_{ad} d-axis mutual reactance
X_{aq} q-axis mutual reactance

The d-axis mutual reactance is sensitive to magnetic saturation whilst the q-axis reactance saturation depends on rotor construction. For normal synchronous machines usually, $X_{sd} > X_{sq}$ such that the second term in (3.7) gives positive contribution to the power [13]. For permanent magnet machines this power term might differ based on how the magnets are built into the rotor [13].

Torque is given by Chapman at.al [7] as (3.9):

$$T_{em} = \frac{P_{em}}{\omega_m} \quad (3.9)$$

Such that (3.7) turns into (3.10):

$$T_{em} = \frac{3}{\omega_m} * \left[\frac{V_1 E_f}{X_{sd}} * \sin(\delta) + \frac{V_1^2}{2} * \left(\frac{1}{X_{sq}} - \frac{1}{X_{sd}} \right) * \sin(2 * \delta) \right] \quad (3.10)$$

The second term in (3.10) is referred to as reluctance torque [17]. This exists only for salient pole generators because the machine tries to minimize the energy in the air-gap by keeping it as small as possible. If the air gap is uniform no reluctance torque is present.

In electromagnetic exited and PM motors a cage windings is frequently mounted on salient-pole rotors to provide asynchronous starting, and to damp oscillations under transient conditions [13]. Figure 21 shows two permanent magnet machine rotors with salient pole rotor.

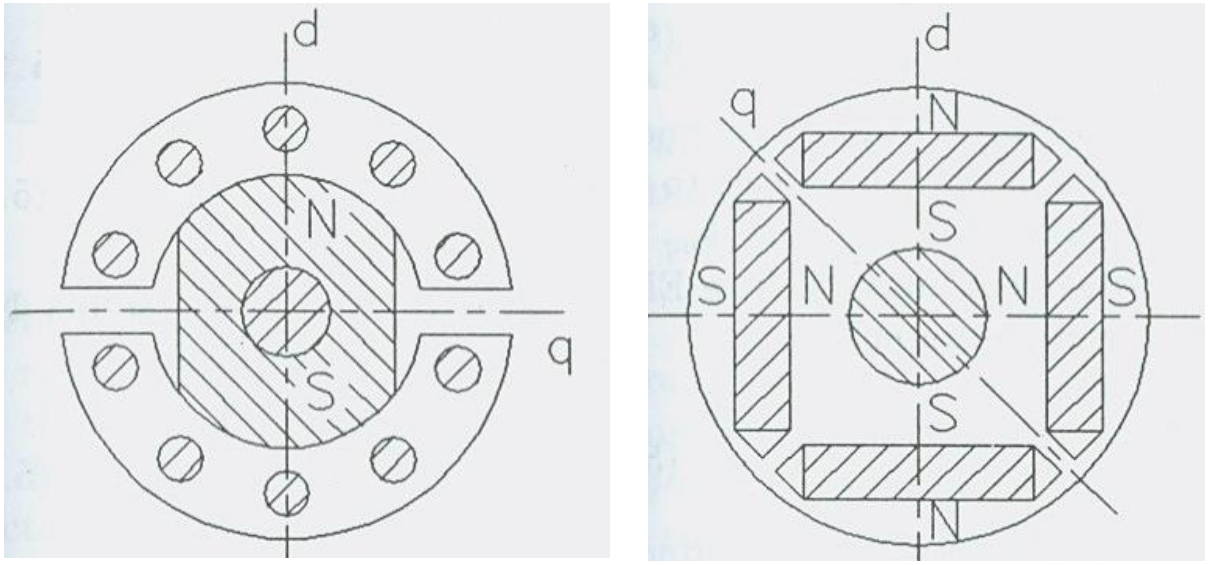

Figure 21 - Salient pole permanent magnet machine rotor with damper windings

The left configuration above was the first successful construction for high speed applications [13]. A different rotor configuration is shown in the right part of the figure. Here it can be seen that the q-axis magnetic flux sees a lower reluctance then that in the d-axis, because of the slot of high relative permeability between the magnets. Therefor the d-axis reactance is lower then that of the q-axis, and the reluctance torque is opposing the electromagnetic torque mentioned before. See equation (3.10).

Rotor configuration strongly affects how the source sees the machine. With knowledge of the power and torque equations shown above in the design process the type of machine may be adapted to the system needs [10]. Knowledge about rotor reluctance may also be exploited in sensorless control systems to determine rotor position such that dynamic control strategies can be used [28]. This is not covered here because the system studied has no feedback.

3.5.2 Damping power

Oscillations in the machine power angle are usually damped by the power provided by damper windings [17]. These windings act in similar way as short circuited squirrel cage rotor windings in an induction machine providing opposing torque when the rotor moves asynchronous to the electrical frequency. In round rotor machines the solid steel body provides paths for eddy currents which have the same effect as damper windings [17].

Machowski [17] derives expressions for damping power based on an induction machine equivalent for both round and salient rotors with the following assumptions:

(a) Resistance of the armature winding are neglected
(b) Damping is produced only by damper windings
(c) The leakages reactance of the armature winding can be neglected
(d) Excitation does not affect the damping torque

The final expression for a round rotor damping power is then (3.11):

$$P_D^{round} = V_1^2 \frac{X_d' - X_d''}{(X + X_d')^2} * \frac{X_d'}{X_d''} * \frac{T_d'' \Delta\omega}{1 + (T_d'' \Delta\omega)^2} \quad (3.11)$$

For a salient rotor the driving voltage V_S is replaced by the d- and q-axis voltage components,

V_d=-V_1*sin(δ) and V_q=V_1*cos(δ), to give (3.12):

$$P_D^{salient} = V_1^2 \left[\frac{X_d' - X_d''}{(X + X_d')^2} * \frac{X_d'}{X_d''} * \frac{T_d'' \Delta\omega}{1 + (T_d'' \Delta\omega)^2} * \sin^2 \delta + \frac{X_q' - X_q''}{\left(X + X_q'\right)^2} * \frac{X_q'}{X_q''} * \frac{T_q'' \Delta\omega}{1 + \left(T_q'' \Delta\omega\right)^2} * \cos^2 \delta \right] \quad (3.12)$$

Where besides the above notation:

X_x‘	Transient d- or q-axis reactance
X_x’’	Sub transient d- or q-axis reactance
T_x’	Transient short circuit time constant in d- or q-axis
T_x’’	Sub transient short circuit time constant in d- or q-axis
Δω	Speed deviation, $\Delta\omega = \frac{d\delta}{dt}$

As can be seen in the next chapter damping power is not included in the SimPowerSystems™ permanent magnet machine model, but is included in the load model. The damping power will improve the ability of the machine to reach synchronism during starting. Therefor the simulation base cases represent a worse case then the real situation. According to Pyrönen et. al. [10] damping in PMSM’s may be achieved by placing aluminum or copper plates on top of the magnets. The amount of torque produced depends on the reactance/resistance ratio for the damper windings, or the equivalent for a solid steel core. This ratio may be modified in the design process of the machine. Thicker aluminum or copper plates gives winder air gap, and may effect the electromagnetic torque produced.

3.5.3 Saturation

Machine saturation may occur if voltage/frequency ratio is higher at the cable end. Because of the voltage drop in the cable it is assumed that this ratio is lower then or equal to rated such that saturation in machine may safely be neglected.

3.5.4 Simulink model

Two main aspects are important when the electrical system load is modeled.

1. Electrical system
   a. Production of electromagnetic torque dependent on internal voltage
2. Mechanical load torque
   a. Stiction torque at stand still
   b. Speed dependent torque

The electrical system of the machine is modeled in the d- q-reference frame using a predefined SimPowerSystems™ permanent machine block. See Figure 22.

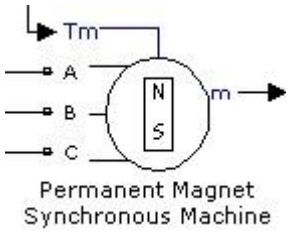

Figure 22 - Permanent magnet SM SimPowerSystems block

The equations of the electrical machine are (3.13)(3.14)(3.15) [29]:

$$\frac{d}{dt}i_d = \frac{1}{L_d}v_d - \frac{R}{L_d}i_d + \frac{L_q}{L_d}p\omega_r i_q \tag{3.13}$$

$$\frac{d}{dt}i_q = \frac{1}{L_q}v_q - \frac{R}{L_q}i_q - \frac{L_d}{L_q}p\omega_r i_d - \frac{\lambda p\omega_r}{L_q} \tag{3.14}$$

$$T_{em} = 1{,}5 * p * \left[\lambda i_q + \left(L_d - L_q\right)i_d i_q\right] \tag{3.15}$$

Where:

i_d	d-axis current
i_q	q-axis current
v_d	d-axis voltage
v_q	q-axis voltage
R	Stator resistance
L_d	d-axis inductance
L_q	q-axis inductance
ω_r	Rotor speed
λ	Amplitude of flux induced in stator phase by the rotor
p	Number of pole pairs
T_{em}	Electromagnetic torque

In cases studied where rotor is locked the q-axis current becomes an alternating current such that also electromagnetic torque shown in the equation above fluctuates. This corresponds to theory presented e.g. by Machowski [17] where torque is a sinusoidal function of power angle.

d- and q- axis voltages are given by the phase voltages on the motor terminals. Then currents are calculated with an appropriate solver in Matlab. Electromagnetic torque is calculated and combined with the load torque to obtain the machine speed by the equation (3.16):

$$\frac{d\omega_r}{dt} = \frac{1}{J_{tot}}\left[T_{em} - T_L(\omega) - F * \omega\right] \tag{3.16}$$

Where:

J_{tot}	Inertia of load and machine
ω	Rotor speed
$T_L(\omega)$	Load torque as function of rotor speed
F	Friction factor. Friction assumed to increase linear with speed

Defining the load torque as a function of speed is important. The torque at zero speed is typical 30 % of rated [8]. When the machine starts to move the torque drops significantly, and then increase as a function of speed defined by the type of load [8]. The system must produce sufficient torque to overcome this torque even at low frequency.

3.5.5 The chosen machine

In this work a round rotor machine with the parameters shown in Table 5 is used.

Table 5 - Motor data [30]

Nominal shaft power	P_N	[kW]	2800
Nominal voltage	U_N	[V]	6000
Power factor	PF		0.836
Efficiency	η		0.924
Nominal frequency	f_N	[Hz]	66.67
Induced flux by PM in rotor	ψ	[Wb]	10.4
Nominal apparent power	S_N	[kVA]	3624.8
Nominal current	I_N	[A]	348.8
Nominal speed	ω_N	[rad/sec]	418.9
Nominal torque	T_N	[Nm]	6684.5
Nominal impedance	Z_N	[ohm]	9.93
Stator resistance	R_S	[pu]	0.00585
Stator inductance	L_S	[pu]	0.61872
Stator resistance	R_S	[ohm]	0.0581
Stator inductance	L_S	[H]	0.0147

There is no difference in d- and q- axis inductance for this machine. Hence the rotor is magnetically round as previously discussed. Reluctance torque in this machine is therefor zero.

3.6 Mechanical load model

3.6.1 Mechanical torque and start sequence

The load usually requires a torque in some way proportional to rotor speed [31]. As mentioned there is also a stiction torque that must be overcome to get the machine from standstill. The load model developed in SimPowerSystems™ therefor has two sequences:

1. Standstill. The electromagnetic torque, T_{em}, must exceed some predefined threshold before the rotor starts to accelerate.
2. Acceleration and steady state. The load torque is proportional to rotor speed to some power defined by the type of load [31].

The calculated load torque is an input to the model of the permanent magnet machine. See Figure 23.

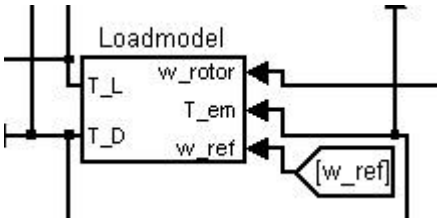

Figure 23 - Load model block as it appears in SIMULINK. Input: Rotor speed and electromagnetic torque. Output: Load torque

The block calculates the term T_L (3) and T_D (5) in the mechanical equation (3.17):

$$\overset{(1)}{T_{em}} = \overset{(2)}{J_{tot}\frac{d\omega}{dt}} + \overset{(3)}{T_L} + \overset{(4)}{F * \omega} + \overset{(5)}{T_D} \qquad (3.17)$$

Where:

(1) Electromagnetic torque. The driving force of the motor
(2) Torque needed to accelerate or decelerate the rotor
(3) Load torque defined by the type of load the motor drives. Also used to account for the higher torque during the first few cycles of starting due to stiction.
(4) Friction torque during normal operation. Included in standard machine model
(5) Damping torque

In Appendix F the implementation of the load model is shown in detail. The modeling of T_L is based on assumptions on how the mechanical system behaves during start. From standstill the bearing lubrication is assumed to be very viscous, and need some time to heat up.

3.6.2 Including damping torque in load model

The damping torque may be expressed mathematically for small frequency deviations as (3.18) [17]:

$$T_D = \frac{\omega_{ref} - \omega_{mech}}{\omega_{ref}} * D = \Delta\omega * D \quad segment\ (1) \qquad (3.18)$$

Damping is not included in the SimPowerSystem machine model for permanent magnet synchronous machine [29]. The torque effect is therefor included in the mechanical load model described above. In the real case the synchronous reactance change when rotor speed deviates from electrical frequency. With the chosen model this effect is not included. Therefor the real machine reactance in

the transient state is smaller then the reactance in these simulations. The equation describing torque is only valid for a small frequency deviation from rated as can be seen in typical torque speed curves for induction machines [7]. Using a low start frequency ensures that the speed deviation is limited at starting.

3.6.3 Example

The load model is constructed to take negative starting into account. That is if the rotor angle is in front of the initial stator flux linkage angle. Then the torque would be negative, and the rotor pulled in opposite direction. In Figure 24 an example of negative pullout is shown. As long as the speed is negative the load torque opposes this movement before it changes sign when the rotor speed becomes positive.

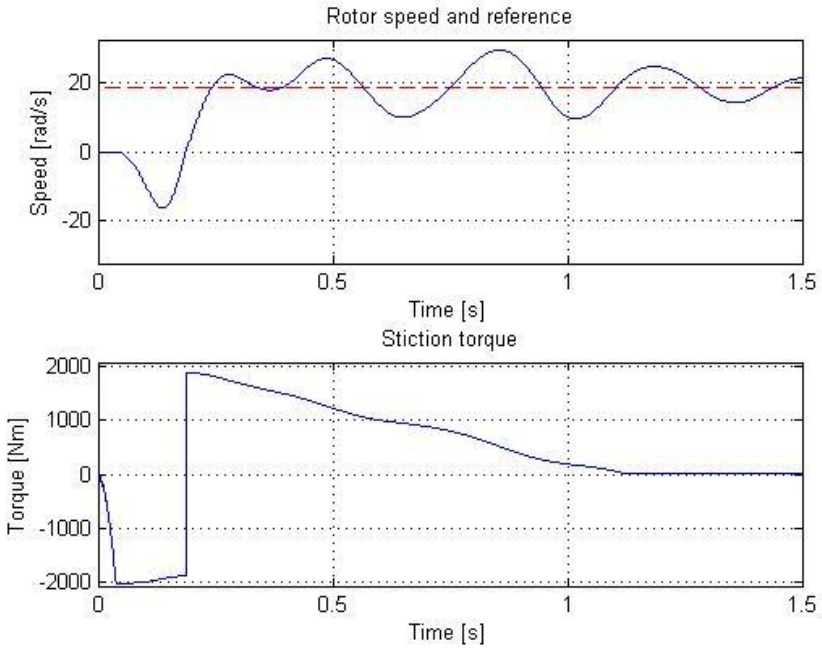

Figure 24 - Rotor speed and T_{LOAD} during initial synchronization. Typical sequence.

Above it can be seen that the friction torque due to viscous oil drops to zero as it is argued for earlier in this chapter. Including some amount of damping may prevent oscillations. This is covered in simulations. Note that torque shown Figure 24 does not include the terms (2), (4) and (5) in equation (3.17).

With the parameters shown in Appendix F the torque for each term in (3.17) at starting- and steady state frequency would be:

Table 6 - Torque values before and after synchronization. f_{rated} = 66.67 Hz. Rotor initially locked.

Initially (ω_{rotor} = 0)		**When synchronized (ω_{rotor} = 2*π*f_{start})**		
f_{start} [Hz]	3	**f_{start} [Hz]**	3	66.67
(1) [Nm]	0*	**(1) [Nm]**	32	6685
(2) [Nm]	0	**(2) [Nm]**	0	0
(3) [Nm]	T_{EM}+T_D*	**(3) [Nm]**	13	6266
(4) [Nm]	0	**(4) [Nm]**	19	419
(5) [Nm]	-T_D**	**(5) [Nm]**	0	0

***The rotor is locked until $T_{EM}+T_D>T_{STICTION}$ = 0.3*T_{RATED}(Typically) ≈ 2000 Nm**
****Damping is present from $t=0^+$**

The table shows that very high torque is needed when the rotor is locked compared to when it is synchronized. This illustrates one of the major challenges with a long step out system including magnetic couplings e.g. transformers and motors. Figure 24 also shows oscillations in rotor speed which means that the torque from the second term in equation (3.17) may be significant.

Voltage drop in the cable at low frequency makes it difficult to achieve the high torque needed to overcome stiction, and to synchronize the rotor. If starting is successful the torque demand drops dramatically after the first few mechanical revolutions.

3.6.4 Load data

The load data used in this work is given in Table 7.

Table 7 - Load data [30]

Pump inertia	J_P	[kg*m^2]	7.37
Machine inertia	J_M	[kg*m^2]	11.51
Total inertia	J_{TOT}	[kg*m^2]	18.88
Load exponent		[]	2
Nominal pump torque	T_P	[Nm]	6685
Nominal pump speed	f_N	[Hz]	66.67
Break away/stiction torque	$T_{stiction}$	[Nm]	*

***A range of stiction torques is investigated in simulations**

These values are inserted into the configuration script used to initiate the SimPowerSystem™ simulations. See Appendix E.

3.7 Power system characteristics

The power system seen by the source depends on the relationship between cable and transformer series inductance, and parallel capacitance of the cable. Impedances of cable and transformers as function of length and frequency have been calculated in Appendix B.

Table 8 - Cable/Transformer series reactance compared to cable shunt reactance

Length	Frequency [Hz]	Series reactance	Shunt reactance	Series resistance
10	3	0.83	39008.56	2.14*
	66.67	18.37	1755.30	2.14
50	3	1.39	7801.71	10.70*
	66.67	30.87	351.06	10.70

***assuming unchanged resistance at low frequency.**

Appendix A1, A2 and A3 presents power flow calculations for the system at 3 Hz starting frequency when rotor is locked, and for steady state 66.67 Hz with running rotor. The results for currents, voltages and power are shown in Table 9 and Table 10. Steady state power flow results are also used to adjust topside transformer winding ratio as cable length is increased.

Table 9 - Locked rotor starting frequency power flow. 10 km.

f = 3 Hz		Value	Angle [degrees]
Source voltage	[$V_{ph\text{-}ph,RMS}$]	246.24	-29.68
Source current	[A]	550.52	-78.15
Machine voltage	[$V_{ph\text{-}ph,RMS}$]	155.88	0
Machine current	[A]	550.58	-78.16
Apparent source power	[kVA]	406.67	-
Active source power	[kW]	269.59	-
Reactive source power	[kVAr]	304.47	-
Apparent machine power	[kVA]	257.47	-
Active machine power	[kW]	52.84	-
Reactive machine power	[kVAr]	251.99	-

Table 10 – Results for rated conditions. 10 km.

f = 66.67 Hz		Value	Angle [degrees]
Source voltage	[$V_{ph\text{-}ph,RMS}$]	6544.4	5.03
Source current	[A]	333.0	-29.41
Machine voltage	[$V_{ph\text{-}ph,RMS}$]	6000.0	0
Machine current	[A]	348.8	-33.28
Apparent source power	[kVA]	3775.0	-
Active source power	[kW]	3113.6	-
Reactive source power	[kVAr]	2134.6	-
Apparent machine power	[kVA]	3624.8	-
Active machine power	[kW]	3030.4	-
Reactive machine power	[kVAr]	1989.1	-

The above calculated results are also verified by the SimPowerSystem-model. In the model the motor voltage required is chosen, and the source voltage is calculated. Thus one may see what the source voltage must be to achieve high enough motor voltage to produce sufficient torque.

Table 9 and Table 10 shows that cable capacitance may be neglected at low frequency, as also may be seen from Table 8. This is because charging current is small at low frequencies such that machine and source current are almost identical.

The power flow results are also shown in Figure 25 and Figure 26. These figures are included to show the big difference in voltage drop between the locked rotor case and steady state.

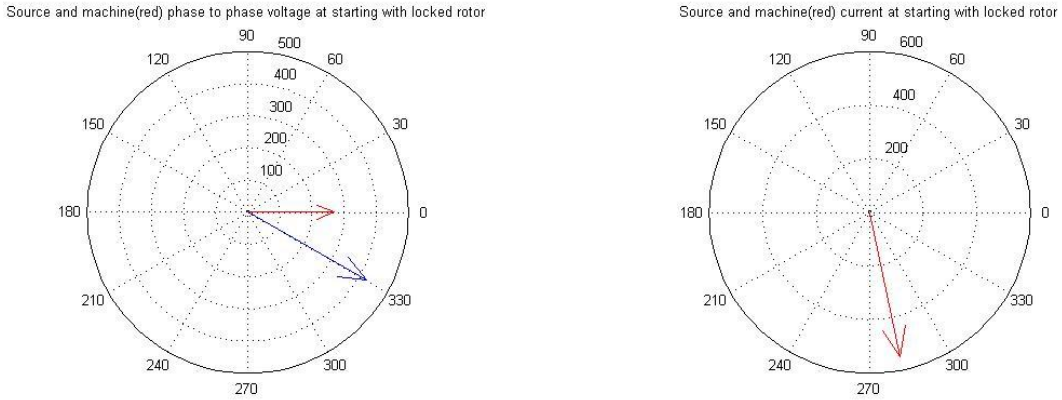

Figure 25 – Left: Machine (red) and source (blue) voltage phasors. Right: Machine (red) and source (blue) current phasors. 3 Hz, Locked rotor, 10 km cable.

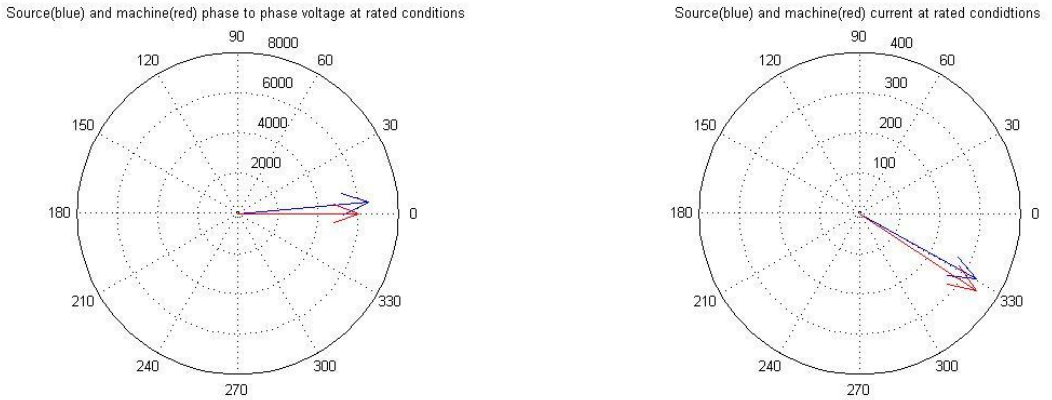

Figure 26 - Left: Machine (red) and source (blue) voltage phasors. Right: Machine (red) and source (blue) current phasors. 66.67 Hz, running rotor, 10 km cable.

The very large source voltage required at starting is not acceptable when transformer iron saturation is included in the model. These unacceptable voltage conditions are further illustrated if the cable is extended to 50 km as shown in the figure below.

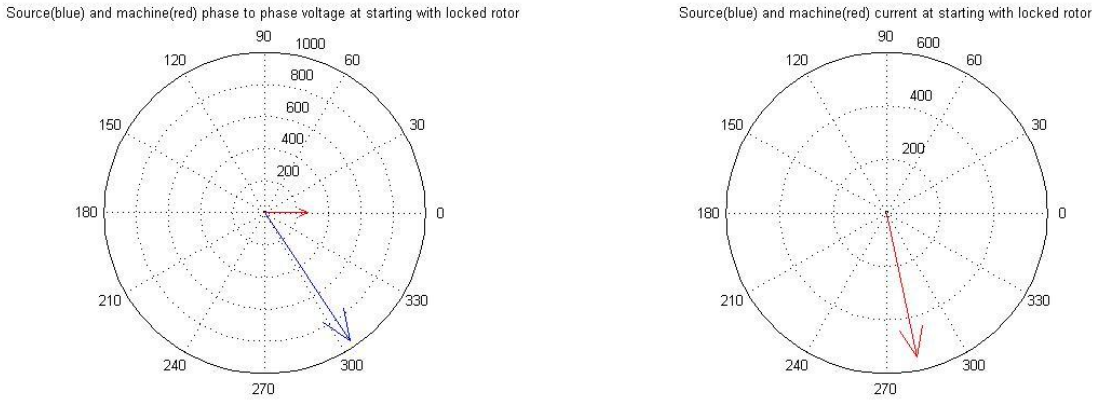

Figure 27 – Left: Machine (red) and source (blue) voltage phasors. Right: Machine (red) and source (blue) current phasors. 3 Hz, Locked rotor, 50 km cable.

These results indicate that the voltage on the machine terminals should be minimized to keep the source voltage within the boundaries set by saturation in transformer. In other words: The limit on source voltage requires that the machine is started at lower voltage then rated.

4 SIMULATIONS

4.1 Introduction

The developed system and SimPowerSystem blocks are to be used to simulate the start of a permanent magnet synchronous machine powered by an adjustable frequency AC source with a single, long, 3-phase cable between source and load. The expected challenges with these solutions have been presented and discussed in previous chapters. In the following subchapters the reference system is modified one part at a time to test how different proposed solutions effect starting of the machine.

Simulations are divided into base cases, source modification, cable modification and machine modifications. The base cases are intended to be the reference for the other tests. Two cable lengths are used, 10 km and 50 km, which are considered to represent normal and long step out umbilicals. For the other cases only 50 km cable is used as it is considered most relevant in this work.

In source modifications the voltage to frequency ratio is increased above rated. The machine torque problem at starting is mainly due to high voltage drop in the cable, and increasing source voltage thus seems to be a potential solution. Transformer saturation is the main problem with this option, and 15 % and 30 % higher ratio is to be tested. Custom saturation curves used in this case gives results that may not be accurate for general purposes. However they may indicate how voltage boost may affect a step out system with transformers. Voltage boost generally increase magnetizing current, and may not give the desired secondary side voltage [9]. This is discussed in more detail in transformer chapter.

Operating with a cable with lower resistance is also tested using 80 % and 90 % of the base case series resistance. This effectively means to reduce the cable length seen by the source to increase machine terminal voltage and machine current. Simulations of these cases illuminate the benefit in choosing low resistance cables compared to the other solutions. Lower resistance cable is one solution mentioned in recent literature for step out systems using asynchronous machine [11]. Therefor this is tested here. Decrease in resistance compared to rated conditions because of less skin effect is not considered, but may improve start conditions.

Damping torque ensures that a net positive electromagnetic torque is produced in the machine. According to Chapman [7] an induction machine, which work in the same way as damper windings or eddy currents in steel core [7], may have typically a pullout torque equal to 200 % of rated torque. This is with reference to direct on line starting which in this case means 66,67 Hz slip. Using the formula from Machowski [17] shown in machine chapter and implemented in SimPowerSystems™ to find an approximate damping constant gives: D = 31,92 which means a damping torque of 600 Nm at starting frequency.

The main assumption here is that rated torque of the damper windings is the same as the synchronous machine, and that the damping torque increase linearly with a slip as high as the rated frequency. It is not realistic that the damper windings would be able to produce the same torque as the synchronous motor for a direct online starting. This indicates that the damping torque also at starting frequency should be smaller then indicated above. Consulting relevant sources as Chapman [7] and Machowski [17] shows also that the second of the assumptions is not correct, but also that induction machines usually have a peak torque at lower slip then maximum. This means that the

damping torque may be higher then what is calculated above. These two facts may outweigh each other. Therefor a damping torque of 500 Nm at starting frequency is assumed realistic for normal steel rotor machines. Higher damping torque is also tested to indicate if specially designed rotors could be relevant to consider.

Table 11 - Damping torque at starting frequency tested

	Damping torque [Nm]
D_1	500
D_2	1000
D_3	1500

The main results of the simulations are presented in the following chapters before each of them are compared in a summary and discussion chapter.

4.2 Base cases

4.2.1 Base case 10 km and 50 km

These results are obtained with the system parameters from power system description and 6 kV source voltage. Results presented graphically here are the ones thought to be of highest relevance to understand and work with the system. Other results may be found in appendix D.

Steady state analysis of both cable lengths for locked rotor, and steady state case is performed. Here voltages and currents are presented in phasor diagrams. Apparent, active and reactive power are also presented in the base case to illuminate the difference between starting conditions and steady state. Thereafter the SimPowerSystems™ model developed is used to simulate a motor start. In the presentation of this base case the rotor is started first with no stiction torque, and then with a stiction torque thought to be representative [8]. The motor start is performed for both the ideal case when rotor is aligned to the stator field flux, and the worst case scenario when rotor is displaced by 180 degrees in relation to stator field at starting.

The below cases for 10 km and 50 km cable is studied without any modification in components or control.

4.2.1.1 10 km

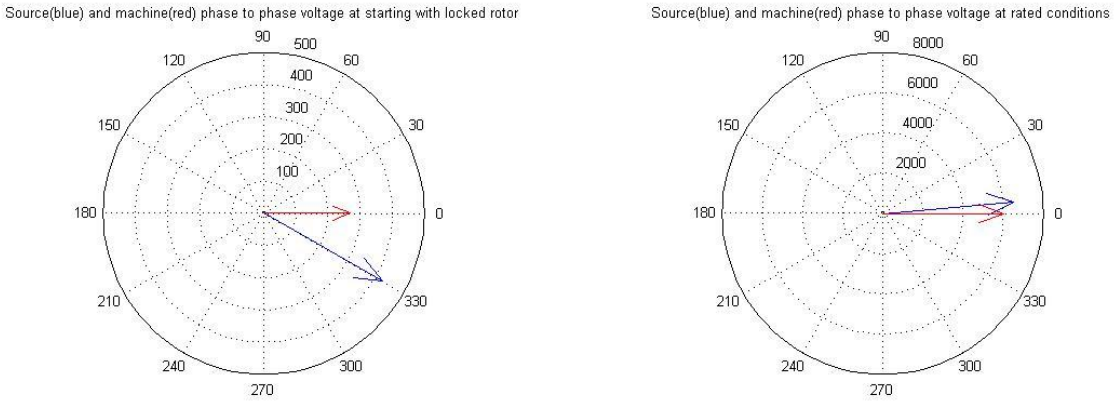

Figure 28 – VOLTAGES 10 KM CABLE. Left: 3 Hz, locked rotor. Right: 66.67 Hz, running rotor. Machine (red), Source (blue)

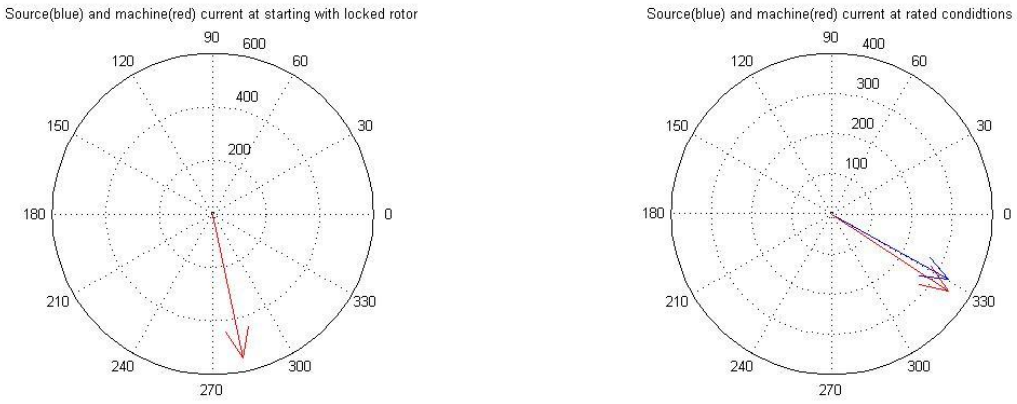

Figure 29 – CURRENTS 10 KM CABLE. Left: 3 Hz, locked rotor. Right: 66.67 Hz, running rotor. Machine (red), Source (blue)

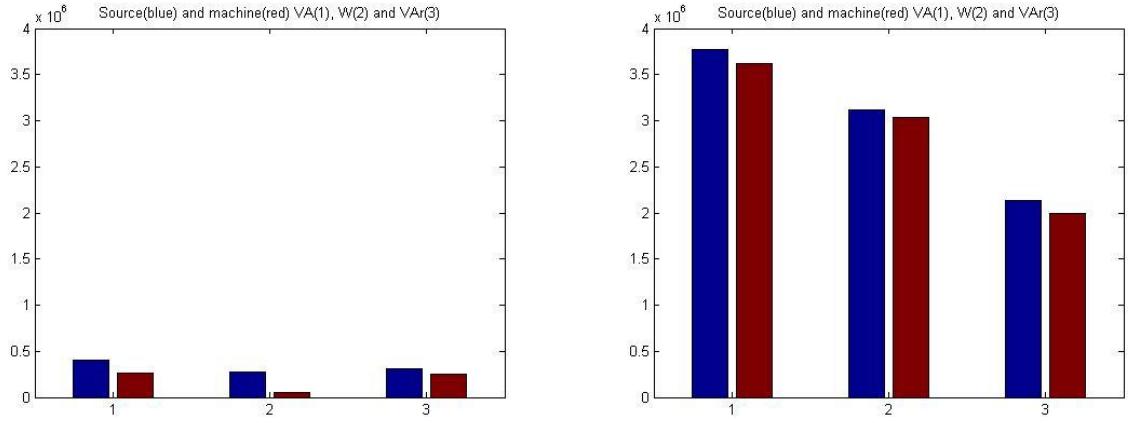

Figure 30 – POWER 10 KM CABLE. Left: 3 Hz, locked rotor. Right: 66.67 Hz, running rotor. Machine (red), Source (blue). Apparent- (1), Real- (2) and Reactive (3) power.

In Figure 28, Figure 29 and Figure 30 steady state results are presented for locked and running rotor at starting and full speed frequency respectively. The right part of Figure 30 confirms the steady state machine characteristic given in the description. The most interesting observation is the very high voltage drop initially and that the source and machine current may be considered equal at low frequency. This is because the charging current of the cable is small for low frequencies, because the phase to ground admittance is small. Figure 31 and Figure 32 shows a motor start with and without stiction torque.

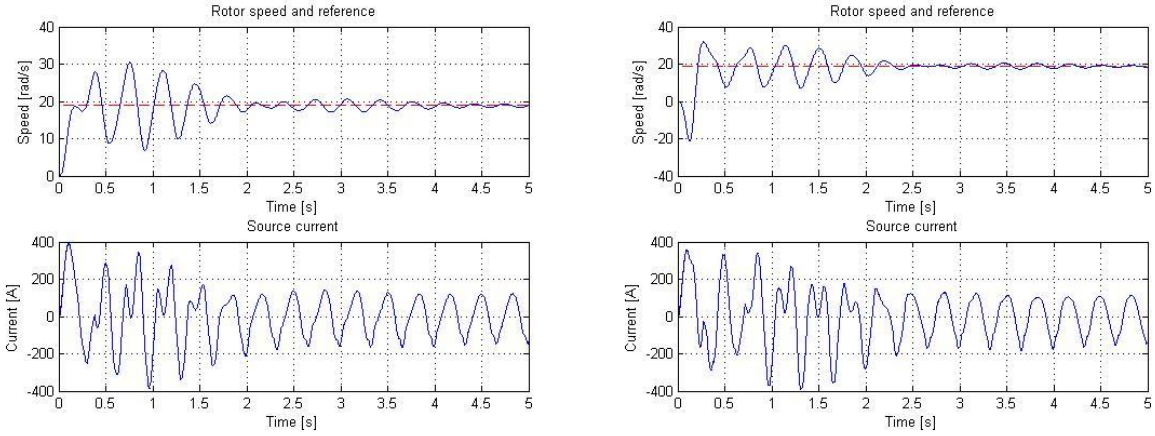

Figure 31 – SPEED AND CURRENT for 10 KM CABLE. Left: 3 Hz, zero degree initial power angle. Right: 3 Hz, 180 degree initial power angle. $T_{STICTION}$ = 0 Nm.

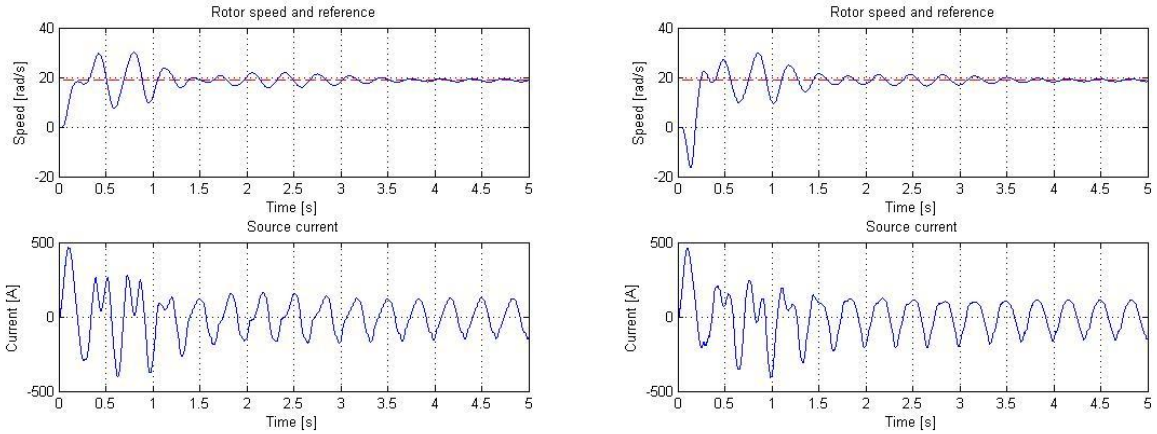

Figure 32 – SPEED AND CURRENT for 10 KM CABLE. Left: 3 Hz, zero degree initial power angle. Right: 3 Hz, 180 degree initial power angle. $T_{STICTION}$ = 2006 Nm (30 % of rated torque).

For the 10 km case the voltage drop is low, and when no stiction torque is present the machine achieves synchronous operation fast as shown in Figure 31. The base case is also investigated with a stiction torque equal to 30 % of rated machine torque with result shown in Figure 32 for zero and 180 degree initial power angle. Even with this stiction torque synchronization is fast. Increasing it further leads to several oscillations below zero speed. See Appendix D. With the oscillations follows negative induced voltage in stator turns which in turn give higher current then locked rotor. Results show that static torque holding the rotor initially impacts the dynamic behavior of the machine during starting. Rotor oscillations give increased mechanical and electrical strain on the system.

4.2.1.2 50 km

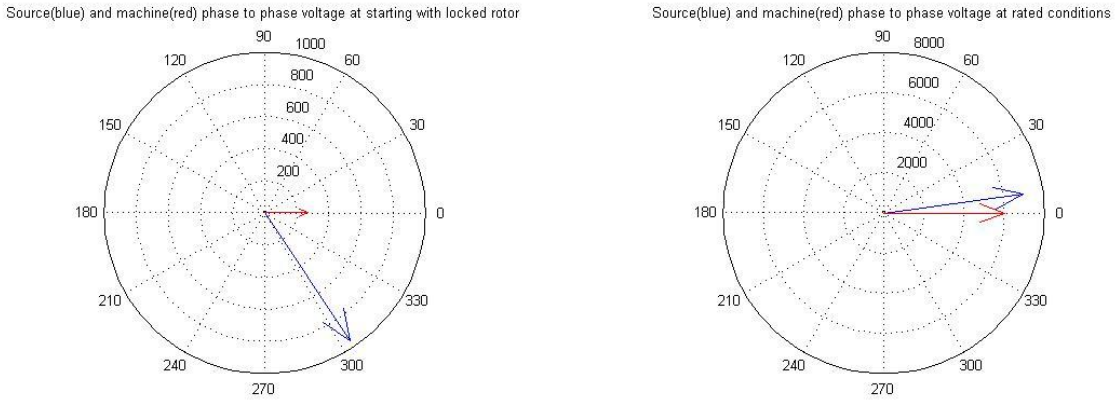

Figure 33 – VOLTAGES 50 KM CABLE. Left: 3 Hz, locked rotor. Right: 66.67 Hz, running rotor. Machine (red), Source (blue).

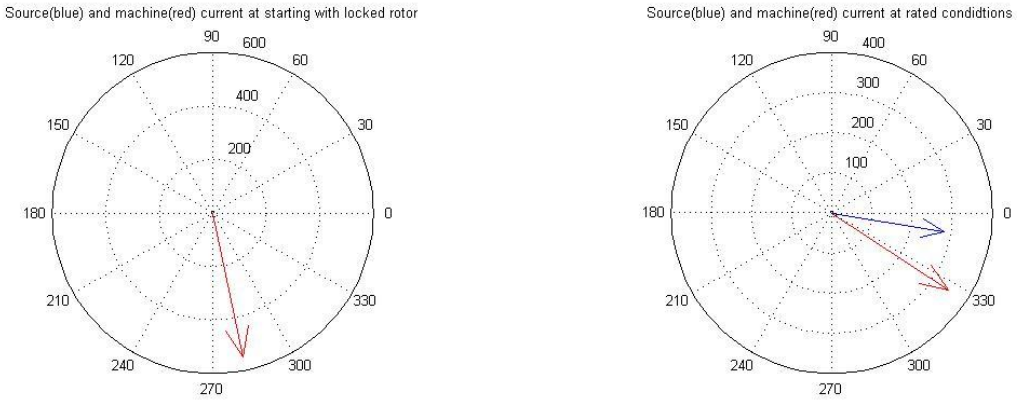

Figure 34 – CURRENTS 50 KM CABLE. Left: 3 Hz, locked rotor. Right: 66.67 Hz, running rotor. Machine (red), Source (blue).

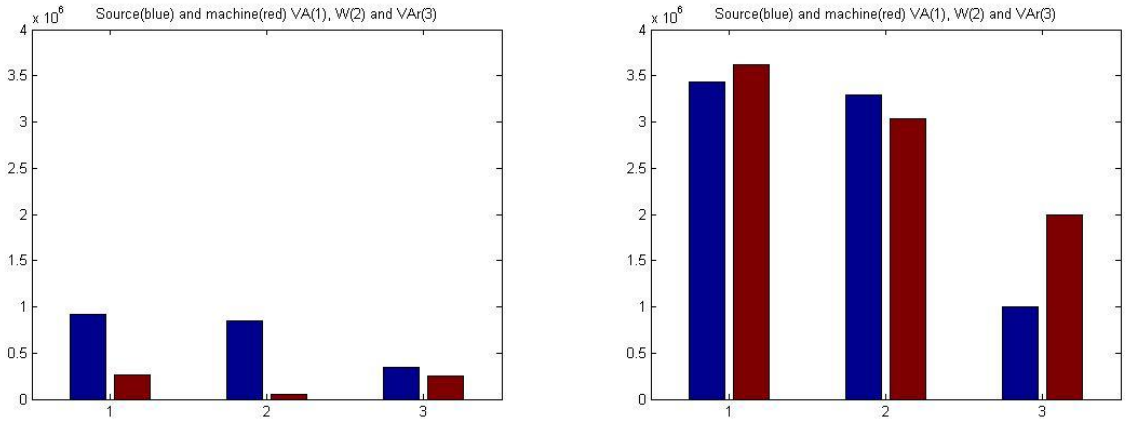

Figure 35 – POWER 50 KM CABLE. Left: 3 Hz, locked rotor. Right: 66.67 Hz, running rotor. Machine (red), Source (blue). Apparent- (1), Real- (2) and Reactive (3) power.

As for the 10 km cable Figure 33, Figure 34 and Figure 35 shows the steady state conditions in the cable. Comparing the cable length the most notable difference is that the voltage drop is higher, and that the cable capacitance is high enough to balance out the series reactance of cable and transformers in the full speed case. For starting frequency the same result as in Figure 30 may be seen, but for the longer it can be seen that the resistive power loss becomes more dominant at starting.

Note: The current is equal for the two cable lengths at starting. This is because motor terminal voltage is chosen as reference such that both cases draw the same amount of current. The difference is the voltage drop. Both source voltages require to high voltage to frequency ratio, and this situation gets worse as the length increases. In SimPowerSystems™ simulations source voltage is the reference but the ratio between source and load voltage is approximately the same.

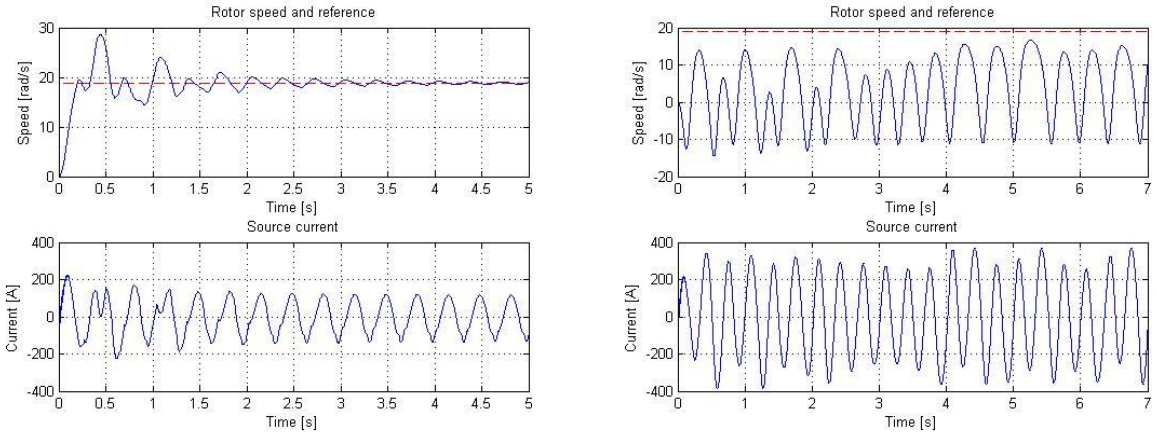

Figure 36 – SPEED AND CURRENT for 50 KM CABLE. Left: 3 Hz, zero degree initial power angle. Right: 3 Hz, 180 degree initial power angle. $T_{STICTION}$ = 0 Nm.

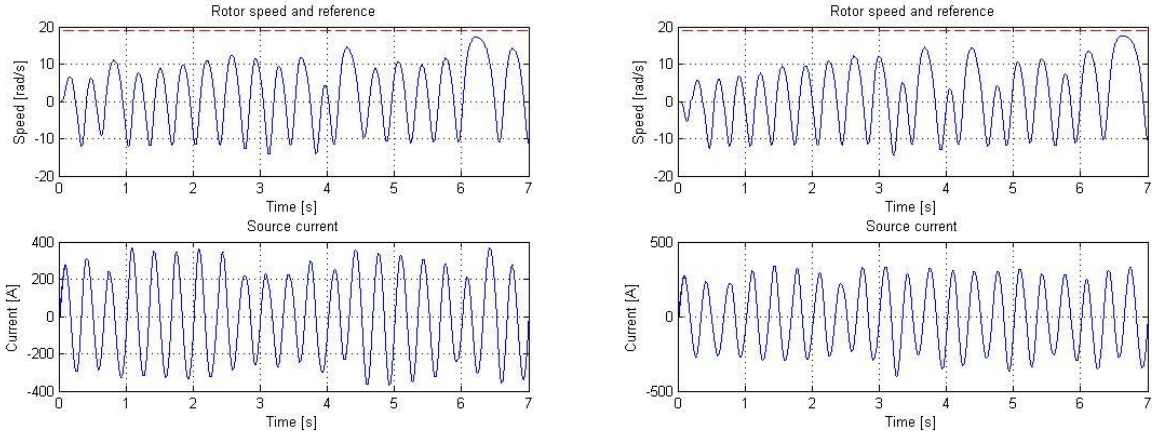

Figure 37 – SPEED AND CURRENT for 50 KM CABLE. Left: 3 Hz, zero degree initial power angle. Right: 3 Hz, 180 degree initial power angle. $T_{STICTION}$ = 2006 Nm (30 % of rated torque).

Comparing the 50 km to the 10 km base case it is evident that the ability to reach synchronization is reduced as the cable length is increased.

4.3 Voltage boost

One of the hypotheses presented in papers related to long step out systems is to oversize the topside transformer such that higher voltage to frequency may be applied during the initial low frequency sequence [1]. Voltage boost is tested without modifying the saturation curves to see how these transformers react to higher voltage to frequency ratio.

Figure 38 shows simulation results for a motor start with zero stiction torque, and 15 % voltage boost. High source current is observed as the rotor accelerates and oscillates. This is mainly due to the oscillations, not the higher source voltage. See Appendix A1. Thus the current drawn from the source is higher for the case when the rotor is running backwards. As only 15 % and 30 % voltage boost is tested here the topside transformer magnetizing current is not very high compared to rated. Testing with 100 % voltage boost and locked rotor gave 10 times the source current compared to 0 % boost. See Appendix D. Saturation to this degree draw to high current from the converter and is not studied further.

In Figure 39 a stiction torque of 2006 Nm is holding the rotor back until the electromagnetic torque exceeds this value.

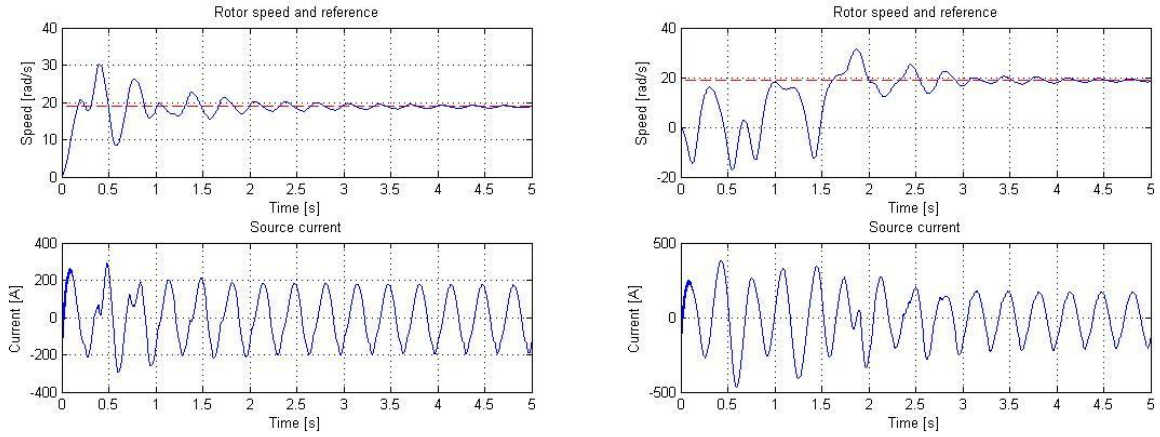

Figure 38 – SPEED AND CURRENT for 50 KM CABLE for 15 % voltage boost. Left: 3 Hz, zero degree initial power angle. Right: 3 Hz, 180 degree initial power angle. $T_{STICTION}$ = 0 Nm.

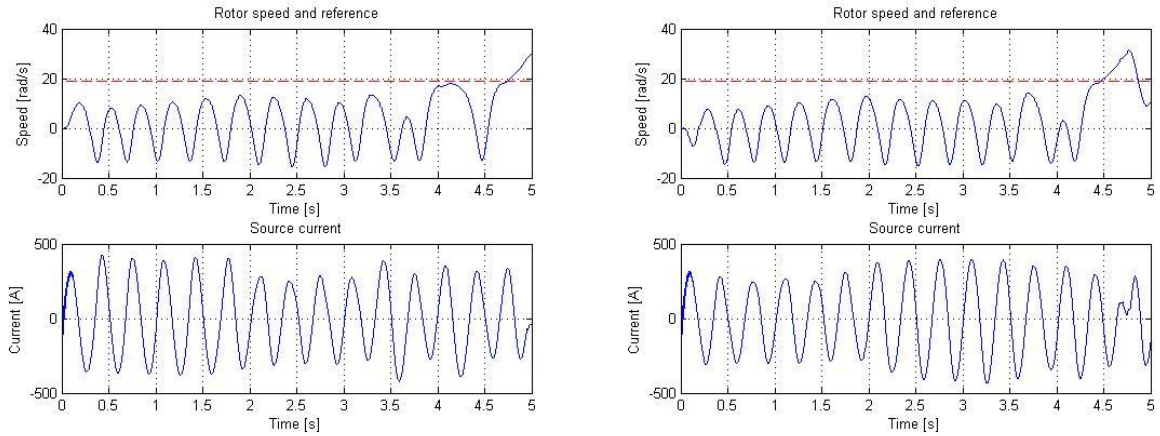

Figure 39 – SPEED AND CURRENT for 50 KM CABLE for 15 % voltage boost. Left: 3 Hz, zero degree initial power angle. Right: 3 Hz, 180 degree initial power angle. $T_{STICTION}$ = 2006 Nm (30 % of T_{RATED}).

Comparing the two above examples it can be seen that stiction torque reduce the ability of the machine to reach synchronism and gives rotor oscillations. Figure 39 shows that the machine is

synchronized to the electrical frequency at almost the same instance independently of the initial power angle. The oscillatory motion in the rotor is not dependent on starting direction, and the stiction torque is reduced at the same rate both for positive and negative speeds. This is an interesting observation because it means that one does not have to think about the initial rotor position. If the system is constructed to withstand oscillations the rotor position does not affect mechanical strain on the machinery.

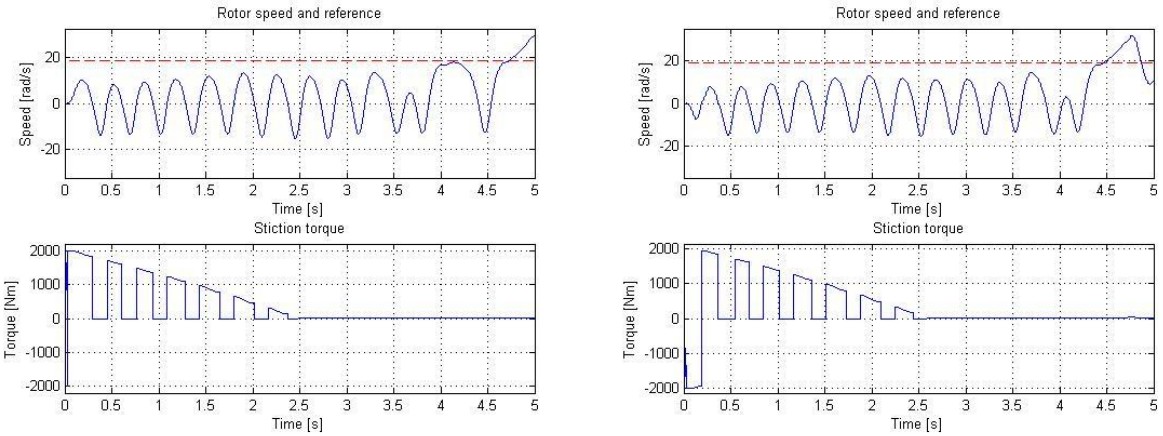

Figure 40 – TORQUE and SPEED for 50 KM CABLE for 15 % voltage boost. Left: 3 Hz, zero degree initial power angle. Right: 3 Hz, 180 degree initial power angle. $T_{STICTION}$ = 2006 Nm (30 % of T_{RATED}).

According to the load model developed in this work. The stiction torque is reduced as a function of the integral of speed. As can be seen in Figure 40 the rotor oscillation is assumed to reduce the stiction torque down to a value close to zero. For 180 degree initial power angle the machine starts in negative direction. The simulations show that when stiction torque is eliminated the rotor behaves almost like the situation in Figure 38 where no static torque is applied. However the rotor is already in motion and this motion result in that it takes a few more electrical cycles before synchronization is obtained. Source control should not increase frequency before synchronous operation is obtained. This statement supported by observations in Figure 41 where acceleration is initiated with and without synchronization.

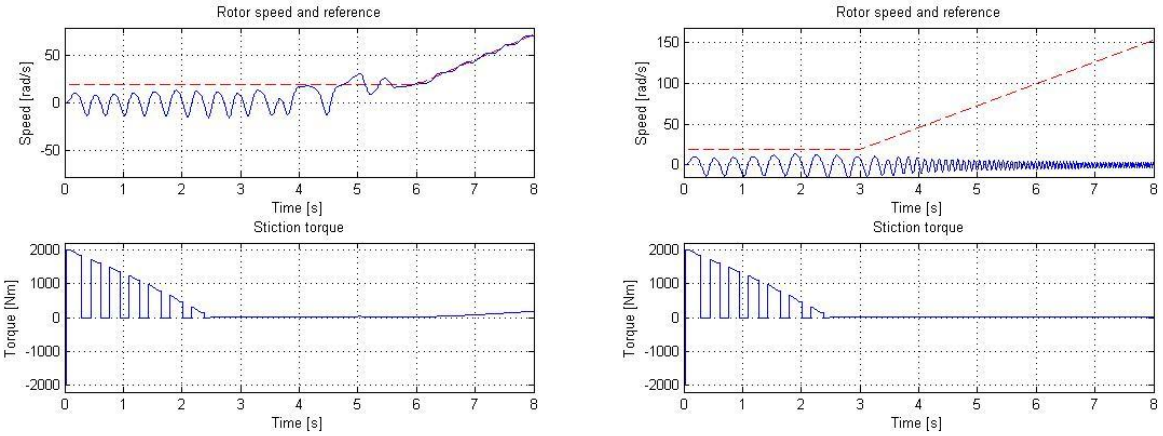

Figure 41 – TORQUE and SPEED for 50 KM CABLE for 15 % voltage boost. Left: 3 Hz, zero degree initial power angle, ramping after synchronization. Successful. Right: 3 Hz, zero degree initial power angle, frequency increase before synchronization. Unsuccessful. $T_{STICTION}$ = 2006 Nm. (30 % of T_{RATED}) Note: Extended simulation time.

The same behavior is assumed for all cases. Therefor this is not investigated further. However the measurement of current amplitude as an option to ensure that synchronous operation is achieved is discussed briefly later.

The motor start simulations where also performed with 30 % source voltage boost. As mentioned before it should be noted that the topside transformer may differ from system to system, and the results with higher voltage/frequency ratios depend strongly on the saturation curves shown in transformer chapter.

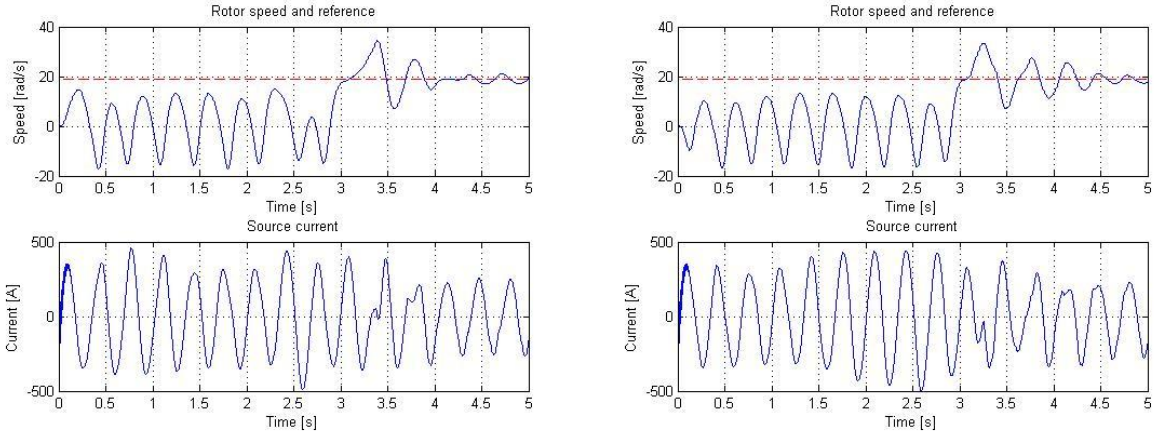

Figure 42 – SPEED AND CURRENT for 50 KM CABLE for 30 % voltage boost. Left: 3 Hz, , zero degree initial power angle. Right: 3 Hz, 180 degree initial power angle. $T_{STICTION}$ = 2006 Nm. (30 % of T_{RATED}) Note: Extended simulation time.

As for 15 % voltage boost the ability to reach synchronization improves both with and without stiction torque. Figure 42 confirms the results from before that oscillations are independent of initial power angle. Comparing 15 % and 30 % voltage boost the difference is the number of electrical cycles needed to synchronize the machine. Higher voltage gives, as expected, faster synchronization. This indicates that as long as the source can deliver the current, and the transformer iron is able to transfer the flux more voltage boost is beneficial.

The time before the rotor reach the predefined start frequency in this case is reduced by about 30 % compared to the 15 % voltage boost case. Compared to unmodified system where no synchronization is achieved the performance is very good. However the motor-pump assembly must still be able to withstand oscillations for several seconds while stiction torque is reduced.

4.4 Reduced resistance

The resistance was modified in the Matlab initializing script by multiplying the resistance per km by 0.9. Reducing the resistance by 10 % would be approximately equal to making the cable 10 % shorter. Resistance is the dominant factor at low frequency. It is therefor assumed that the series reactance is the same for both cases. In practice the inductance might be different.

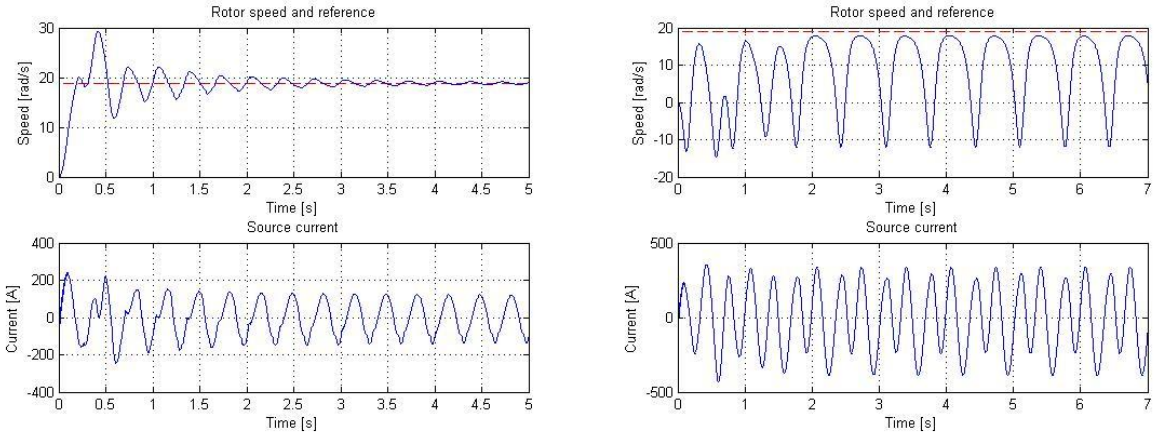

Figure 43 – SPEED AND CURRENT for 50 KM CABLE for 90 % cable resistance. Left: 3 Hz, zero degree initial power angle. Right: 3 Hz, 180 degree initial power angle. $T_{STICTION}$ = 0 Nm. Note: Extended simulation time.

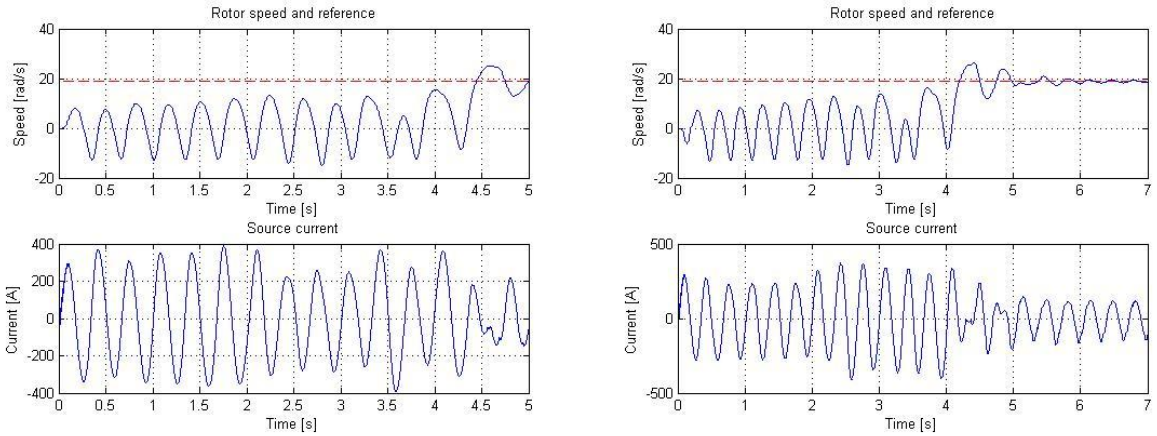

Figure 44 – SPEED AND CURRENT for 50 KM CABLE for 90 % cable resistance. Left: 3 Hz, zero degree initial power angle. Right: 3 Hz, 180 degree initial power angle. $T_{STICTION}$ = 2006 Nm (30 % of T_{RATED}). Note: Extended simulation time.

Studying and comparing the results in Figure 43 and Figure 44 it can be seen that successful synchronization is achieved when stiction torque is applied. With no stiction torque and 180 degree initial power angle the machine fails to achieve synchronous operation. This is the only exception where starting fails. For all stiction torques and initial power angle the machine reaches synchronism.

The result for zero stiction is not easy to explain. The rotor swings gets into a pattern similar to the base case where synchronism is not reached. Comparing to stiction torque the situation should be almost equal as the stiction torque is reduced to zero before the machine reach synchronism. Oscillations are different in these situations as the amplitude of speed swings increase as stiction decrease. However the results show that reducing resistance by only 10 % do not give the security of start as the previous solution where the machine started independently of initial rotor position.

The result in Figure 44 shows that the current amplitude is approximately double prior to synchronization compared to after. Monitoring this current and comparing to system models may give a very simple start success indication.

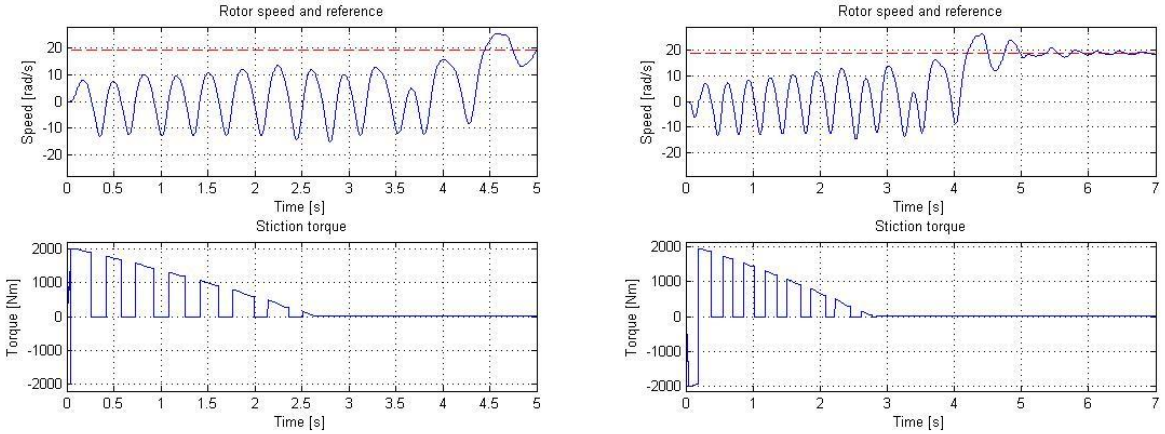

Figure 45 – TORQUE and SPEED for 50 KM CABLE for 90 % cable resistance. Left: 3 Hz, zero degree initial power angle. Right: 3 Hz, 180 degree initial power angle. $T_{STICTION}$ = 2006 Nm (30 % of T_{RATED}). Note: Extended simulation time.

Figure 45 shows stiction torque decay and a clear resemblance to other cases studied. Stiction torque goes to zero, and machine rotor reaches synchronism. This support the early indications that as long as stiction torque is overcome, and the machine start to move it is just a question of time, and that the machinery can handle the strain, before synchronous operation is achieved.

Tests have also been performed with 20 % resistance reduction for comparison. See Appendix D and simulations summary. Some improvement was achieved, but not significant.

4.5 Damping

Including damping in the model is a machine modification. Previous simulations have experimented with changing parameters in other parts of the system. The amount of damping torque present is a function of slip speed, and is easily adjustable in the initializing script. See appendix E. In this case 1000 Nm damping is present at 3 Hz rotor slip. That is: 1000 Nm net positive torque when frequency is locked. As mentioned in the introduction different damping torques are tested. All results are shown in appendix D.

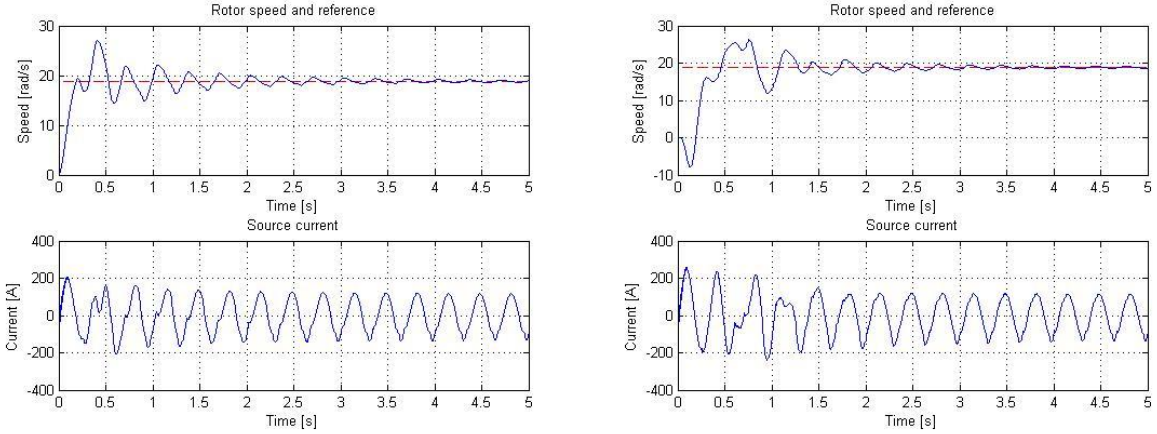

Figure 46 – SPEED AND CURRENT for 50 KM CABLE for 1000 Nm damping at 3 Hz slip. Left: 3 Hz, zero degree initial power angle. Right: 3 Hz, 180 degree initial power angle. $T_{STICTION}$ = 0 Nm.

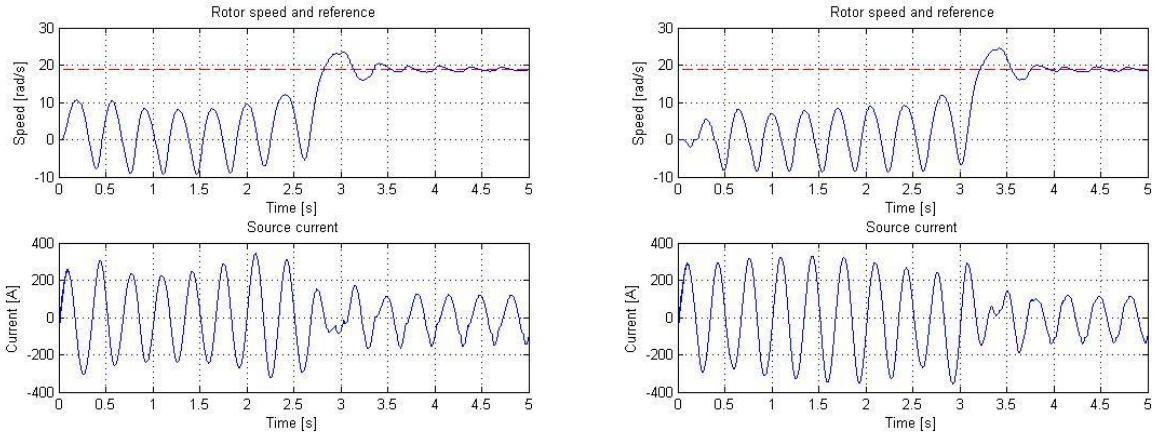

Figure 47 – SPEED AND CURRENT for 50 KM CABLE for 1000 Nm damping at 3 Hz slip. Left: 3 Hz, zero degree initial power angle. Right: 3 Hz, 180 degree initial power angle. $T_{STICTION}$ = 2006 Nm (30 % of T_{RATED}).

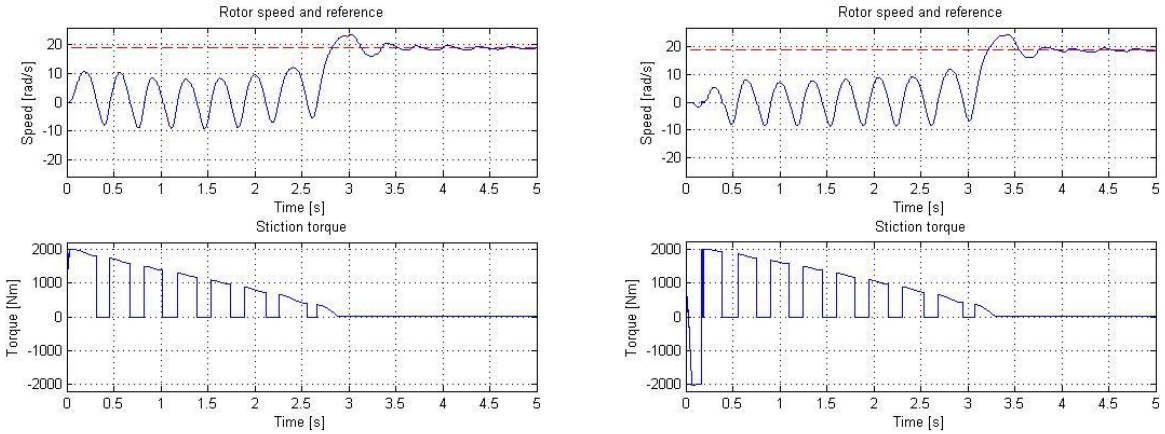

Figure 48 – TORQUE and SPEED for 50 KM CABLE for 1000 Nm damping at 3 Hz slip. Left: 3 Hz, zero degree initial power angle. Right: 3 Hz, 180 degree initial power angle. $T_{STICTION}$ = 2006 Nm (30 % of T_{RATED}).

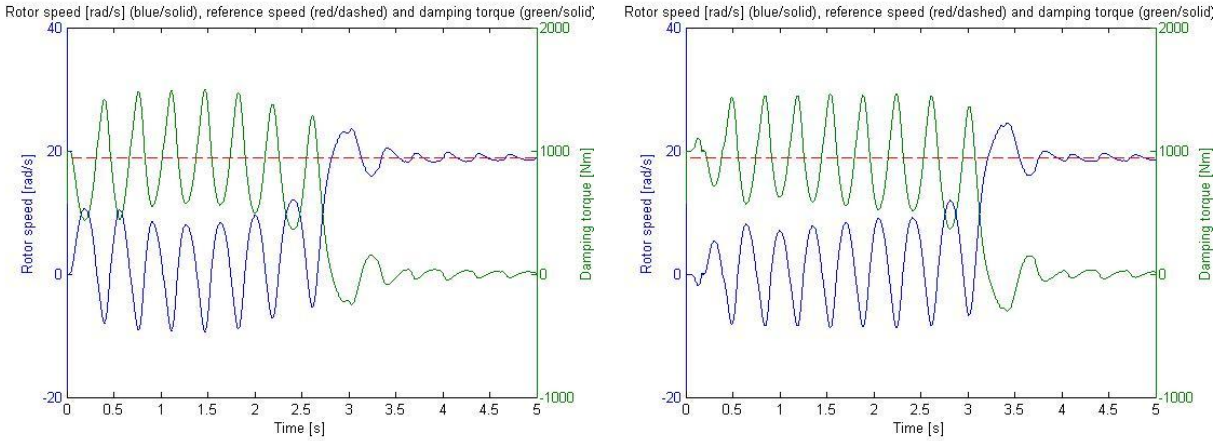

Figure 49 – DAMPING TORQUE and SPEED for 50 KM CABLE for 1000 Nm damping at 3 Hz slip. Left: 3 Hz, zero degree initial power angle. Right: 3 Hz, zero degree initial power angle. $T_{STICTION}$ = 2006 Nm (30 % of T_{RATED}).

Comparing to the base case presented earlier the performance of the machine when damping is included is remarkably better. Figure 47 and Figure 48 shows load torque, current and speed, and shows that the machine reaches synchronous speed faster then any of the previously tested cases.

Some of the results indicate that damping may prevent negative start because the net torque is always positive and ads to the stiction torque. In this way the rotor is not loosened before the machine torque is positive. However the results show that oscillations are present until the static friction is sufficiently reduced.

Figure 49 shows damping torque and speed on right and left axis respectively. The machine oscillations are damped out fast, and the additional damping torque goes to zero. A slipping synchronous rotor will still experience high mechanical forces due to oscillations. Rotor oscillations are, as long as stiction torque is present, not avoided.

If the results when 30 % voltage boost was applied is compared to the 1000 Nm damping torque one may see that the time before synchronous speed is reached is almost identical for this stiction torque magnitude. This means that if the transformer can not be oversized topside due to space requirements using a rotor type with high degree of damping included gives an equivalent start sequence. However, as can be seen in the simulations summary, time until synchronization is achieved does not follow the same pattern for the two options. To clarify this: both lower and higher

degree of damping where tested but not discussed in detail. See appendix D, or simulation summary chapter.

Comparisons of synchronization time for the different damping torques are shown Figure 50 and Figure 51.

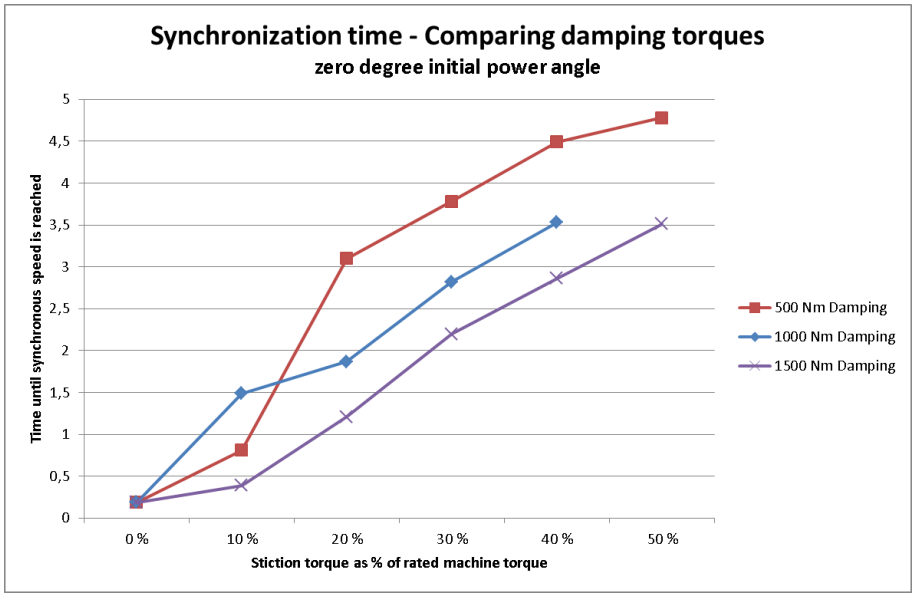

Figure 50 - Time until synchronization is reached as a function of stiction torque (% of rated machine torque) and damping torque. Zero degree initial power angle

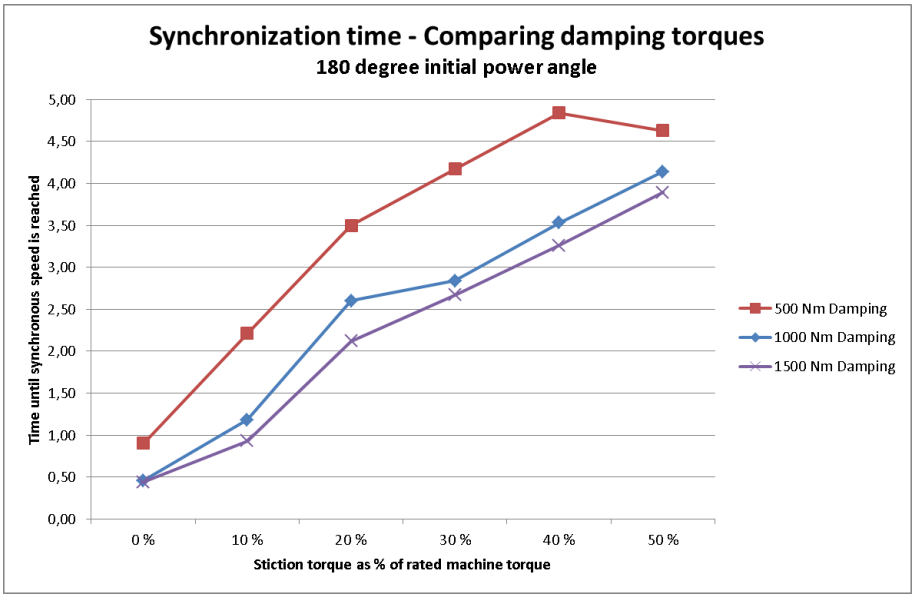

Figure 51 - Time until synchronization is reached as function of different stiction torques (% of rated machine torque) and damping torque. 180 degree initial power angle.

As discussed before the synchronization time is important because acceleration towards rated speed may not begin before the rotor is in synchronous operation with the start frequency. The results show more improvement from 500 Nm to 1000 Nm, then from 1000 Nm to 1500 Nm damping torque. All are, as mentioned, remarkably better then the base case. Damping torque is a design

parameter for a machine, and for starting purposes it should be as high as possible for fast synchronization and settling time.

4.6 Discussion and summary of results

In the above chapters different modifications of a long step out system with topside AC source and a permanent magnet synchronous machine is tested using a developed SimPowerSystems™ model. All modifications are compared to a previously presented base case. Here the different modifications are compared to summarize the system behavior for the attempts to improve starting conditions. Figure 52 and Figure 53 shows graphically how the time until synchronous speed is as a function of stiction torque. Figure 52 shows the best case scenario where the rotor flux is aligned with stator field flux initially whilst Figure 53 shows the situation with 180 degree initial displacement. The latter case must be dimensioning since one does not know the rotor position, and the motor must be able to start for all cases.

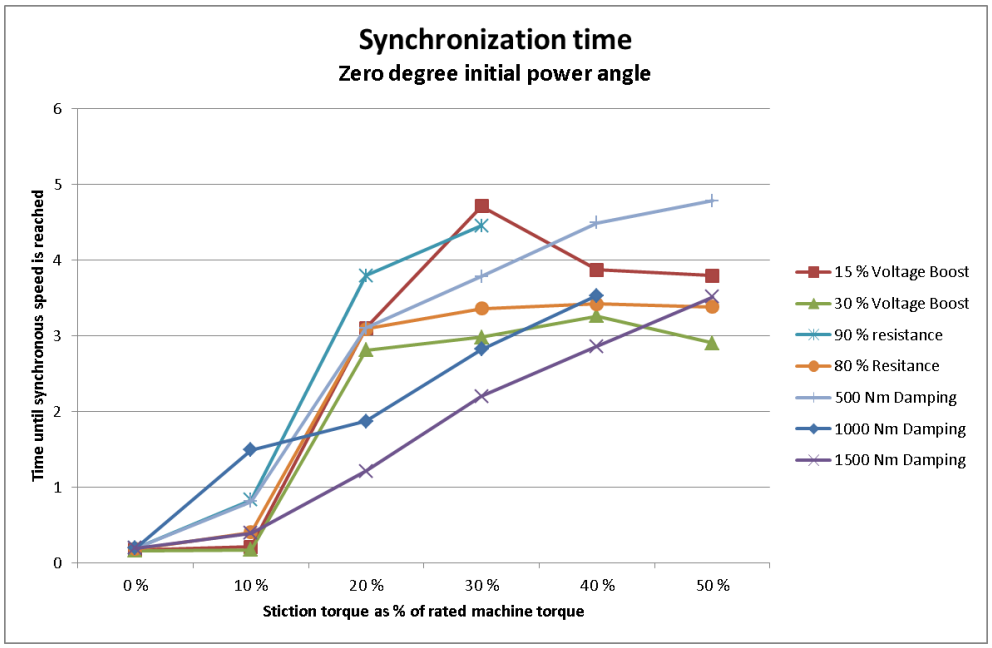

Figure 52 - Synchronization time as a function of stiction torque for zero degree initial power angle. All cases.

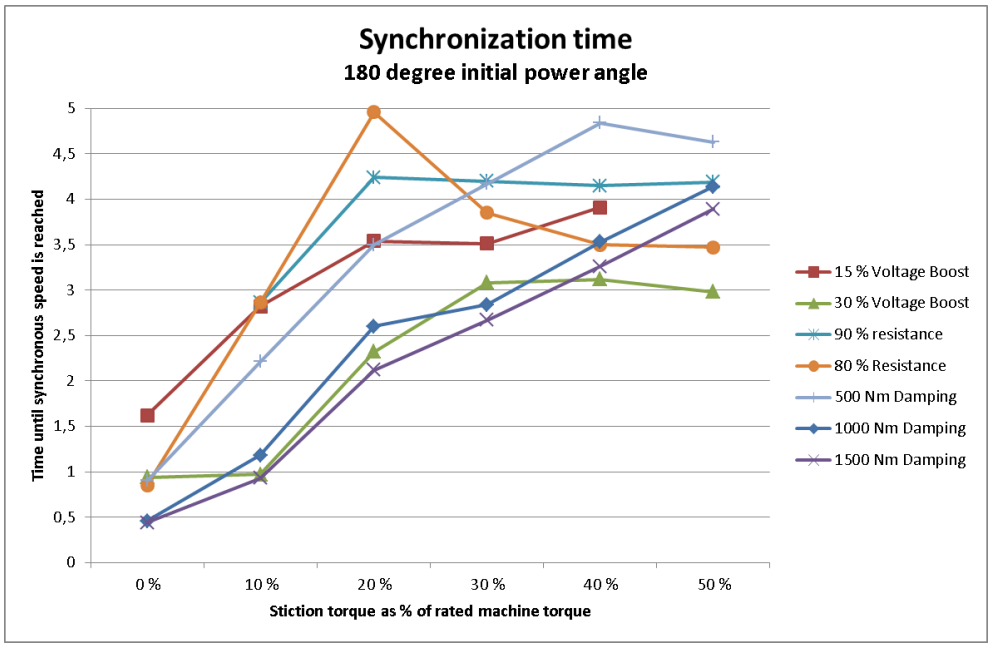

Figure 53 - Synchronization time as a function of stiction torque for 180 degree initial power angle. All cases.

Voltage boost and a high degree of damping stand out as the two methods which has the best performance over a wide variety of stiction torques. Reducing the series resistance in the cable gives improvement compared to the base case, but generally gives longer synchronization time then other alternative methods. Other methods to reduce voltage drop in the cable such as increased transfer voltage might be a better option. Both increase cable cost by increase conductor and insulation cost respectively.

As can be seen in Figure 52 and Figure 53 most cases give a successful motor start as long as maximum torque is reached and the rotor is unlocked. Then follows a sequence of oscillations around zero speed before the rotor manage to reach synchronism. The oscillations give high current due to negative induced voltage in the machine. Transformers and converter must be constructed to withstand this high current.

It is also shown that further acceleration towards full speed may not start until the rotor has reached synchronous speed. Observing the current amplitude in all tests and cases it can be seen that the current is dramatically reduced when synchronism occur. See e.g. Figure 47. This is due to the back induced emf produced by the rotor field, and may help to ensure that synchronous operation is achieved before the ramping is initiated.

5 Conclusion and recommendations for further work

A dynamic simulation model of a long step out umbilical system powered by a variable frequency drive has been developed in SIMULINK™ SimPowerSystems™. The system load is a Permanent Magnet Synchronous Machine, PMSM, and transformers are included because of long transfer distance. The adjustable frequency drive gives the possibility to use frequency reduction to synchronize the machine to the electrical frequency. Reducing the frequency require reduced voltage to avoid iron core saturation, especially in topside transformer.

At low frequency cable resistance is the dominant factor in the total impedance magnitude resulting in a high voltage drop, and low machine terminal voltage. One of the main assumptions is that the mechanical load is held back by a static torque at starting which gradually decrease as the rotor moves. This means that the machine must produce a very high torque even at low frequency and voltage such that successful start may be achieved. Voltage boost, reduced cable resistance and rotor damping have been tested to improve start conditions.

All cases shows improvement compared to the base cases, and damping and voltage boost is the modifications showing the most promising results. This is an expected result as increasing voltage directly improves machine terminal conditions, and that damping torque gives a net positive torque contribution. It was shown in the previous chapter that 30 % voltage boost gave approximately the same result in synchronization time as 1000 Nm damping torque at start frequency slip. Synchronization time is thought to be important because of mechanical strain on the system, and because further acceleration cannot be started before synchronization occur.

None of the cases tested eliminates rotor oscillations around zero speed for stiction torques around 30 % and 40 % thought representative for this application. One of the assumptions made was that both positive and negative rotor speed helps to decrease the static friction torque. The results presented before shows that the machine oscillates until the stiction torque is eliminated. Then the start sequence runs almost as if no stiction is present. The synchronization time might be extended because of oscillations. Therefor the mechanical system must be constructed to withstand rotor oscillations during starting. Another conclusion drawn from these results is that start sequence is very much independent of initial power angle. The synchronization time is very similar for both zero- and 180 degree initial power angle. See Figure 52 and Figure 53 for comparison.

The model developed in this work has the possibility to accelerate the machine up to rated speed. However the frequency dependent parameters in cable and machine have to be changed as the frequency increases. This feature in the voltage source could be exploited in future work on the subject if the above frequency variations are accounted for. Also the assumption that stiction torque is equally reduced for positive and negative speed should be tested in either a laboratory set up, or doing measurements on existing installations similar to what is presented here.

In this work no cost- or size considerations are included. On offshore installations size minimizing of equipment if often an issue because of limited space available. Such considerations are connected closely to each different project such that the tradeoff between cost and size might be difficult to put in a general context.

6 References

[1] G. Scheuer, B. Monsen, K. Rongve, T.-E. Moen, E. Virtanen og S. Ashmore, Subsea compact gas compression with high-speed VSDs and very long step-out cables, ABB, Statoil, QVARx inc., 2009.

[2] X. Liang, Influence of Subsea Cables on Offshore Power Distribution Systems, IEEE, 2009.

[3] S. Rahimi, W. Wiechowski, M. Randrup, J. Østergaard og A. H. Nielsen, Identification of Problems when Using Long High Voltage AC Cable in Transmission Systems II: Resonance and Harmonic Resonance, IEEE, 2008.

[4] L. Xiaodong, R. Laughy og J. Liu, Investigation of induction motors starting and operation with variable frequency drives, IEEE, 2007.

[5] Z. E. Al-Haiki og A. N. Shaikh-Nasser, Power Transmission to Distant Offshore Facilities, IEEE, 2011.

[6] S. Demmig, J. Andrews og R.-D. Klub, Control of Subsea Motors on Multi-km Cable Lengths by Variable Frequency Drives, IEEE, 2011.

[7] S. J. Chapman, Electric Machine Fundamentals 4th edition, 2005.

[8] R. Osman, A medium-voltage drive utilizing series-cell multilevel topology for outstanding power quality, IEEE, 1999.

[9] J. J. Winders, Power Transformers - Principles and Applications, New York - Basel: Marvel Dekker Inc., 2002.

[10] J. Pyrhonen, T. Jokinen og V. Hrabovcova, Design of Rotating Electrical Machines, Wiley, 2008.

[11] S. O. Faried og X. Liang, Subsea Cables Application in Electrical Submersible Pump Systems, IEEE, 2009.

[12] ABB, Subsea Electrification Solutions, Presentation, ABB Offshore systems AS, 2003.

[13] J. F. Gieras og M. Wing, Permanent Magnet Motor Technology - Design and Applications, Marcel Dekker, Inc., 1997.

[14] P. R. Nilssen, Verbal information.

[15] I. Siemens Energy & Automation, WCIII Product User Manual, Siemens Energy & Automation, Inc., 2007.

[16] A. McIntyre, J. Andrews, G. Davis, P. Hammond og R. Mukul, Medium Voltage Drives for Sub-Sea Application, SPE GCS: ESP Workshop. NTNU, 2002.

[17] J. Machowski, J. W. Bialek og J. R. Bumby, Power System Dynamics - Stability and Control, Wiley, 2008.

[18] Siemens, Harmonic analysis. Filters and Study of Resonance effect, Siemens, 2011.

[19] R. Råd, Converter Fed Subsea Motor Drives, Trondheim: Norges Tekniske Høgskole, 1995.

[20] H. J. H., Electric Power Transformer Engineering, CRC Press, 2004.

[21] J. J. Grainger og W. D. Stevenson Jr., Power System Analysis, McGraw-Hill, 1994.

[22] A. Nysveen, Maritime and offshore power systems, 2011.

[23] Mathworks, "Three-Phase Transformer (Two Windings)," [Online]. Available: http://www.mathworks.se/help/toolbox/physmod/powersys/ref/threephasetransformertwowindings.html. [Accessed October 2011].

[24] Mathworks, Saturable Transformer, Mathworks, 2012.

[25] FRAMO, Transformer data sheet - Eds00902_01 NORSOK, Trondheim: Siemens, 2011.

[26] Mathworks, Single phase PI section line, Mathworks inc., 2010.

[27] C.-M. Ong, Dynamic Simulation of Electric Machinery Using Matlab®/SIMULINK, Prentice Hall PTR, 1998.

[28] F. Briz og M. W. Degner, Rotor Position Estimation - A Review of High Frequency Methods, IEEE, 2011.

[29] Mathworks, Permanent Magnet Synchronous Machine, Mathworks, 2011.

[30] FMC og Siemens, MOTOR and LOAD data, FMC, 2011.

[31] N. Mohan, Electric Drives - An Intergrative Approach, MNPERE, 2003.

[32] J. Rodriguez, J.-S. Lai og F. Z. Peng, Multilevel inverters; A survey of Topologies, Controls, and Applications, IEEE Transaction on industrial electronics, Vol 49, 2002.

[33] M. Say, Performance and Design of A.C. Machines, English Language Book Society, 1948.

[34] H. K. Høidalen, Compendium in course: Overspenninger og overspenningsvern, 2010.

[35] IEEE, Recommended Practices and Requirements for Harmonic Control in Electrical Power Systems, 519-1992.

[36] J. Smith, A. Al-Mashgari og R. Slater, Operation of subsea electrical submersible pumps supplied over extended length cable systems, IEEE, 2000.

[37] N. Mohan, Advanced Electric Drives, 2001.

7 Appendix

7.1 APPENDIX A1 – POWER SYSTEM PERFORMANCE

Grainger and Stevenson [21] shows that the sending, denoted S, and receiving, denoted R, end voltage are linked by the long line equation as

$$\begin{bmatrix} \underline{V_S} \\ \underline{I_S} \end{bmatrix} = \begin{bmatrix} \cosh(\underline{\gamma} l) & \underline{Z_C}\sinh(\underline{\gamma} l) \\ \sinh(\underline{\gamma} l/\underline{Z_C}) & \cosh(\underline{\gamma} l) \end{bmatrix} \begin{bmatrix} \underline{V_R} \\ \underline{I_R} \end{bmatrix} \quad \text{(A1)}$$

where $\underline{Z_C} = \sqrt{\underline{z}/\underline{y}}$ is the characteristic impedance of the line, and $\underline{\gamma} = \sqrt{\underline{z}\underline{y}} = \alpha + j\beta$ is the propagation constant [17]. $\underline{z}$ and $\underline{y}$ is the per km series impedance and shunt admittance.

7.1.1 Power transmission

As shown in the cable chapter the cable series resistance should not be neglected at startup because the resistance is the dominant part of the cable impedance for low frequencies.

It is chosen to study the situation at starting frequency and steady state for comparison. That is 3 and 66.67 Hz. Table 12, Table 13 and Table 15 gives the basis for calculation. Cable lengths are assumed to be 10 and 50 km.

Table 12 - Transformer data used in simulations [18]. 10 km.

Transformer data		Topside step up	Subsea step down
Rated power	[MVA]	5.00	5.00
Rated frequency	[Hz]	66.67	66.67
Primary side voltage	[kV]	6	22
Secondary side voltage	[kV]	24	6
Reactance, ux	pu	0.06	0.086
Resistance, ur	pu	0.005	0.006
Magnetizing reactance	pu	"Saturation curve"	"Saturation curve"
Magnetizing resistance	pu	426	870

Table 13 Cable parameters. Nexans 22 kV umbilical (Revisited)

Resistance	R_C [ohm/km]	0.214	
Inductance	L_C [H/km]	$0.746 * 10^{-3}$	
Reactance @ 3 Hz	X_C [ohm/km]	0.014	Typical starting frequency
Reactance @ 66.67 Hz	*X_C [ohm/km]*	*0.313*	
Capacitance	C_C [F/km]	$0.136 * 10^{-6}$	

Table 14 - Motor data [30]

Nominal shaft power	P_N	[kW]	2800
Nominal voltage	U_N	[V]	6000
Power factor	PF		0.836
Efficiency	η		0.924
Nominal frequency	f_N	[Hz]	66.67
Induced flux by PM in rotor	ψ	[Wb]	10.4

Nominal apparent power	S_N	[kVA]	3624.8
Nominal current	I_N	[A]	348.8
Nominal speed	ω_N	[rad/sec]	418.9
Nominal torque	T_N	[Nm]	6684.5
Nominal impedance	Z_N	[ohm]	9.93
Stator resistance	R_S	[pu]	0.00585
Stator inductance	L_S	[pu]	0.61872
Stator resistance	R_S	[ohm]	0.0581
Stator inductance	L_S	[H]	0.0147

With the assumption that the objective is to get rated voltage/frequency ratio at machine terminals becomes $V_R = \frac{6000}{\sqrt{3}} * \frac{f}{f_{rated}}$. At 3 Hz V_R = 155.88 V phase to neutral. The back induced emf is assumed to be zero because the speed is zero when rotor is locked [17] . See Figure 54.

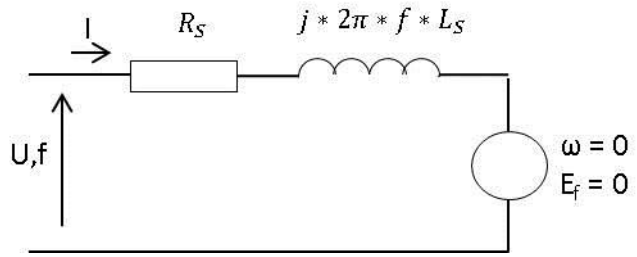

Figure 54 - Motor per phase equivalent for locked rotor

Choosing V_R as reference machine current may be calculated as (A2):

$$\mathrm{I}_{MACHINE} = \frac{V_R}{R_S + j * 2 * \pi * f * L_S} = I_R \qquad \text{(A2)}$$

Thus V_R and I_R are known, and equation (A1) may be used to calculate the necessary source voltage for the locked rotor condition. ABCD-equivalent matrices are calculated for transformers and cable. The total system may then be expressed by multiplying these matrices. The magnetizing current is neglected, and the transformers are represented by its series resistance and reactance. All values are referred to the low voltage side. A sketch of the method is shown in Figure 55.

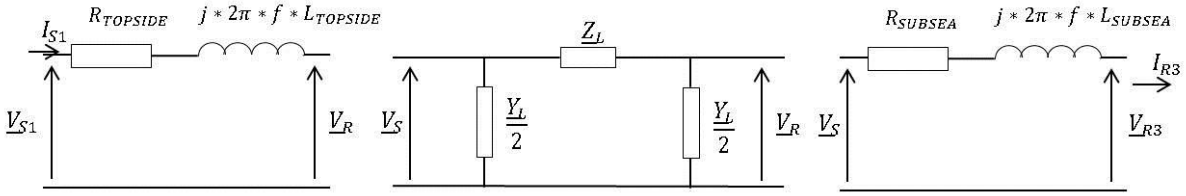

$$\begin{bmatrix} A_1 & B_1 \\ C_1 & D_1 \end{bmatrix} \qquad \begin{bmatrix} A_2 & B_2 \\ C_2 & D_2 \end{bmatrix} \qquad \begin{bmatrix} A_3 & B_3 \\ C_3 & D_3 \end{bmatrix}$$

$$\begin{bmatrix} V_{S1} \\ I_{S1} \end{bmatrix} = \begin{bmatrix} A_1 & B_1 \\ C_1 & D_1 \end{bmatrix} \begin{bmatrix} A_2 & B_2 \\ C_2 & D_2 \end{bmatrix} \begin{bmatrix} A_3 & B_3 \\ C_3 & D_3 \end{bmatrix} \begin{bmatrix} V_{R3} \\ I_{R3} \end{bmatrix}$$

Figure 55 - ABCD-system of transformers and cable

The values in Figure 55 are calculated in a dedicated MATLAB-script. Two scripts are developed. One for the initial state with locked rotor and one for the steady state case. The scripts are shown in appendix A2 and A3.

Calculation results for voltage, current and power for are shown next.

7.1.2 Results for locked rotor

Table 15 - Locked rotor at starting frequency. Power flow. 10 km.

f = 3 Hz		Value	Angle [degrees]
Source voltage	[$V_{ph\text{-}ph,RMS}$]	246.24	-29.68
Source current	[A]	550.52	-78.15
Machine voltage	[$V_{ph\text{-}ph,RMS}$]	155.88	0
Machine current	[A]	550.58	-78.16
Apparent source power	[kVA]	406.67	-
Active source power	[kW]	269.59	-
Reactive source power	[kVAr]	304.47	-
Apparent machine power	[kVA]	257.47	-
Active machine power	[kW]	52.84	-
Reactive machine power	[kVAr]	251.99	-

The results show that charging current to capacitors is very small at low frequency, and that the machine draws a substantial amount of reactive power. Voltages and currents are shown in phasor diagrams below.

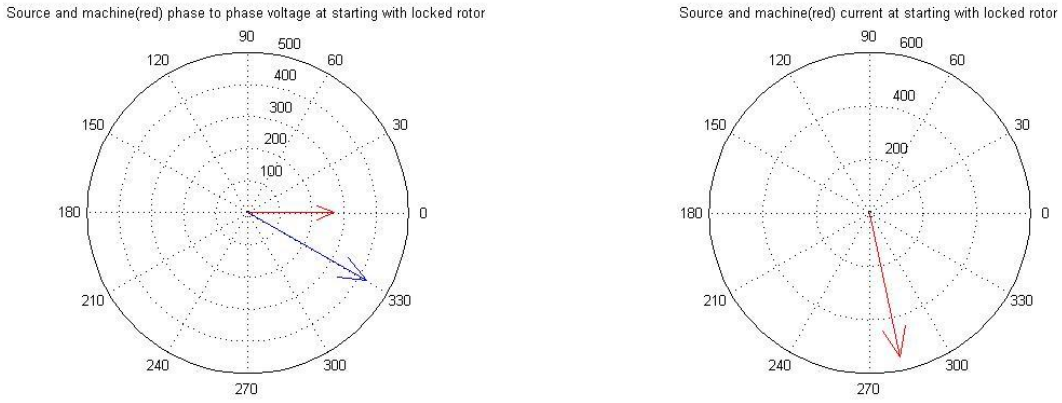

Figure 56 – 10 km cable. Left: Voltage phasors. Red phasor is the desired machine voltage. Blue is the source voltage needed to achieve this result. Right: Current phasors. Since charging current is small source and machine current is equal.

To avoid saturation in transformer iron the source voltage must be limited at low frequency. The source voltage calculated here is not acceptable.

7.1.3 Results for steady state

The steady state situation is also studied. Here it assumed that the machine draws its rated current at the rated power factor. From these assumption the source voltage, current and power is calculated. Machine voltage is the reference as in the locked rotor calculations. Results are shown in Table 16.

Table 16 – Results for rated conditions. 10 km

f = 66.67 Hz		Value	Angle [degrees]
Source voltage	[$V_{ph\text{-}ph,RMS}$]	6544.4	5.03
Source current	[A]	333.0	-29.41
Machine voltage	[$V_{ph\text{-}ph,RMS}$]	6000.0	0
Machine current	[A]	348.8	-33.28
Apparent source power	[kVA]	3775.0	-
Active source power	[kW]	3113.6	-
Reactive source power	[kVAr]	2134.6	-
Apparent machine power	[kVA]	3624.8	-
Active machine power	[kW]	3030.4	-
Reactive machine power	[kVAr]	1989.1	-

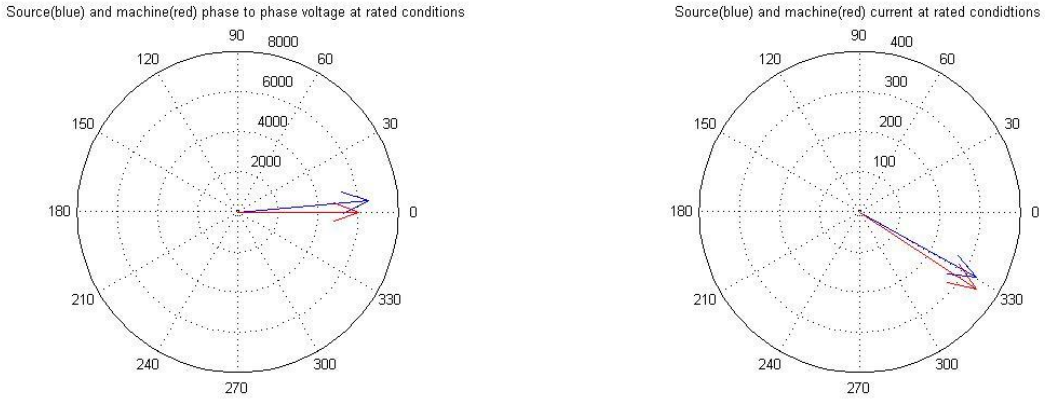

Figure 57 – 10 km cable. Left: Voltage phasors. Red phasor is the desired machine voltage. Blue is the source voltage needed to achieve this result. Right: Current phasors. Red phasor is machine current, blue phasor is source current.

Some steady state results for 50 km cable are included to argue that transformer ratio should be adjusted for this cable length.

Table 17 – Results for rated conditions 50 km

f = 66.67 Hz		Value	Angle [degrees]
Source voltage	[$V_{ph\text{-}ph,RMS}$]	6976.7	7.56
Machine voltage	[$V_{ph\text{-}ph,RMS}$]	6000.0	0

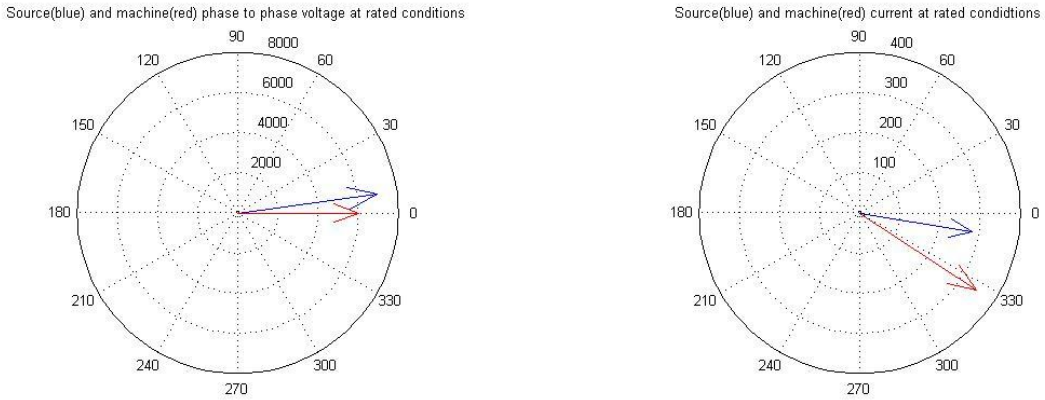

Figure 58 - 50 km cable. Left: Voltage phasors. Red phasor is the desired machine voltage. Blue is the source voltage needed to achieve this result. Right: Current phasors. Red phasor is machine current, blue phasor is source current.

The conditions shown in Figure 57 and Figure 58 are what one may expect. At steady state it is desired to run the converter at 6 kV. To compensate the voltage drop in the cable the topside cable voltage should be ($6544 * \frac{22}{6} \cong 24000$) 24:6. Correspondingly the turns ratio for 50 km cable should be ($6977 * \frac{22}{6} \cong 25600$) 25.6:6. See Table 16 and Table 17 for steady state voltage results.

The SimPowerSystem model used to verify successful start give corresponding results for voltage drop and power factor. Thus the models may be approved for further use.

7.2 APPENDIX A2 – LOCKED ROTOR CALCULATIONS

```
%% SCRIPT FOR LOCKED ROTOR CALCULATIONS %%
%% PARAMETERS %%
clear all;

length = 10; %The cable length studied
f = 3;

f_rated = 66.67;

Rs = 0.0581; % [ohm] Machine stator resistance
Ls = 0.0147; % [H] Machine stator inductance
ux_ss = 0.086; % Reactance voltage drop in subsea transformer
ur_ss = 0.006;
Xss = (f/f_rated)*(6^2/5)*ux_ss;
Rss = (6^2/5)*ur_ss;

ux_ts = 0.06; % Reactance voltage drop in subsea transformer
ur_ts = 0.005;
Xts = (f/f_rated)*(6^2/5)*ux_ts;
Rts = (6^2/5)*ur_ts;

r = 0.214; % [ohm/km]
l = 0.746e-3; % [H/km]
c = 0.136e-6; % [C/km]

z = (r + 1i*2*pi*f*l)*((6/22)^2); % Impedance per unit km REF to LV-side
y = 1i*2*pi*f*c*((22/6)^2); % Admittance per unit km REF to LV-side

%% TRANSFORMER CALCULATIONS
%Neglecting magnetizing current (assuming rated voltage/Hz ratio) for this
%example
%TOPSIDE
A1 = 1;
B1 = Rts + 1i*Xts;
C1 = 0;
D1 = A1;
ABCD_1 = [A1 B1;C1 D1]; % Used in equation: [Vs Is]' = ABCD*[Vr Ir]';

%SUBSEA
A3 = 1;
B3 = Rss + 1i*Xss;
C3 = 0;
D3 = A3;
ABCD_3 = [A3 B3;C3 D3]; % Used in equation: [Vs Is]' = ABCD*[Vr Ir]';

%% LONG LINE CALCULATIONS
Zc = sqrt(z/y); % Characteristic impedance of the line
delta = sqrt(z*y); % propagation constant

A2 = cosh(delta*length);
B2 = Zc*sinh(delta*length);
C2 = sinh(delta*length)/Zc;
D2 = A2;

ABCD_2 = [A2 B2;C2 D2]; % Used in equation: [Vs Is]' = ABCD*[Vr Ir]';

%% PI EQUIVALENT CALCULATIONS %%
```

```
Z = z*length;
Y = y*length;

%corrected impedance values
ZL = Z*(sinh(delta*length)/(delta*length));
YL = Y*(tanh(delta*length/2)/(delta*length/2));
%%

%% VOLTAGE AND CURRENT CALCULATIONS LOCKED ROTOR %%
dr = 0;
% Desired machine voltage at starting at cable side of subsea transformer
Vmachine = (6000/sqrt(3))*(f/f_rated) * (cos(dr) + 1i*sin(dr)); %Including
subsea transformer voltage drop

% Machine current for locked rotor with chosen Vr. Assuming Eback = 0, as
% w = 0.
Imachine = Vmachine/(Rs + 1i*(2*pi*f*Ls));

ABCD_SYSTEM = ABCD_1*ABCD_2*ABCD_3;

% Using ABCD-matrix to calculate neccessary source voltage and current
SYST = ABCD_SYSTEM*[Vmachine; Imachine];

Vsource = SYST(1);
Isource = SYST(2);

figure
%Plotting phase to phase voltages
compass(sqrt(3)*Vsource)
hold on
compass(sqrt(3)*Vmachine,'r')
title('Source and machine(red) phase to phase voltage at starting with
locked rotor')

figure
%Plotting currents in machine and source
compass(Isource)
hold on
compass(Imachine,'r')
title('Source and machine(red) current at starting with locked rotor')

%% POWER CALCULATION AND PRINTOUT%%
Smachine = 3*Vmachine*conj(Imachine);
Ssource = 3*Vsource*conj(Isource);

Pmachine = real(Smachine);
Qmachine = imag(Smachine);
Psource = real(Ssource);
Qsource = imag(Ssource);

POWER_LOCKED = [abs(Ssource) abs(Smachine); Psource Pmachine; Qsource
Qmachine];
figure; bar(POWER_LOCKED); title('Source(left) and machine(right) VA(1),
W(2) and VAr(3) initially');
```

7.3 APPENDIX A3 – STEADY STATE CALCULATIONS

```
%% SCRIPT FOR STEADY STATE CALCULATIONS %%
%% PARAMETERS %%
clear all;

length = 10; %The cable length studied
f = 66.67;

f_rated = 66.67;

Rs = 0.0581; % [ohm] Machine stator resistance
Ls = 0.0147; % [H] Machine stator inductance

ux_ss = 0.086; % Reactance voltage drop in subsea transformer
ur_ss = 0.006;
Xss = (f/f_rated)*(6^2/5)*ux_ss;
Rss = (6^2/5)*ur_ss;

ux_ts = 0.06; % Reactance voltage drop in subsea transformer
ur_ts = 0.005;
Xts = (f/f_rated)*(6^2/5)*ux_ts;
Rts = (6^2/5)*ur_ts;

r = 0.214; % [ohm/km]
l = 0.746e-3; % [H/km]
c = 0.136e-6; % [C/km]

z = (r + 1i*2*pi*f*l)*((6/22)^2); % Impedance per unit km REF to LV-side
y = 1i*2*pi*f*c*((22/6)^2); % Admittance per unit km REF to LV-side

%% TRANSFORMER CALCULATIONS
%Neglecting magnetizing current (assuming rated voltage/Hz ratio) for this
%example
%TOPSIDE
A1 = 1;
B1 = Rts + 1i*Xts;
C1 = 0;
D1 = A1;
ABCD_1 = [A1 B1;C1 D1]; % Used in equation: [Vs Is]' = ABCD*[Vr Ir]';

%SUBSEA
A3 = 1;
B3 = Rss + 1i*Xss;
C3 = 0;
D3 = A3;
ABCD_3 = [A3 B3;C3 D3]; % Used in equation: [Vs Is]' = ABCD*[Vr Ir]';

%% LONG LINE CALCULATIONS
Zc = sqrt(z/y); % Characteristic impedance of the line
delta = sqrt(z*y); % propagation constant

A2 = cosh(delta*length);
B2 = Zc*sinh(delta*length);
C2 = sinh(delta*length)/Zc;
D2 = A2;

ABCD_2 = [A2 B2;C2 D2]; % Used in equation: [Vs Is]' = ABCD*[Vr Ir]';
```

```
%% PI EQUIVALENT CALCULATIONS %%
Z = z*length;
Y = y*length;

%corrected impedance values
ZL = Z*(sinh(delta*length)/(delta*length));
YL = Y*(tanh(delta*length/2)/(delta*length/2));
%%

%% VOLTAGE AND CURRENT CALCULATIONS RUNNING ROTOR RATED %%
%Choosing this voltage as reference
dr = 0;
% Desired machine voltage at starting at cable side of subsea transformer
Vmachine = (6000/sqrt(3))*(f/f_rated) * (cos(dr) + 1i*sin(dr)); %Including
subsea transformer voltage drop

% Machine back induced voltage at rated conditions. See motor data table
Imachine = 348.8*(0.836 - 1i*sqrt(1-0.836^2)); %Using rated PF and I
Eback_rated = Vmachine - Imachine*(Rs + 1i*2*pi*f*Ls);

ABCD_SYSTEM = ABCD_1*ABCD_2*ABCD_3;

% Using ABCD-matrix to calculate neccessary source voltage and current
SYST = ABCD_SYSTEM*[Vmachine; Imachine];

Vsource = SYST(1);
Isource = SYST(2);

figure
%Plotting phase to phase voltages
compass(sqrt(3)*Vsource)
hold on
compass(sqrt(3)*Vmachine,'r')
title('Source(blue) and machine(red) phase to phase voltage at rated
conditions')

figure
%Plotting currents in machine and source
compass(Isource)
hold on
compass(Imachine,'r')
title('Source(blue) and machine(red) current at rated condidtions')

%% POWER CALCULATION AND PRINTOUT %%
Smachine_rated = 3*Vmachine*conj(Imachine);
Ssource_rated = 3*Vsource*conj(Isource);

Pmachine_rated = real(Smachine_rated);
Qmachine_rated = imag(Smachine_rated);
Psource_rated = real(Ssource_rated);
Qsource_rated = imag(Ssource_rated);

POWER_RATED = [abs(Ssource_rated) abs(Smachine_rated); Psource_rated
Pmachine_rated; Qsource_rated Qmachine_rated];
figure; bar(POWER_RATED); title('Source(left) and machine(right) VA(1),
W(2) and VAr(3) at steady state');
```

7.4 APPENDIX B – CALCULATING CABLE AND TRANSFORMER REACTANCES

The below calculations are made to give an impression on how the reactive power production or consumption. Simplified per phase models of the transformers, cable and synchronous machine are shown below.

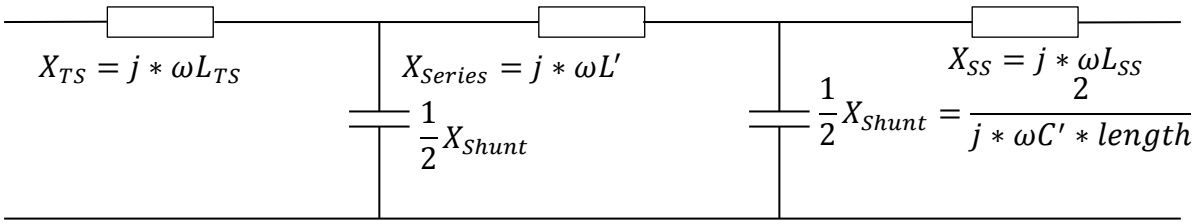

Figure 59 - System per phase sketch

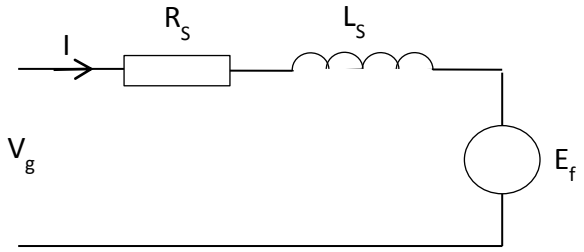

Figure 60 – Simplified per phase synchronous machine model [2]

The transformer data are shown in Table 18.

Table 18 - Transformer data used in simulations [18]

Transformer data		Topside step up	Subsea step down
Rated power	[MVA]	5.00	5.00
Rated frequency	[Hz]	66.67	66.67
Primary side voltage	[kV]	6	22
Secondary side voltage	[kV]	24	6
Reactance, ux	pu	0.06	0.086
Resistance, ur	pu	0.005	0.006
Magnetizing reactance	pu	"Saturation curve"	"Saturation curve"
Magnetizing resistance	pu	426	870

Motor data are shown in Table 19.

Table 19 - Synchronous machine data [18]

Machine data		
Stator resistance, R_S	[ohm]	0.0581
Stator inductance, L_S	[H]	0.0147
Flux linkage from rotor	[Wb]	10.7

From Table 2 the series inductance may be calculated by calculating the impedance base value.

$$L_{Transformer} = \frac{X_{Transformer}}{2 * \pi * f_{rated}} = \frac{ux * Z_{base}}{2 * \pi * f_{rated}} = \frac{ux * \frac{U_{base}^2}{S_{base}}}{2 * \pi * f_{rated}}$$

Inserting numerical values from Table 2 provides the following answers:

$$L_{series,topside} = \frac{0.06 * \frac{24^2}{5}}{2 * \pi * 66.67} = 16.48 * 10^{-3} H$$

$$L_{series,subsea} = \frac{0.086 * \frac{22^2}{5}}{2 * \pi * 66.67} = 19.90 * 10^{-3} H$$

These inductances do not change with cable length as the cable inductance does.

From cable chapter:

$$L'_{cable} = 0.746 * 10^{-3} \, {}^{H}/_{km}$$

$$C'_{cable} = 0.136 * 10^{-6} \, {}^{F}/_{km}$$

The series- and shunt reactance is therefor:

$$X_{series} = 2 * \pi * f(L_{series,topside} + L_{series,subsea} + L'_{cable} * length)$$

$$X_{shunt} = \frac{1}{2 * \pi * f * C' * length}$$

Results for relevant frequencies and cable lengths are summed up in Table 20.

Table 20 - Cable/Transformer series reactance compared to cable shunt reactance

Length	Frequency [Hz]	Series reactance	Shunt reactance	Series resistance
10	3	0.83	39008.56	2.14*
	66.67	18.37	1755.30	2.14
50	3	1.39	7801.71	10.70*
	66.67	30.87	351.06	10.70

***assuming unchanged resistance at the low frequency.**

The machine reactance and resistance is added to the impedance values shown in Table 20. For the low frequencies the shunt reactance caused by the cable capacitance is high compared to series impedance. It is therefor assumed that for low frequency the approximate per phase cable current may be calculated using series impedance only. Note also that the resistance is the dominating parameter in the cable for low frequencies.

7.5 APPENDIX C – VOLTAGE SOURCE

The source is developed in SimPowerSystems™ and the block included in the start system is shown in Figure 9.

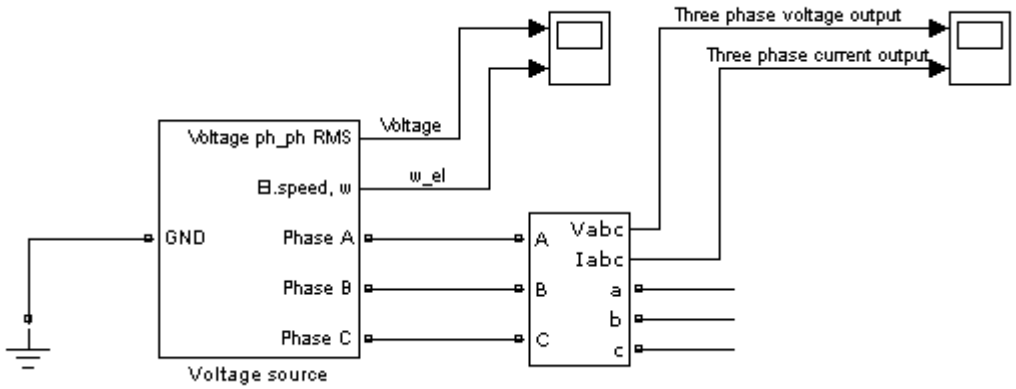

Figure 61 - Three phase source

The block shown in Figure 61 contains several subsystems. All phases are equal except for a 120^{o} phase shift, and that the reference signals for voltage and frequency are obtained from phase A only. The subsystem of Figure 61 can be seen below.

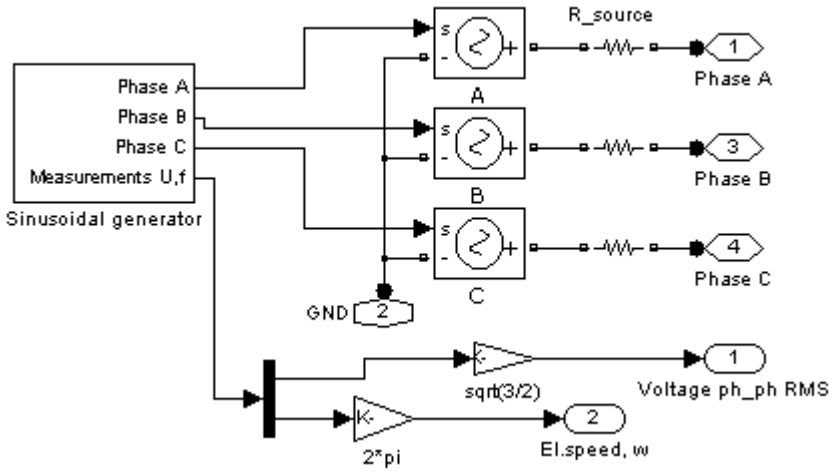

Figure 62 - Three phase signal generator

Three single phase controllable voltage sources get signals from the Sinusoidal generator shown in Figure 62. The generated voltage is driven by the input signal of the block. This signal is generated in the blocks shown in Figure 63.

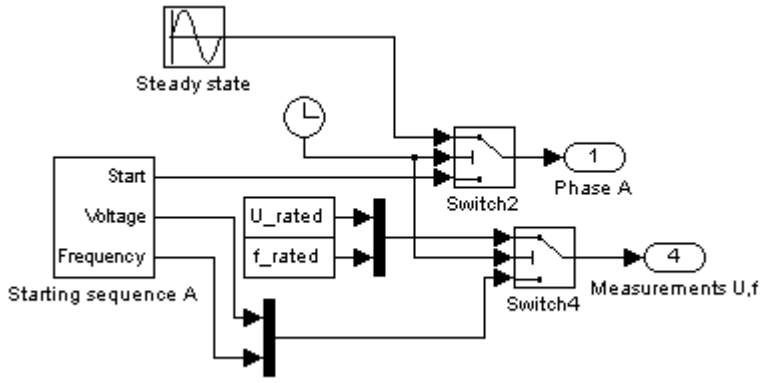

Figure 63 - Single phase signal generator

When the starting sequence is finalized Switch2 shifts over to the steady state signal. At that instant in time the frequency and voltage is ramped up to desired values. The phase of the steady state signal is calculated from frequency of starting and steady state and the sequence duration such that the transition from start sequence to steady state is smooth. The subsystem Starting sequence A is shown in Figure 64.

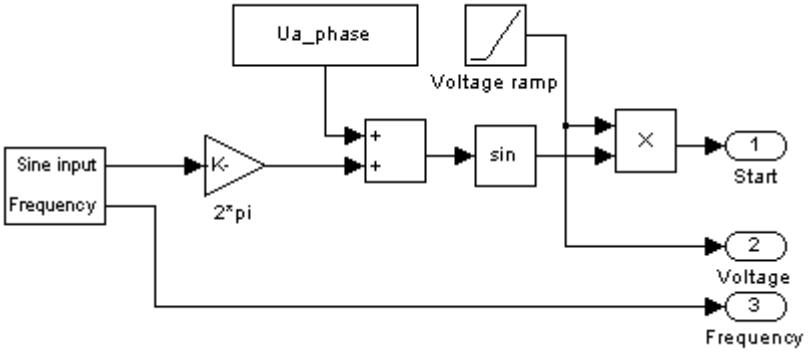

Figure 64 - Ramp generator

In Figure 64 it can be seen that the reference signals for voltage and frequency are obtained at the input to the sine function on the form:

$$K(t) = \mathrm{U(t)} * \sin(2 * \pi * \mathrm{X(t)}) \qquad \text{(C1)}$$

Where f(t) and U(t) is sent to input 2 and 3 in Figure 64 respectively. Finally Figure 65 shows how the time-dependent frequency is obtained.

$$\mathrm{X(t)} = \mathrm{t} * \mathrm{f(t)} \qquad \text{(C2)}$$

Where t denotes simulation time.

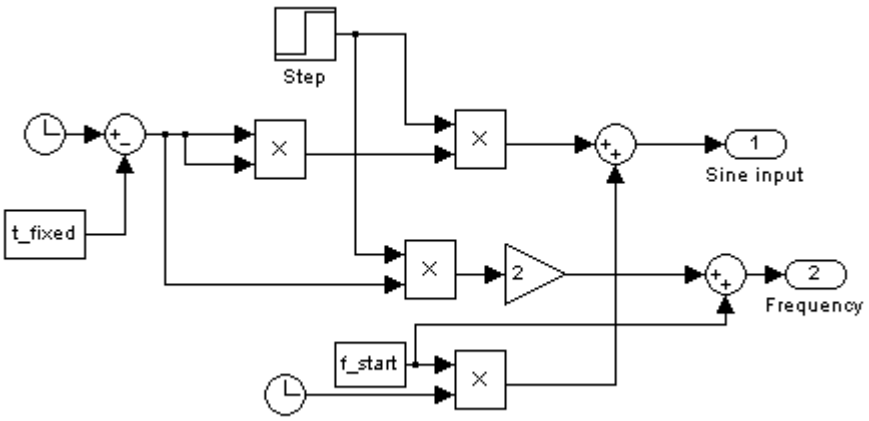

Figure 65 - Frequency signal generator

With reference to Figure 65 the signal on output 1 is given by the following equation.

$$\mathrm{X(t)} = \begin{cases} f_{start} * t, 0 < t < t_{fixed} \\ f_{slope} * \left(t - t_{fixed}\right)^2 + f_{start} * t, t_{fixed} < t < (t_{fixed} + t_{ramp}) \end{cases} \quad \text{(C3)}$$

The frequency of the sinusoidal signal is given by the time derivative of X(t) such that the frequency is given by:

$$\mathrm{f(t)} = \begin{cases} f_{start}, 0 < t < t_{fixed} \\ 2 * f_{slope} * \left(t - t_{fixed}\right) + f_{start}, t_{fixed} < t < (t_{fixed} + t_{ramp}) \end{cases} \quad \text{(C4)}$$

When the duration of fixed frequency, t_{fixed}, and the time the machine is intended to use for accelerating to rated speed, t_{ramp}, is chosen the f_{slope} may be calculated. This is done in the script shown below. Here the start and end frequency, rated voltage, and other characteristics may be specified.

```
%%Spec
U_rated = 660*sqrt(2/3); % [V] Phase-Gnd peak
f_rated = 20; % [Hz]
w_rated = 2*pi*f_rated; % [rad/s]

R_source = 0.01; %Internal resistance in voltage source.
%Nonzero if capacitor is in parallel with voltage source

%Initial phase.
Ua_phase = 0;
Ub_phase = 2*pi/3;
Uc_phase = 4*pi/3;

%Load data
Tm_rated = 2500; % [Nm]
Friction = 0.01;

%%LINE MODEL - PI-equivalent
R_line = 0.65; %Ohm
L_line = 2.14e-3; %H
C_line = 0.6e-6; %F

%%Start sequence (Ramps voltage/frequency from start to rated)
U_f_boost = 2.0; %Ratio of voltage boost at starting
f_start = 5; % [Hz]
t_fixed = 0.5; % [sec]
t_ramp = 3; % [sec]

U_start = (U_rated/f_rated)*f_start*U_f_boost;
f_slope = (f_rated-f_start)/(2*t_ramp); % Coefficient in t^2 function
U_slope = (U_rated - U_start)/t_ramp; % [V/sec]

%The steady state voltage must be phased in with the ramped signals
Ua_phase_ss = 2*pi*(f_slope*t_ramp^2 + (f_start-f_rated)*(t_fixed + t_ramp));
Ub_phase_ss = Ua_phase_ss + 2*pi/3;
Uc_phase_ss = Ub_phase_ss + 2*pi/3;
```

As an example the three phase voltage output when the frequency is ramped from five to 20 Hz in 3 seconds is shown in Figure 67. Initially the voltage per frequency ratio is 1.0 times rated. This feature is included to overcome stiction torque which is common at startup. As higher voltage per voltage ratio may be needed. The single phase output with voltage and frequency references are shown in Figure 66.

Initially the ratio between voltage and frequency is “U_f_boost” times rated. At the end of the start sequence rated conditions are achieved.

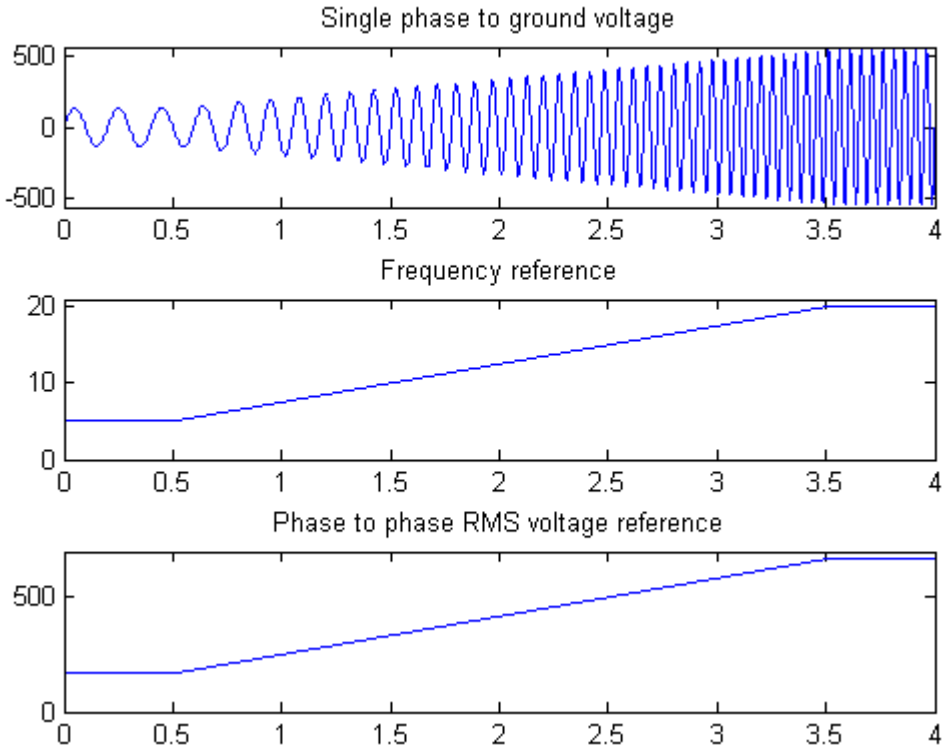

Figure 66- Single phase output with references

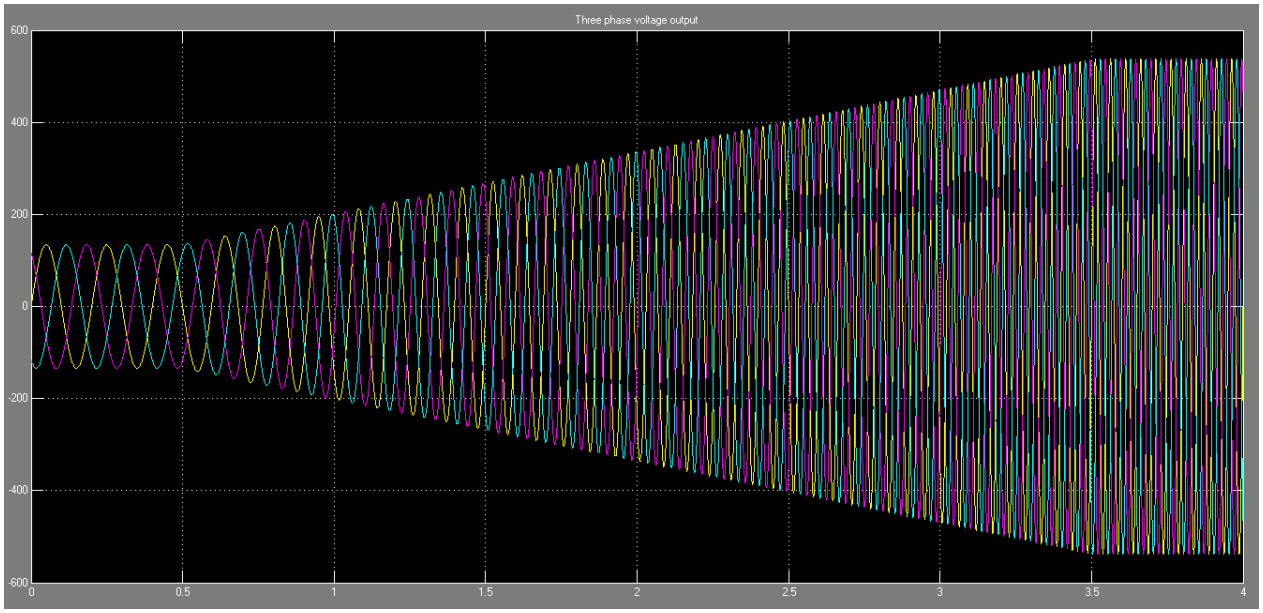

Figure 67 - Three phase voltage output corresponding to Figure 10. Example

7.6 APPENDIX D – SIMULATION RESULTS EXCEL

The results presented below are a result of the simulations performed in the developed SimPowerSystems™ model. Parameters thought to be most important are included.

MAIN PARAMTERS PRESENTED IN EXCEL SHEETS	
VALUE	**EXPLANATION**
T_{MAX_LOCKED}	The maximum torque the machine produced if the rotor is locked. This must exceed the stiction torque of the mechanical load.
$T_{STICTION}$	The electromagnetic torque the machine must produced to move the rotor initially. Results in the range of 30 %-40 % of rated pump torque are thought to be most relevant, but it probably depends strongly on the type of fluid and pump.
$w_{rotorMAX}/w_{START}$	The maximum speed during the start cycle. Give an impression of the overshoot as the machine reach synchronous speed.
$w_{rotorMIN}/w_{START}$	The minimum speed. If zero crossings or negative start occur it is interesting to see how fast the rotor runs backwards.
Neg. Start	The results script found in Appendix E works out if negative start occurs.
# of zero crossings	If zero crossings occur the script in Appendix E calculates how many times the rotor oscillates before synchronism is reached. Not a relevant number if rotor is not synchronized.
Synchronized	Yes / No
$I_{sourceMAX}$	The maximum source current drawn from the converter. The converter must always be able to provide enough current. If transformers are driven into saturation very high magnetizing currents may be the result which may destruct the transistors.
t_{SYNCH}	How much time the rotor uses before it accelerates up to synchronous speed. It has been found that further acceleration must not be initiated before the rotor reach synchronism.

Locked rotor current and torque results

From SimPowerSystems-model

Maximum electromagnetic torque, T_{EM} [Nm]

10 km	Vs/Vsrated				
Frequency	1,00	1,05	1,10	1,15	2,00
3	8229	8643	9058	9474	14445
6	10578	11111	11652	12186	19646
9	11593	12176	12770	13358	22030

Locking rotor and using Tmax = max(T_em.signals.values); to identify max torqe.

Locked rotor -> **Maximum RMS-current drawn from source, I_{vfd} [A]**

10 km	Vs/Vsrated				
Frequency	1,00	1,05	1,10	1,15	2,00
3	434	456	480	503	2159
6	596	629	662	695	2303
9	679	717	756	794	2420

Maximum electromagnetic torque, T_{EM}

50 km	Vs/Vsrated				
Frequency	1,00	1,05	1,10	1,15	2,00
3	3961	4171	4383	4599	9358
6	6662	7023	7392	7761	13436
9	8509	8969	9558	9912	17435

Locked rotor -> **Maximum RMS-current drawn from source, I_{vfd} [A]**

50 km	Vs/Vsrated				
Frequency	1,00	1,05	1,10	1,15	2,00
3	209	221	232	245	2029
6	355	376	398	420	2218
9	454	481	511	538	2293

Base case 10 km

Length [km]	10
Tmax_locked [km]	8229
Isource_max_locked [A]	434
Trated [Nm]	6685
Voltage boost	1
Start frequency [Hz]	3
Damping [Nm]	0
Initial power angle [deg]	0

Tstiction/Trated	**Tstiction**	**w_max/w_start**	**w_min/w_start**	**Neg. Start?**	**# of zero crossings***	**Synchronized**	**Isource_max [A]**	**t_synch [sec]**
0 %	0	1,62	0	NO	0	YES	277	0,29
10 %	669	1,64	0	NO	0	YES	296	0,30
20 %	1337	1,64	0	NO	0	YES	315	0,30
30 %	2006	1,60	0	NO	0	YES	333	0,32
40 %	2674	1,67	0	NO	0	YES	350	0,35
50 %	3343	2,07	-1,27	NO	2	YES	537	0,99
60 %	4011	1,64	-1,23	NO	1	YES	451	0,54
70 %	4680	1,59	-1,20	NO	2	YES	571	1,06
100 %	6685	0,69	-0,96	NO	-	NO	423	-
Tmax_locked [Nm]	8229	-	-	-	-	-	-	-

*Within first 5 sec

Length [km]	10
Tmax_locked [km]	8229
Isource_max_locked [A]	434
Trated [Nm]	6685
Voltage boost	1
Start frequency [Hz]	3
Damping [Nm]	0
Initial power angle [deg]	180 worst case

Tstiction/Trated	**Tstiction**	**w_max/w_start**	**w_min/w_start**	**Neg. Start?**	**# of zero crossings***	**Synchronized**	**Isource_max [A]**	**t_synch [sec]**
0 %	0	1,69	-1,13	YES	0	YES	252	0,22
10 %	669	1,60	-1,05	YES	0	YES	280	0,22
20 %	1337	1,59	-0,96	YES	0	YES	304	0,23
30 %	2006	1,57	-0,87	YES	0	YES	325	0,24
40 %	2674	1,62	-0,78	YES	0	YES	342	0,27
50 %	3343	1,92	-1,21	YES	2	YES	426	1,11
60 %	4011	1,70	-1,22	YES	1	YES	489	0,65
70 %	4680	1,52	-1,19	YES	2	YES	469	1,13
100 %	6685	1,78	-1,22	YES	3	YES	421	1,26
Tmax_locked [Nm]	8229	-	-	YES	-	NO	515	-

*Within first 5 sec

Base case 50 km

Length [km]	50
Tmax_locked [Nm]	3961
Isource_max_locked [A]	209
Trated [Nm]	6685
Voltage boost	1
Start frequency [Hz]	3
Damping [Nm]	0
Initial power angle [deg]	0

Tstiction/Trated	**Tstiction**	**w_max/w_start**	**w_min/w_start**	**Neg. Start?**	**# of zero crossings***	**Synchronized**	**Isource_max [A]**	**t_synch [sec]**	
0 %	0	1,52	0,00	NO	0	YES	159	0,20	fig
10 %	669	0,93	-0,81	NO	18	NO**	260	-	fig
20 %	1337	0,95	-0,73	NO	18	NO**	256	-	fig
30 %	2006	0,91	-0,75	NO	18	NO**	261	-	fig
50 %	3343	-	-	-	-	-	-	-	
Tmax_locked [Nm]	3961	-	-	-	-	-	-	-	

*within first 5 sec

** Fixed frequency extended to 7 sec

Length [km]	50
Tmax_locked [Nm]	3960
Isource_max_locked [A]	209
Trated [Nm]	6685
Voltage boost	1
Start frequency [Hz]	3
Damping [Nm]	0
Initial power angle [deg]	180 *worst case*

Tstiction/Trated	**Tstiction**	**w_max/w_start**	**w_min/w_start**	**Neg. Start?**	**# of zero crossings***	**Synchronized**	**Isource_max [A]**	**t_synch [sec]**	
0 %	0	0,88	-0,78	YES	17**	NO**	261	-	fig
10 %	669	1,45	-0,77	YES	13**	YES**	239	4,94	fig
20 %	1337	1,44	-0,69	YES	15**	YES**	244	5,55	fig
30 %	2006	0,94	-0,77	YES	19**	NO**	243	-	fig
40 %	2674	0,77	-0,67	YES	20**	NO**	242	-	fig
Tmax_locked [Nm]	3960	-	-	-	-	-	-	-	

*within first 5 sec

** Fixed frequency extended to 7 sec

15 % Voltage boost

Length [km]	50
Tmax_locked [Nm]	4599
Isource_max_locked [A]	245
Trated [Nm]	6685
Voltage boost	1,15
Start frequency [Hz]	3
Damping [Nm]	0
Initial power angle [deg]	0

Tstiction/Trated	**Tstiction**	**w_max/w_start**	**w_min/w_start**	**Neg. Start?**	**# of zero crossings***	**Synchronized**	**Isource_max [A]**	**t_synch [sec]**	
0 %	0	1,62	0	NO	0	YES	208	0,17	fig
10 %	669	1,52	0	NO	0	YES	199	0,21	fig
20 %	1337	1,7	-0,87	NO	8	YES	258	3,1	fig
30 %	2006	1,58	-0,82	NO	12	YES	301	4,71	fig
40 %	2674	1,67	-0,85	NO	10	YES	263	3,87	fig
50 %	3343	1,63	-0,71	NO	10	YES	279	3,79	fig
Tmax_locked [Nm]	4599	-	-	-	-	-	-	-	Simulation hangs

*within first 5 sec

Length [km]	50
Tmax_locked [Nm]	4599
Isource_max_locked [A]	245
Trated [Nm]	6685
Voltage boost	1,15
Start frequency [Hz]	3
Damping [Nm]	0
Initial power angle [deg]	180 *worst case*

Tstiction/Trated	**Tstiction**	**w_max/w_start**	**w_min/w_start**	**Neg. Start?**	**# of zero crossings***	**Synchronized**	**Isource_max [A]**	**t_synch [sec]**	
0 %	0	1,66	-0,91	YES	3	YES	268	1,62	fig
10 %	669	1,68	-0,89	YES	7	YES	273	2,82	fig
20 %	1337	1,56	-0,93	YES	9	YES	278	3,54	fig
30 %	2006	1,47	-1,08	YES	9	YES	274	3,51	fig
40 %	2674	1,68	-0,84	YES	10	YES	289	3,91	fig
50 %	3343	-	-	-	-	-	-		fig
Tmax_locked [Nm]	4599	-	-	-	-	-	-	-	

*within first 5 sec

** Fixed frequency extended to 7 sec

30 % Voltage boost

Length [km]	50
Tmax_locked [Nm]	5271
Isource_max_locked [A]	283
Trated [Nm]	6685
Voltage boost	1,30
Start frequency [Hz]	3
Damping [Nm]	0
Initial power angle [deg]	0

Tstiction/Trated	**Tstiction**	**w_max/w_start**	**w_min/w_start**	**Neg. Start?**	**# of zero crossings***	**Synchronized**	**Isource_max [A]**	**t_synch [sec]**		
0 %	0	1,67	0	NO	0	YES	255	0,16	fig	
10 %	669	1,66	0	NO	0	YES	224	0,17	fig	
20 %	1337	1,70	-0,81	NO	7	YES	325	2,81	fig	
30 %	2006	1,76	-0,92	NO	8	YES	326	2,98	fig	
40 %	2674	1,79	-0,92	NO	9	YES	334	3,26	fig	
50 %	3343	1,81	-0,95	NO	8	YES	332	2,90	fig	
Tmax_locked [Nm]	5271	-	-	-	-	-	-	-	fig	Sim. H.

*within first 5 sec

** Fixed frequency extended to 7 sec

Length [km]	50
Tmax_locked [Nm]	5271
Isource_max_locked [A]	283
Trated [Nm]	6685
Voltage boost	1,30
Start frequency [Hz]	3
Damping [Nm]	0
Initial power angle [deg]	180 *worst case*

Tstiction/Trated	**Tstiction**	**w_max/w_start**	**w_min/w_start**	**Neg. Start?**	**# of zero crossings***	**Synchronized**	**Isource_max [A]**	**t_synch [sec]**		
0 %	0	1,83	-0,96	YES	1	YES	294	0,94	fig	
10 %	669	1,68	-1,02	YES	2	YES	305	0,97	fig	
20 %	1337	1,79	-0,95	YES	6	YES	304	2,32	fig	
30 %	2006	1,78	-0,89	YES	8	YES	312	3,08	fig	
40 %	2674	1,59	-0,92	YES	8	YES	308	3,12	fig	
50 %	3343	1,79	-0,87	YES	8	YES	310	2,98	fig	
Tmax_locked [Nm]	5271	-	-	-	-	-	-	-	Simulation hangs	

*within first 5 sec

** Fixed frequency extended to 7 sec

90 % cable resistance

Length [km]	50
Tmax_locked [Nm]	4085
Isource_max_locked [A]	225
Trated [Nm]	6685
Voltage boost	1,00
Start frequency [Hz]	3
Damping [Nm]	0
Initial power angle [deg]	0

Tstiction/Trated	**Tstiction**	**w_max/w_start**	**w_min/w_start**	**Neg. Start?**	**# of zero crossings***	**Synchronized**	**Isource_max [A]**	**t_synch [sec]**	
0 %	0	1,55	0	NO	0	YES	170	0,19	fig
10 %	669	1,46	-0,38	NO	1	YES	260	0,83	fig
20 %	1337	1,34	-0,77	NO	10	YES	252	3,79	fig
30 %	2006	1,33	-0,8	NO	12	YES	275	4,45	fig
40 %	2674	0,96	-0,77	NO	16**	NO**	277		fig
Tmax_locked [Nm]	4085	-	-	-	-	-	-	-	Simulation hangs

*within first 5 sec

** Fixed frequency extended to 7 sec

Length [km]	50
Tmax_locked [Nm]	4085
Isource_max_locked [A]	225
Trated [Nm]	6685
Voltage boost	1,00
Start frequency [Hz]	3
Damping [Nm]	0
Initial power angle [deg]	180 *worst case*

Tstiction/Trated	**Tstiction**	**w_max/w_start**	**w_min/w_start**	**Neg. Start?**	**# of zero crossings***	**Synchronized**	**Isource_max [A]**	**t_synch [sec]**	
0 %	0	0,95	-0,78	YES	12**	NO**	252		fig
10 %	669	1,41	-0,84	YES	7	YES**	263	2,86	fig
20 %	1337	1,53	-0,75	YES	11	YES**	271	4,24	fig
30 %	2006	1,50	-0,79	YES	11	YES**	261	4,20	fig
40 %	2674	1,31	-0,76	YES	11	YES**	269	4,15	fig
50 %	3343	1,51	-0,68	YES	11	YES**	278	4,19	fig
Tmax_locked [Nm]	4085	1,5	-0,67	YES	11	YES**	283	4,18	fig

*within first 5 sec

** Fixed frequency extended to 7 sec

80 % cable resistance

Length [km]	50
Tmax_locked [Nm]	4404
Isource_max_locked [A]	244
Trated [Nm]	6685
Voltage boost	1,00
Start frequency [Hz]	3
Damping [Nm]	0
Initial power angle [deg]	0

Tstiction/Trated	**Tstiction**	**w_max/w_start**	**w_min/w_start**	**Neg. Start?**	**# of zero crossings***	**Synchronized**	**Isource_max [A]**	**t_synch [sec]**
0 %	0	1,56	0	NO	0	YES	190	0,18
10 %	669	1,47	0	NO	0	YES	221	0,40
20 %	1337	1,43	-0,8	NO	8	YES	286	3,09
30 %	2006	1,53	-0,84	NO	9	YES	310	3,36
40 %	2674	1,45	-0,86	NO	9	YES	296	3,42
50 %	3343	1,62	-0,85	NO	9	YES	305	3,38
Tmax_locked [Nm]	4404	-	-	-	-	-	-	-

*within first 5 sec

** Fixed frequency extended to 7 sec

Length [km]	50
Tmax_locked [Nm]	4404
Isource_max_locked [A]	244
Trated [Nm]	6685
Voltage boost	1,00
Start frequency [Hz]	3
Damping [Nm]	0
Initial power angle [deg]	180 *worst case*

Tstiction/Trated	**Tstiction**	**w_max/w_start**	**w_min/w_start**	**Neg. Start?**	**# of zero crossings***	**Synchronized**	**Isource_max [A]**	**t_synch [sec]**
0 %	0	1,36	-0,74	YES	1	YES	243	0,85
10 %	669	1,55	-0,80	YES	7	YES	263	2,86
20 %	1337	1,55	-0,82	YES	11**	YES	308	4,96
30 %	2006	1,58	-0,78	YES	10**	YES	291	3,85
40 %	2674	1,31	-0,84	YES	9	YES	291	3,50
50 %	3343	1,63	-0,82	YES	9	YES	291	3,47
Tmax_locked [Nm]	4404	-	-	-	-	-	-	-

*within first 5 sec

** Fixed frequency extended to 7 sec

500 Nm damping at starting frequency

Length [km]	50	
Tmax_locked [Nm]	4461	*EM + damping at starting frequency*
Isource_max_locked [A]	209	
Trated [Nm]	6685	
Voltage boost	1,00	
Start frequency [Hz]	3	
Damping [Nm]	500	*At slip equal to starting frequency*
Initial power angle [deg]	0	

Tstiction/Trated	**Tstiction**	**w_max/w_start**	**w_min/w_start**	**Neg. Start?**	**# of zero crossings***	**Synchronized**	**Isource_max [A]**	**t_synch [sec]**
0 %	0	1,48	0	NO	0	YES	152	0,19
10 %	669	1,30	-0,24	NO	1	YES	236	0,81
20 %	1337	1,27	-0,61	NO	8	YES	249	3,10
30 %	2006	1,27	-0,62	NO	10	YES	248	3,78
40 %	2674	1,37	-0,64	NO	12	YES	248	4,49
50 %	3343	1,37	-0,63	NO	13	YES	242	4,78
Tmax_locked [Nm]	4461	-	-	-	-	-	-	-

*within first 5 sec

Length [km]	50	
Tmax_locked [Nm]	4461	*EM + damping at starting frequency*
Isource_max_locked [A]	209	
Trated [Nm]	6685	
Voltage boost	1,00	
Start frequency [Hz]	3	
Damping [Nm]	500	*At slip equal to starting frequency*
Initial power angle [deg]	180	*worst case*

Tstiction/Trated	**Tstiction**	**w_max/w_start**	**w_min/w_start**	**Neg. Start?**	**# of zero crossings***	**Synchronized**	**Isource_max [A]**	**t_synch [sec]**
0 %	0	1,46	-0,53	YES	1	YES	229	0,90
10 %	669	1,35	-0,62	YES	5	YES	225	2,21
20 %	1337	1,34	-0,61	YES	9	YES	236	3,50
30 %	2006	1,36	-0,58	YES	11	YES	238	4,17
40 %	2674	1,31	-0,6	YES	13	YES	237	4,84
50 %	3343	1,4	-0,65	YEs	12	YES	237	4,63
Tmax_locked [Nm]	4461	-	-	-	-	-	-	-

*within first 5 sec

1000 Nm damping at starting frequency

Length [km]	50	
Tmax_locked [Nm]	4961	*EM + damping at starting frequency*
Isource_max_locked [A]	209	
Trated [Nm]	6685	
Voltage boost	1,00	
Start frequency [Hz]	3	
Damping [Nm]	1000	*At slip equal to starting frequency*
Initial power angle [deg]	0	

Tstiction/Trated	**Tstiction**	**w_max/w_start**	**w_min/w_start**	**Neg. Start?**	**# of zero crossings***	**Synchronized**	**Isource_max [A]**	**t_synch [sec]**	
0 %	0	1,44	0	NO	0	YES	144	0,19	fig
10 %	669	1,35	-0,33	NO	1	YES	241	1,49	fig
20 %	1337	1,35	-0,59	NO	5	YES	233	1,87	fig
30 %	2006	1,25	-0,50	NO	7	YES	242	2,82	fig
40 %	2674	1,32	-0,50	NO	9	YES	244	3,53	fig
50 %	3343	-	-	-	-	-	-	-	fig, simulation hangs
Tmax_locked [Nm]	4961	-	-	-	-	-	-	-	

*within first 5 sec

Length [km]	50	
Tmax_locked [Nm]	4961	*EM + damping at starting frequency*
Isource_max_locked [A]	209	
Trated [Nm]	6685	
Voltage boost	1,00	
Start frequency [Hz]	3	
Damping [Nm]	1000	*At slip equal to starting frequency*
Initial power angle [deg]	180	*worst case*

Tstiction/Trated	**Tstiction**	**w_max/w_start**	**w_min/w_start**	**Neg. Start?**	**# of zero crossings***	**Synchronized**	**Isource_max [A]**	**t_synch [sec]**	
0 %	0	1,40	-0,42	YES	1	YES	181	0,46	fig
10 %	669	1,31	-0,53	YES	2	YES	214	1,18	fig
20 %	1337	1,33	-0,6	YES	6	YES	234	2,6	fig
30 %	2006	1,32	-0,66	YES	7	YES	234	2,84	fig
40 %	2674	1,24	-0,68	YES	9	YES	233	3,53	fig
50 %	3343	1,29	-0,47	NO	11	YES	233	4,14	fig
Tmax_locked [Nm]	4961	-	-	-	-	-	-	-	

*within first 5 sec

1500 Nm damping at starting frequency

Length [km]	50	
Tmax_locked [Nm]	5461	*EM + damping at starting frequency*
Isource_max_locked [A]	209	
Trated [Nm]	6685	
Voltage boost	1,00	
Start frequency [Hz]	3	
Damping [Nm]	1500	*At slip equal to starting frequency*
Initial power angle [deg]	0	

Tstiction/Trated	**Tstiction**	**w_max/w_start**	**w_min/w_start**	**Neg. Start?**	**# of zero crossings***	**Synchronized**	**Isource_max [A]**	**t_synch [sec]**
0 %	0	1,4	0	NO	0	YES	138	0,19
10 %	669	1,32	0	NO	0	YES	167	0,39
20 %	1337	1,23	-0,27	NO	2	YES	232	1,21
30 %	2006	1,25	-0,41	NO	5	YES	232	2,20
40 %	2674	1,28	-0,39	NO	7	YES	238	2,86
50 %	3343	1,25	-0,38	NO	9	YES	228	3,51
Tmax_locked [Nm]	5461	-	-	-	-	-	-	-

*within first 5 sec

Length [km]	50	
Tmax_locked [Nm]	5461	*EM + damping at starting frequency*
Isource_max_locked [A]	209	
Trated [Nm]	6685	
Voltage boost	1,00	
Start frequency [Hz]	3	
Damping [Nm]	1500	*At slip equal to starting frequency*
Initial power angle [deg]	180	*worst case*

Tstiction/Trated	**Tstiction**	**w_max/w_start**	**w_min/w_start**	**Neg. Start?**	**# of zero crossings***	**Synchronized**	**Isource_max [A]**	**t_synch [sec]**
0 %	0	1,36	-0,31	YES	1	YES	193	0,44
10 %	669	1,26	-0,42	YES	1	YES	195	0,93
20 %	1337	1,26	-0,43	YES	4	YES	254	2,12
30 %	2006	1,25	-0,37	YES	6	YES	231	2,67
40 %	2674	1,27	-0,37	NO	8	YES	227	3,26
50 %	3343	1,25	-0,38	NO	10	YES	228	3,89
Tmax_locked [Nm]	5461	-	-	-	-	-	-	-

*within first 5 sec

These results are commented in the report.

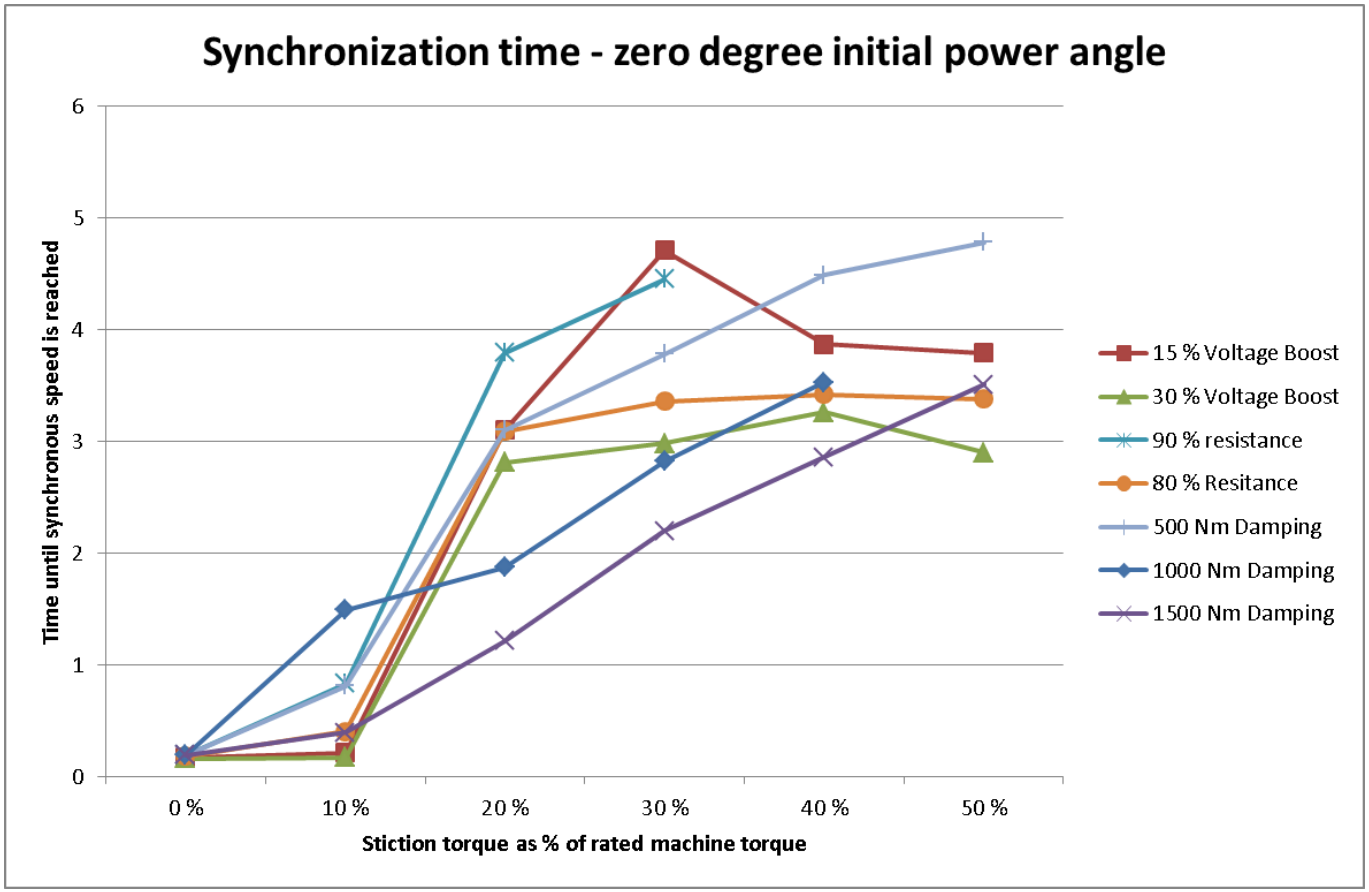

These results are commented in the report.

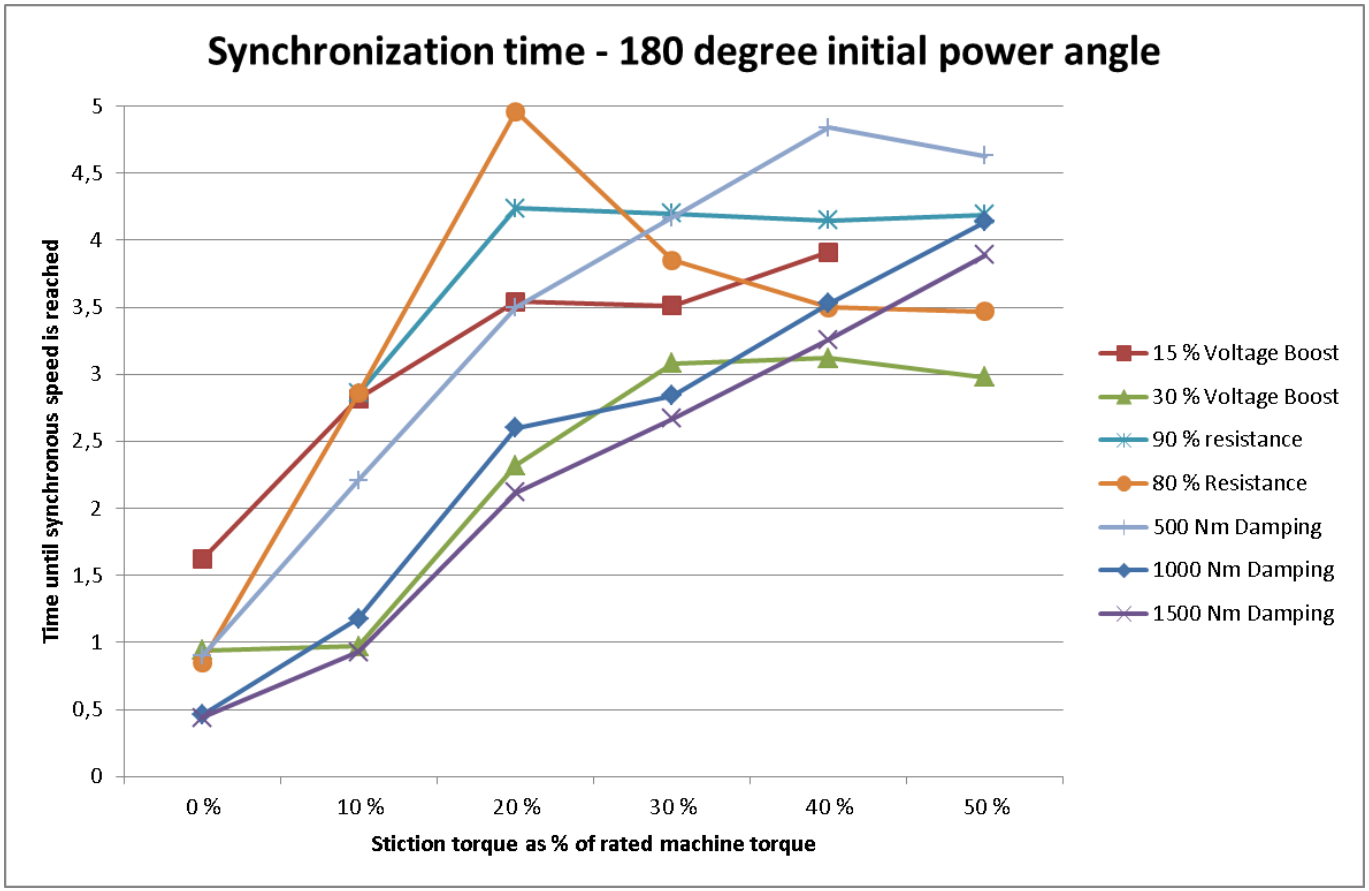

These results are commented in the report.

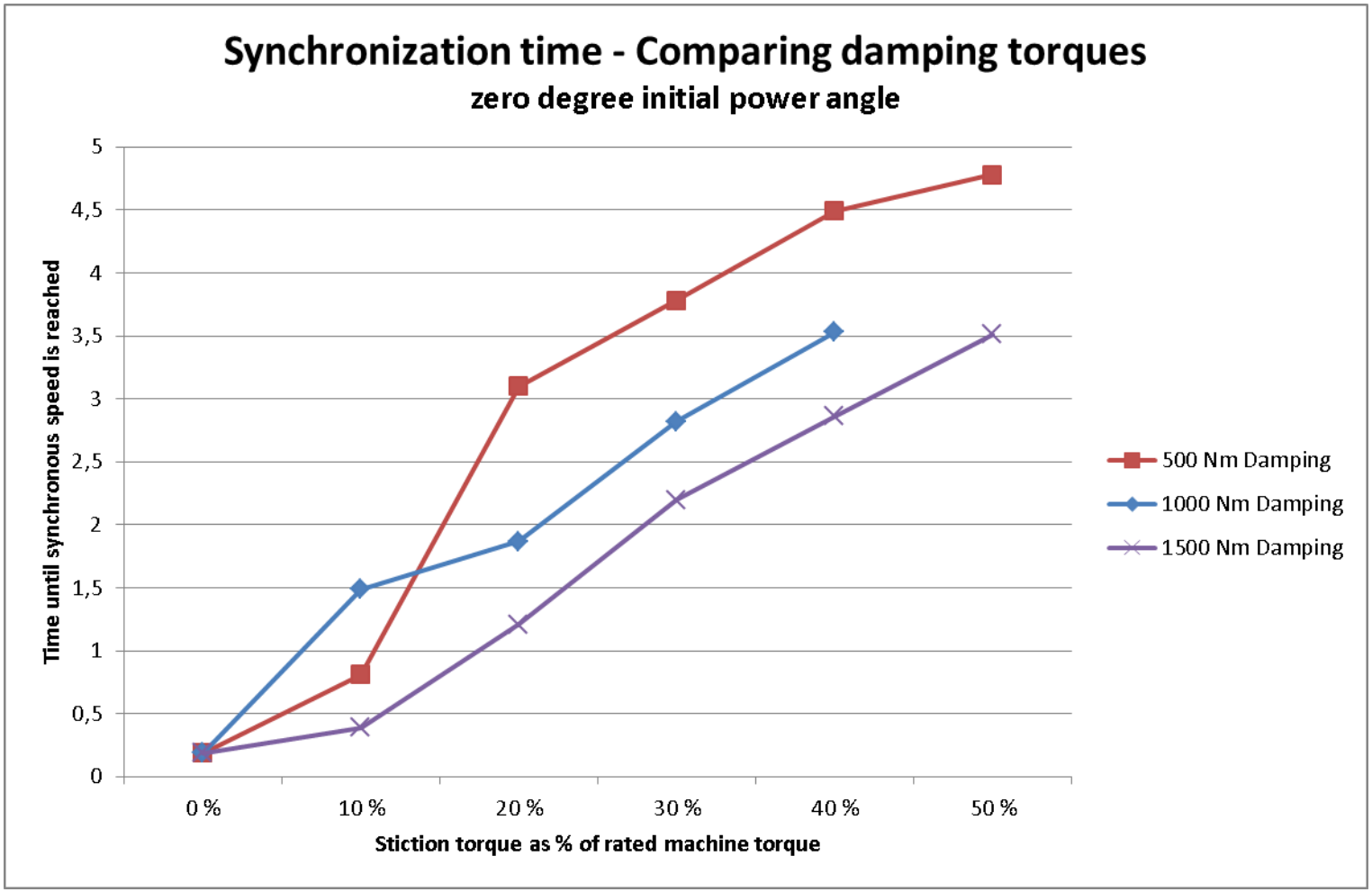

These results are commented in the report.

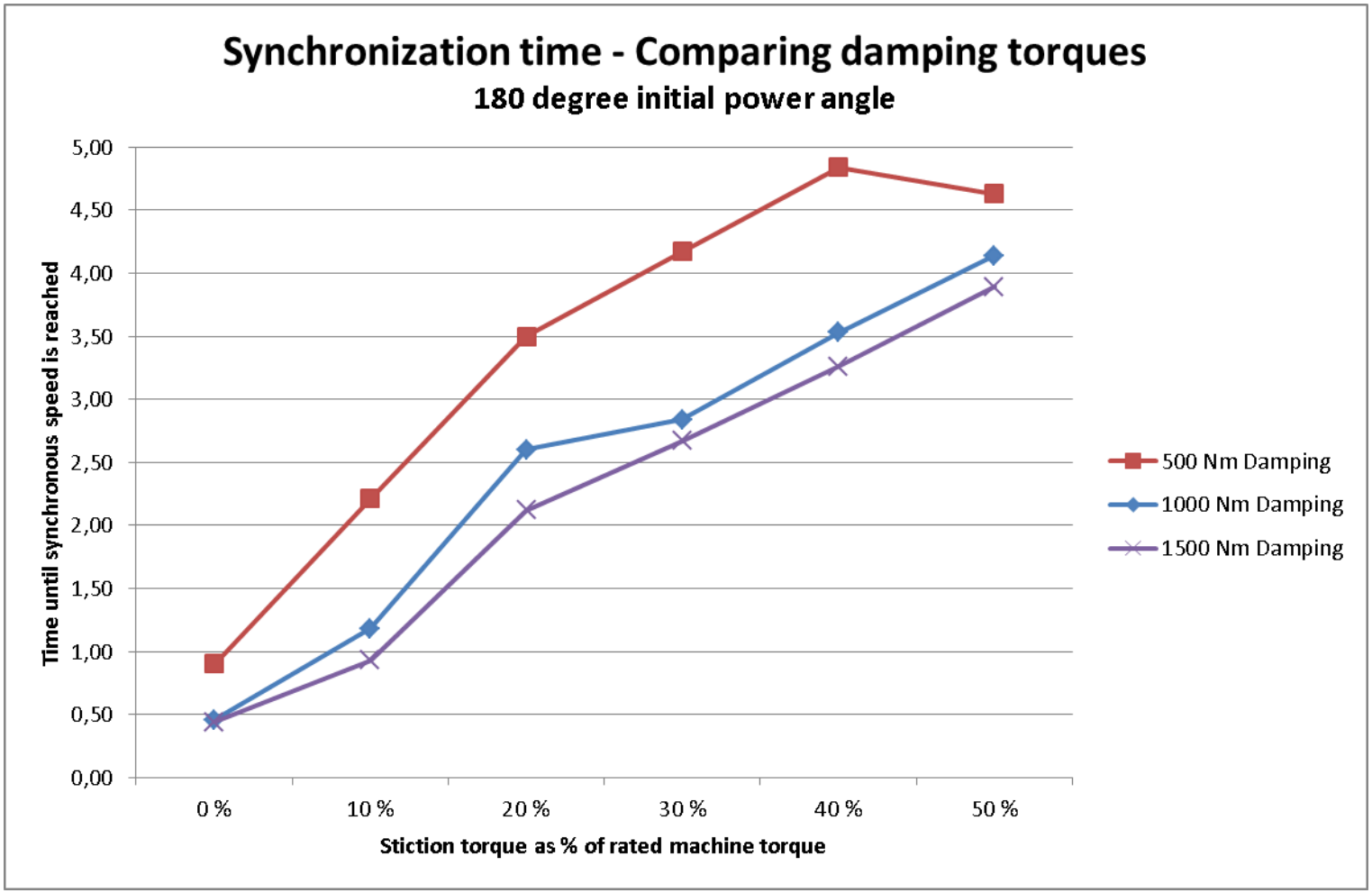

7.7 APPENDIX E – MATLAB MOTOR START SIMULATION SCRIPTS

These scripts initialize and runs the simulations in the SimPowerSystems™ model developed.

7.7.1 Main script

```
%Script for running the simulations of a motor start.
clear all

%Initialize system parameters
Parameters_start_model_simulink

%Length of simulation
t_sim = t_fixed;% + 5;% t_ramp/4;% + 2; % [sec]

%Run SIMULINK SimPowerSystems simulation
sim PM_machine_start_system

%Get values from workspace (torque, rotor_spd, Voltages, currents ...)
struct with time
%... and plot

% Plot of Load torque and electromagnetic torque
% figure(1)
% plot(T_load.time,T_load.signals.values, '--r','LineWidth',2);
% title('(Electromagnetic + Damping)- (black/solid) and Load torque
(red/dashed)')
% xlabel('Time [s]')
% ylabel('Torque [Nm]')
% hold on
% plot(T_em.time,T_em.signals.values+T_D.signals.values, '-k');
% hold off

% Plot some results
disp(['Maximum torque: ', num2str(max(T_em.signals.values)), ' Nm'])
disp(['At frequency ', num2str(frlc), ' Hz and ', num2str(length), ' km'])
disp(['Maximum current ', num2str(max(Ivfd.signals.values/sqrt(2))), '
Arms'])
disp(['Maximum rotor speed: ',
num2str(max(w_rotor.signals.values)/(frlc*2*pi)), ' [w_max/w_start]'])
disp(['Minimum rotor speed: ',
num2str(min(w_rotor.signals.values)/(frlc*2*pi)), ' [w_min/w_start]'])

%Calculate and print the number of times the rotor oscillates around zero
speed
zerocrossings(w_rotor.signals.values, t_sim, frlc);

%Calculate the time before synchronous speed is reached the first time
%Earliest time for speed reference increase
synchtime = reachsynch(w_rotor.signals.values, w_rotor.time, t_sim, frlc);
disp([num2str(synchtime),' seconds until rotor reaches synchronous speed
first time'])

% %Plot of rotor speed, reference and damping torque
figure(2)
[AX] = plotyy(w_rotor.time, w_rotor.signals.values, w_rotor.time,
T_D.signals.values);
hold on
plot(w_rotor.time,w_ref.signals.values, '--r');
```

```
title('Rotor speed [rad/s] (blue/solid), reference speed (red/dashed) and
damping torque (green/solid)')
xlabel('Time [s]')
set(get(AX(1),'Ylabel'),'String','Rotor speed [rad/s]')
set(get(AX(2),'Ylabel'),'String','Damping torque [Nm]')
%
figure(13)
subplot(2,1,1)
plot(w_rotor.time,w_ref.signals.values, '--r');
hold on
grid on
plot(w_rotor.time,w_rotor.signals.values);
axis([0 max(w_rotor.time) -1.1*max(w_rotor.signals.values)
1.1*max([max(w_ref.signals.values) max(w_rotor.signals.values)])])
title('Rotor speed and reference')
xlabel('Time [s]')
ylabel('Speed [rad/s]')
subplot(2,1,2)
plot(T_load.time, T_load.signals.values);
grid on
axis([0 max(T_load.time) -1.1*max(T_load.signals.values)
1.1*max(T_load.signals.values)])
title('Stiction torque')
xlabel('Time [s]')
ylabel('Torque [Nm]')

% % Plot speed, speed reference and current
% figure(3)
% subplot(2,1,1)
% plot(w_rotor.time,w_ref.signals.values, '--r');
% hold on
% grid on
% plot(w_rotor.time,w_rotor.signals.values);
% title('Rotor speed and reference')
% xlabel('Time [s]')
% ylabel('Speed [rad/s]')
% subplot(2,1,2)
% plot(Ivfd.time, Ivfd.signals.values);
% grid on
% title('Source current')
% xlabel('Time [s]')
% ylabel('Current [A]')
%
% %Plot source current and voltage
% figure(4)
% subplot(2,1,1)
% plot(Ivfd.time, Ivfd.signals.values)
% title('Source side data')
% ylabel('Source current [A]')
% subplot(2,1,2)
% plot(Uvfd.time, Uvfd.signals.values)
% ylabel('Source  ph-ph voltage [V]')
% xlabel('Time [s]')
%
% figure(5)
% subplot(2,1,1)
% plot(Icable_in.time, Icable_in.signals.values)
% title('Data from cable side of topside transformer')
% ylabel('Current into cable [A]')
% subplot(2,1,2)
% plot(Ucable_in.time, Ucable_in.signals.values)
```

```
% ylabel('Voltage [V]')
% xlabel('Time [s]')

% figure(6)
% subplot(2,1,1)
% plot(Icable_out.time, Icable_out.signals.values)
% title('Data from cable side of subsea transformer')
% ylabel('Current out of cable [A]')
% subplot(2,1,2)
% plot(Ucable_out.time, Ucable_out.signals.values)
% ylabel('Voltage [V]')
% xlabel('Time [s]')
%
% figure(7)
% subplot(2,1,1)
% plot(Imotor_in.time, Imotor_in.signals.values)
% title('Data from motor side of subsea transformer')
% ylabel('Motor current [A]')
% subplot(2,1,2)
% plot(Umotor_in.time, Umotor_in.signals.values)
% ylabel('Motor terminal ph-ph voltage [V]')
% xlabel('Time [s]')
```

7.7.2 Initialization script

```
%%Specifications
U_rated = 6000*sqrt(2/3); % [V] Phase-Gnd peak
f_rated = 66.67; % [Hz]
w_rated = 2*pi*f_rated; % [rad/s]

R_source = 1e-3; %Internal resistance in voltage source.
%Nonzero if capacitor is in parallel with voltage source

% TOPSIDE TRANSFORMER
Sratedts = 5e6; % [VA]
V1ts = 6e3; % [V] Primary side voltage
V2ts = 25.6e3; % [V] Secondary side voltage
R1ts = 0.002; % [pu]
R2ts = 0.002; % [pu]
L1ts = 0.08; % [pu]
L2ts = 0.08; % [pu]
Rmts = 500; % [pu]
satcurve_tops; % Loads the saturation curve topside.
%Lm = (excluded because of saturation curve)

% SUBSEA TRANSFORMER
Sratedss = 5e6; % [VA]
V1ss = 22e3; % [V] Primary side voltage
V2ss = 6e3; % [V] Secondary side voltage
R1ss = 0.002; % [pu]
R2ss = 0.002; % [pu]
L1ss = 0.08; % [pu]
L2ss = 0.08; % [pu]
Rmss =  0; % [pu] Included in Rm_shunt. Transformerlosses
Rm_shunt = (V2ss^2/10e3); % [ohm] 10kW
satcurve_subs; % Loads the saturation curve subsea.
%Lm = (excluded because of saturation curve)

%Initial phase.
Ua_phase = 0;
Ub_phase = -2*pi/3;
Uc_phase = -4*pi/3;

%%CABLE MODEL - one PI-equivalent per 5 km
length = 50; % [km]
nopi = 10; % # of PI equivalent. Using 1 per 5 km
frlc = 3; % [Hz]. Frequency used for RLC-specification & START FREQUENCY
Rc = 0.214; % [ohm/km]
Lc = 0.746e-3; % [H/km]
Cc = 0.136e-6; % [F/km]

%LOAD DATA
Friction = 1; % [Nm*s]
Tm_rated = 6685-Friction*2*pi*f_rated; % [Nm] Rated torque for the
centrifugal load. Linear friction subtracted
load_exponent = 2.0; % Choose square, cube etc. torque.-> TL =
k*w^load_exponent
stiction_torque = 2674; % [Nm] Rotor goes from fixed stiction torque to
                        %the T=K*w^2 when Te exceed stiction torque that is
w > 0
heating_time = 1; % [s] How much time at "frlc" the machine uses before
bearing oil etc. is heated, and the machine follows exponential torque.
K_start = stiction_torque/(2*pi*frlc*heating_time); % [Nm] How fast the
torque after stand still drops.
```

```
D = 0/(frlc*2*pi);%0.015*Tm_rated; % [Nm*s] T_D = D*w_slip Damping torque
factor. Torque as function of speed deviation.

%%START SEQUENCE (Ramps voltage/frequency from start to rated)
U_f_boost = 1.00; %Ratio of voltage boost at starting
f_start = frlc; % [Hz]
t_fixed = 5; % [sec]
t_ramp = 15; % [sec]
theta_init = -60; % [deg] Initial rotor angle. Worst: 120, Best: -60

U_start = (U_rated/f_rated)*f_start*U_f_boost;
f_slope = (f_rated-f_start)/(2*t_ramp); % Coeffisient in t^2 function
U_slope = (U_rated - U_start)/t_ramp; % [V/sec]

%The steady state voltage must be phased in with the ramped signals.
%Therefor the phase angle is calculated for each phase voltage based on how
%fast the frequency is increased and what the starting frequency was
Ua_phase_ss = 2*pi*(f_slope*t_ramp^2 + (f_start-f_rated)*(t_fixed +
t_ramp));
Ub_phase_ss = Ua_phase_ss - 2*pi/3;
Uc_phase_ss = Ub_phase_ss - 2*pi/3;
```

7.7.3 Saturation curves

```
%%% Saturation curve subsea transformer %%%

satcurve = [0,0 ; 0.05,0.1 ; 0.09,0.2 ; 0.12,0.28 ; 0.16,0.41 ; 0.18,0.5 ;
0.2,0.6 ; 0.22,0.68 ; 0.25,0.8 ; 0.28,0.9 ; 0.31,0.95 ; 0.35,0.98 ; 0.4,1 ;
0.65,1.05 ; 0.95,1.07 ; 15,1.2];

satcurve_subsea = [satcurve(:,1)*0.01 satcurve(:,2)];

% plot(satcurve_subsea(:,1), satcurve_subsea(:,2))
%
% axis([0 0.02 0 1.8])
% %axis([0 0.52 0 1.3])
% xlabel('Current in pu')
% ylabel('Flux in pu')

%Base value of flux linkage: (Base RMS voltage) * sqrt(2) / (2*pi *
base_frequency)


%%% Saturation curve topside transformer %%%

satcurve = [0,0 ;  0.0043,0.45 ; 0.0050,0.5 ; 0.0058,0.55 ; 0.0064,0.6 ;
0.0065,0.65 ; 0.0071,0.7 ; 0.0072,0.75 ; 0.0076,0.8 ; 0.0081,0.85;
0.0089,0.9 ; 0.0092,0.95 ; 0.01,1 ; 0.0110,1.05 ; 0.0132,1.1 ; 0.0153,1.15
; 0.0235,1.2 ; 0.0611,1.25 ; 0.1351,1.3 ; 0.245,1.34 ; 0.5,1.38 ; 1,1.42 ;
1.5,1.43 ; 100,1.44];

satcurve_topside = [satcurve(:,1)*0.15 satcurve(:,2)];

% plot(satcurve_topside(:,1), satcurve_topside(:,2))
% axis([0 0.02 0 1.8])
% xlabel('Current in pu')
% ylabel('Flux in pu')

%Base value of flux linkage: (Base RMS voltage) * sqrt(2) / (2*pi *
base_frequency)
```

7.7.4 Support functions used in main script

7.7.4.1 Function to find if machine reaches synchronism from the rotor speed vector and find the synchronization time

```
function tsynch = reachsynch(X, Y, sim, f)

w_rated = f*2*pi;
tsynch = 0;
temp = 0;
sizew = size(X);

for i = 1:sizew(1)
    if ((X(i)/w_rated) > 1)
        temp = 1;
        for j = i:sizew(1)
            if ((X(j)/w_rated) < 0)
                temp = 0;
            end
        end
    end
    if temp == 1
        break
    end
end

tsynch = Y(i);
if tsynch == sim
    tsynch = 9999;
end

end
```

7.7.4.2 Function to count the number of oscillations around zero speed.

```
function zero = zerocrossings(X, t_sim, frlc)
%Speed oscillations. The number of zero-crossings
zerocrossings = 0;
sizew = size(X);
negstart = 0;
%If pulled in negative direction initially
for i = 1:(sizew(1)-1)
    if X(i) > 0
        break;
    elseif X(i) < 0
        negstart = negstart + 1;
        break
    end
end

if negstart == 1
    disp('Negative start: YES')
elseif negstart == 0
    disp('Negative start: NO')
end

for i = 6:10:(sizew(1)-5)
    %If the speed is positive, and rotor stops and is pulled negative
    if (X(i-5) > 0) && (X(i+5) < 0)
        zerocrossings = zerocrossings + 1;
    end
```

```
end
 disp(['The speed oscillates below zero ', num2str(zerocrossings), ' times
during the first ', num2str(frlc*t_sim),' electrical periods.'])
 zero = 0;
end
```

7.8 APPENDIX F – MECHANICAL LOAD MODEL

7.8.1 Mechanical torque and start sequence

The load usually requires a torque proportional to rotor speed. As mentioned there is also a stiction torque that must be overcome to get the machine from standstill. The load model in SIMULINK has two sequences.

1. Standstill. The electromagnetic torque, T_{em}, must exceed some predefined threshold before the rotor starts to accelerate.
2. Acceleration and steady state. The load torque is proportional to rotor speed to some power defined by the type of load [31].

The calculated load torque is an input to the model of the permanent magnet machine. See Figure 68.

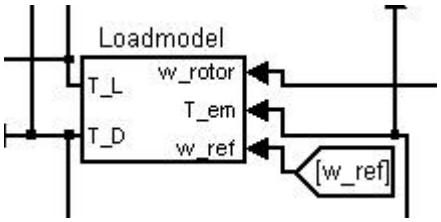

Figure 68 - Load model block as it appears in SIMULINK. Input: Rotor speed and electromagnetic torque. Output: Load torque

The block calculates the term T_L (3) and T_D (5) in the mechanical equation shown below (F1):

$$\overset{(1)}{T_{em}} = \overset{(2)}{J_{tot}\frac{d\omega}{dt}} + \overset{(3)}{T_L} + \overset{(4)}{F * \omega} + \overset{(5)}{T_D} \qquad \text{(F1)}$$

Where:

(1) Electromagnetic torque. The driving force of the motor
(2) Torque needed to accelerate or decelerate the rotor
(3) Load torque defined by the type of load the motor drives. Also used to account for the higher torque during the first few cycles of starting due to stiction.
(4) Friction torque during normal operation. Included in standard machine model
(5) Damping torque

Figure 69 shows the content of the block in Figure 68. For explanation the figure is divided into four segments to explain how each one works. The modeling of T_L is made based on assumptions on how the mechanical system behaves during start. From standstill the lubrication of bearings are assumed to be very viscous, and need some time to heat up.

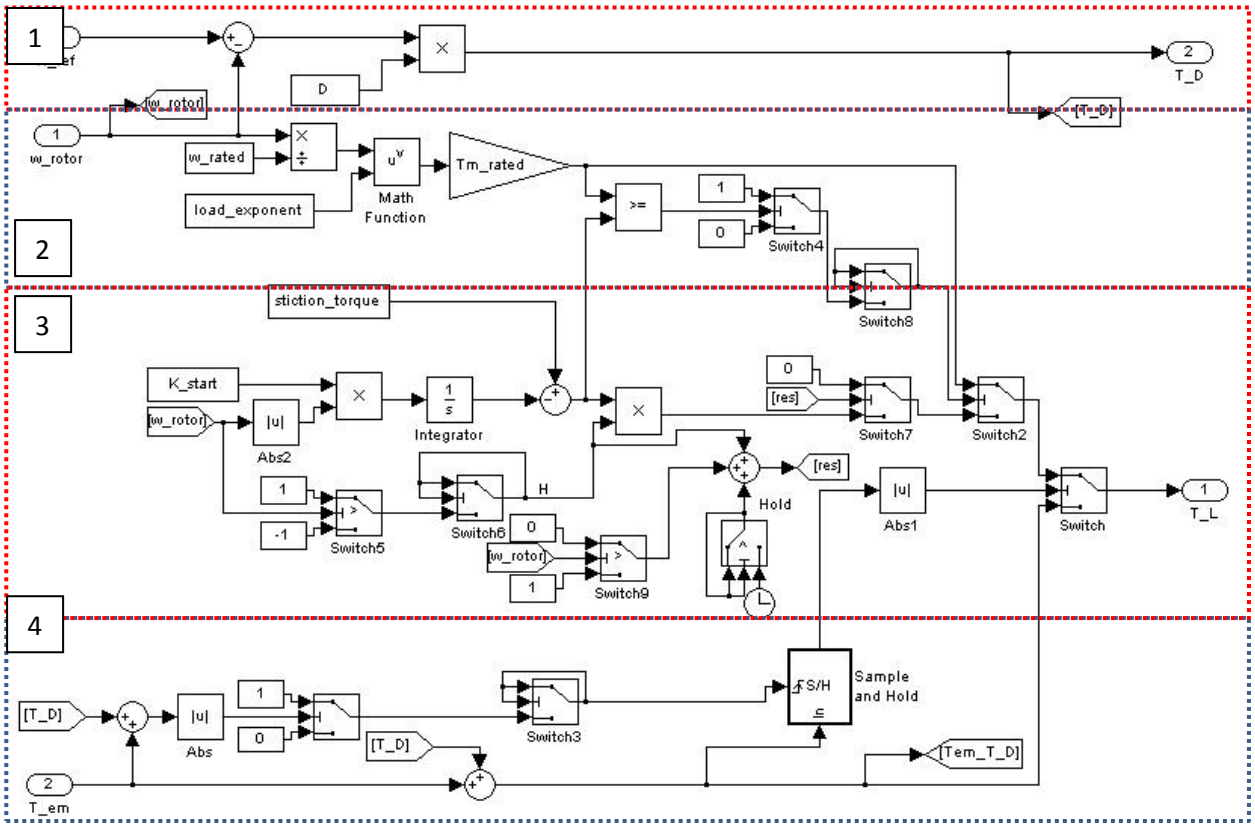

Figure 69 - Load model block content

With reference to Figure 69 each part of the load model is explained below. The colored rectangles are marked with a number from one to four.

1. Damping torque is included in the load model as torque opposing speed deviation. This torque is subtracted from the mechanical load torque. This solution is chosen because of limitations in the standard permanent magnet machine model in SimPowerSystems™
2. Steady state torque. Torque is proportional to speed to the power of some chosen exponent, and a constant value. Mohan [31] suggests the exponent equal to two for centrifugal loads, and one for compressors and rollers
3. After the stiction torque is exceeded the rotor starts to move. The rotor may initially start turning in opposite direction of what is intended. This part of the load model creates a decaying torque whichs drops until it is equal to the steady state torque plus the nominal friction for this speed. If the speed drops below zero T_L also goes to zero if the situation occur after the initial movement of the rotor. This is an approximation to the friction due to quenched bearing oil which would always oppose the speed. If this approximation is not made T_L would act in the same way as the electromagnetic torque when it is negative. This is not realistic. T_L should not be mixed with the torque due to inertia which always opposes change in speed
4. Stiction torque makes the machine stand still until a certain chosen torque is exceeded. By setting load torque equal to electromagnetic torque in this period the machine speed is zero. When the rotor is released the torque decreases for some time (3). Thereafter it increases with speed up to rated value (2)

The segments explained above may be expressed as follows:

$$T_L = \begin{cases} T_{em} \quad \ldots\ldots\ldots\ldots\ldots\ldots\ldots\ldots\ldots\ldots\ldots\ldots\ldots\ldots\ segment\ (2) \\ T_{stiction} - K_{start} \int_o^t |\omega_{rotor}|\, dt \quad segment\ (3) \\ 0 \quad \ldots\ldots\ldots\ldots\ldots\ldots\ special\ case\ of\ segment\ (3) \\ T_{rated} * \left(\frac{\omega_r}{\omega_{rated}}\right)^{load-exponent} \quad segment\ (4) \end{cases} \qquad \text{(F2)}$$

The coefficient K_{start} in (F2) is calculated based on an assumption about how much time the machine would use at starting frequency before the lubrication oil and bearings are heated. With reference to oral discussion with supervisor Norum one second at starting frequency is assumed in this work, but may easily modified for other cases is empirical data is presented to prove other assumptions. Thus K_{start} is calculated with the following equation:

$$K_{start} = \frac{T_{stiction}}{\int_o^{t_{heating}} (2 * pi * f_{start})\, dt} = \frac{T_{stiction}}{2 * pi * f_{start} * t_{heating}} \qquad \text{(F3)}$$

The transition between segment (3) and (4) in Figure 69 occur when the torque assumed related to viscous oil falls below the torque required by the centrifugal load. K_{start} may easily be modified in the configuration script by changing the heating time parameter. See textbox in the end of the chapter.

7.8.2 Including damping torque in load model

The damping torque may be expressed mathematically as [17]:

$$T_D = \frac{\omega_{ref} - \omega_{mech}}{\omega_{ref}} * D = \Delta\omega * D \quad segment\ (1) \qquad \text{(F4)}$$

Damping may not be directly included in the SimPowerSystem machine model for permanent magnet synchronous machine [29]. The torque effect is therefor included in the mechanical load model described above. In the real case the synchronous reactance change when rotor speed deviates from electrical frequency. With the chosen model this effect is not included. Therefor the real machine reactance in the transient state is smaller then the reactance in these simulations.

7.8.3 Example

The load model takes negative starting into account. That is if the rotor angle is in front of the initial stator flux linkage angle. Then the torque would be negative, and the rotor pulled in opposite direction. In Figure 70 an example of negative pullout is shown. As long as the speed is negative the load torque opposes this movement before it changes sign when the rotor speed becomes positive.

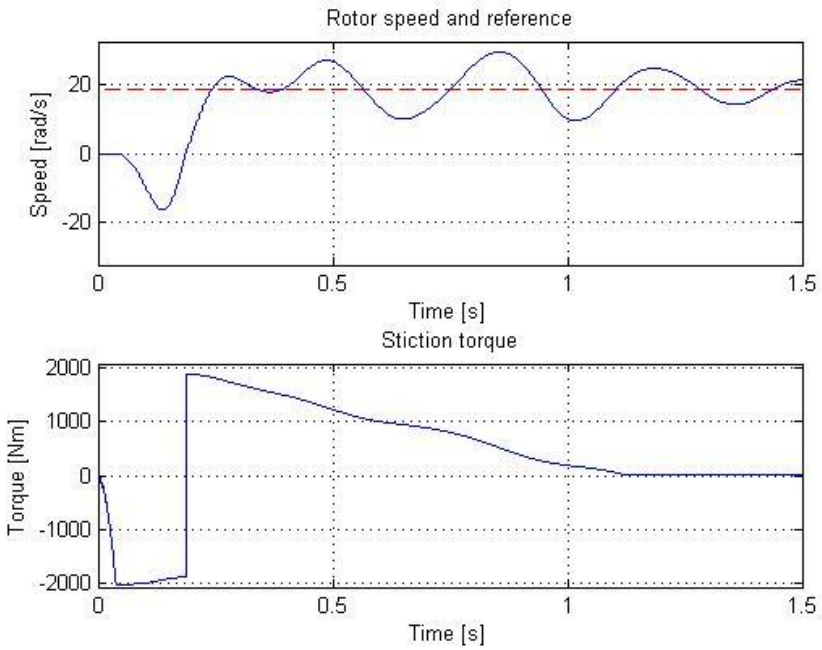

Figure 70 - Rotor speed and T_{LOAD} during initial synchronization. Typical sequence.

Above it can be seen that in the oscillations result in zero crossings in the rotor speed. The friction torque due to viscous oil then drops to zero as it is argued for earlier in this chapter. Including some amount of damping may prevent the rotor from oscillating severely. This is covered in simulations. Note that Figure 24 does not show the terms (2), (4) and (5) in equation (F1).

```
%LOAD DATA (Example)
Friction = 1; % [Nm*s]
Tm_rated = 6685 - Friction*2*pi*f_rated; % [Nm]
load_exponent = 2.0; % Choose linear, square, cube etc. torque.-> TL =
%k*w^load_exponent
stiction_torque = 2000; % [Nm] Rotor goes from fixed stiction torque to the
%T=K*w^2 when Te exceed stiction torque that is w > 0
heating_time = 1; % [s] How much time at "frlc" the machine uses before bearing
%oil etc. is heated, and the machine follows exponential torque.
K_start = stiction_torque/(2*pi*frlc*heating_time); % [Nm] How fast the torque
%after stand still drops.
D = 0.00*Tm_rated; % [Nm*s] T_D = D*w_slip Damping torque factor. Torque as
function of speed deviation.
```

With the parameters shown here the value for each term in (F1) at starting and steady state frequency would be:

Table 21 - Torque values before and after synchronization. f_{rated} = 66.67 Hz. Rotor initially locked.

Initially (ω_{rotor} = 0)		**When synchronized ($\omega_{rotor} = 2*\pi*f_{start}$)**		
f_{start} [Hz]	3	**f_{start} [Hz]**	3	66.67
(1) [Nm]	0*	**(1) [Nm]**	32	6685
(2) [Nm]	0	**(2) [Nm]**	0	0
(3) [Nm]	$T_{EM}+T_D$*	**(3) [Nm]**	13	6266
(4) [Nm]	0	**(4) [Nm]**	19	419
(5) [Nm]	$-T_D$**	**(5) [Nm]**	0	0

***The rotor is locked until $T_{EM}+T_D > T_{STICTION} = 0.3*T_{RATED}$(Typically) ≈ 2000 Nm**

****Damping is present from t=0$^+$**

The table shows that very high torque is needed when the rotor is locked compared to when it is synchronized. This illustrates one of the major challenges with a long step out system including magnetic couplings e.g. transformers and motors. Figure 70 also shows oscillations in rotor speed which means that the torque from the second term in equation (F1) may be significant.

Voltage drop in the cable at low frequency makes it difficult to achieve the high torque needed to overcome stiction, and to synchronize the rotor. If starting is successful the torque demand drops dramatically after the first few mechanical revolutions.

7.8.4 Load data

The load data used in this work is given in Table 22.

Table 22 - Load data [30]

Nominal shaft power	J_P	[kg*m^2]	7.37
Nominal voltage	J_M	[kg*m^2]	11.51
Power factor	J_{TOT}	[kg*m^2]	18.88
Load exponent		[]	2
Nominal pump torque	T_P	[Nm]	6685
Nominal pump speed	f_N	[Hz]	66.67
Break away/stiction torque	$T_{stiction}$	[Nm]	*

***A range of stiction torques is investigated in simulations**

These values are inserted into the configuration script used to initiate the SimPowerSystem simulations. See Appendix E.